EPRI
Electric Power
Research Institute

Keywords:
Decontamination
Chemical Solvents
Light Water Reactors
Radiation Control

EPRI NP-3177
Project 1329-1
Final Report
July 1983

EPRI-NP--3177

DE83 902948

Development of LOMI Chemical Decontamination Technology

Prepared by
Central Electricity Generating Board
Berkeley, Gloucestershire, U.K.

Development of LOMI Chemical Decontamination Technology

NP-3177
Research Project 1329-1

Final Report, July 1983

Prepared by

CENTRAL ELECTRICITY GENERATING BOARD
Technology Planning and Research Division
Berkeley Nuclear Laboratories
Berkeley, Gloucestershire GL13 9PB
United Kingdom

Principal Investigators
D. Bradbury
M. G. Segal
R. M. Sellers
T. Swan
C. J. Wood

Prepared for

Electric Power Research Institute
3412 Hillview Avenue
Palo Alto, California 94304

EPRI Project Manager
R. A. Shaw

Chemistry, Radiation, and Monitoring Program
Nuclear Power Division

ORDERING INFORMATION

Requests for copies of this report should be directed to Research Reports Center (RRC), Box 50490, Palo Alto, CA 94303, (415) 965-4081. There is no charge for reports requested by EPRI member utilities and affiliates, U.S. utility associations, U.S. government agencies (federal, state, and local), media, and foreign organizations with which EPRI has an information exchange agreement. On request, RRC will send a catalog of EPRI reports.

Prepared by
Central Electricity Generating Board
Berkeley, Gloucestershire, U.K.

EPRI PERSPECTIVE

PROJECT DESCRIPTION

This project (RP1329-1) is one of several studies directed at the development of decontamination technology for the reduction of radiation fields in nuclear power plants. Other projects have focused on nonchemical decontamination techniques and testing of a wide range of dilute chemical reagents. This report describes work to develop a new chemical system using low-oxidation-state metal-ion (LOMI) reagents for application to LWRs.

PROJECT OBJECTIVE

The overall objective was to formulate chemical reagents capable of dissolving oxides from pipework and suitable for use in LWRs.

PROJECT RESULTS

The product of this work is the LOMI chemical decontamination reagent, vanadous picolinate/formate. This reagent is effective on BWR corrosion films, has good radiation stability, does not corrode the base metal, and can be processed using conventional ion-exchange technology. Since the work described in this report was carried out, vanadous picolinate/formate has been used extensively by the United Kingdom Atomic Energy Authority to decontaminate the entire circuit including fuel in the Winfirth Steam Generating Heavy Water Reactor, a 100-MW (e) BWR.

Vanadous picolinate/formate is not effective on the chromium-rich corrosion films in PWRs. Central Electricity Generating Board has been developing LOMI systems for PWR use. One of these developments, a dilute oxidizing pretreatment followed by vanadous picolinate/formate, was used to decontaminate one channel head of the ex-Surry steam generator at Battelle, Pacific Northwest Laboratories. This work was carried out by Quadrex Corporation as part of the NRC-directed Surry steam generator project.

These successful plant demonstrations indicate that the LOMI decontaminate system should be considered by utilities evaluating decontamination options. EPRI is

involved in additional work to validate the LOMI system for plant use, including materials corrosion testing at Battelle (RP2296-4). The LOMI technology has been patented and is currently being marketed worldwide.

This report should be of interest to nuclear plant engineers planning special maintenance operations and to plant chemists and health physics engineers with ALARA responsibilities.

Robert A. Shaw, Project Manager
Nuclear Power Division

ABSTRACT

The objective of this project is to develop chemical reagents for the decontamination of nuclear power-reactor coolant circuits with particular emphasis on PWR primary-coolant circuits. These reagents must be effective at dissolving activated corrosion products, must be compatible with reactor coolant circuit materials and must be manageable in terms of radioactive-waste disposal. A fundamental study of metal oxide dissolution has led to the development of low-oxidation-state transition-metal-ion (LOMI) reagents, which dissolve oxides rapidly without affecting the underlying metal. One of these reagents, vanadous picolinate/formate, has been used to decontaminate reactor specimens efficiently. The radiation-stability of this reagent is good, and the released activity can be collected conveniently on ion-exchange resins. Application of these types of reagents to PWR and BWR decontamination is outlined in the report.

CONTENTS

ILLUSTRATIONS

TABLES

APPENDIX ILLUSTRATIONS

APPENDIX ILLUSTRATIONS (Cont'd)

APPENDIX TABLES

SUMMARY

In order to reduce radiation exposure in LWRs, a method of decontamination is being developed to remove the radioactive metal oxide crud in the primary circuit. Ideally low concentrations of cleaning reagents should be employed so as to minimise circuit corrosion and the volume of rad-waste produced.

Experiments have been conducted to determine the factors which control the chemical dissolution of oxides typical of LWR primary circuits. The presence of a one electron reducing agent has been found to result in rapid dissolution of deposited oxides where the predominant species is Fe^{III}. This conclusion has allowed the development of a number of decontaminating agents based on low-oxidation-state transition-metal-ion reductants (LOMI). These are capable of dissolving synthetic oxides up to two orders of magnitude faster than conventional decontaminating reagents based on mixtures of complexing acids, even when the LOMI reagent is present at only one hundredth the concentration of the conventional chemicals. One of these reagents, vanadous picolinate/formic acid has been used successfully to decontaminate active samples removed from a boiling water reactor circuit and accomplished this more rapidly and with less base metal corrosion than conventional, high concentration citric/oxalic acid based reagents. Dissolved radioactivity was removed on ion-exchange resins. The radiation chemistry of these reagents has been examined and reagents have been identified which have sufficient stability for decontamination of a full circuit including the fuelled core. The application of LOMI reagents to a PWR circuit is discussed and methods of reagent preparation are described.

The reagents described in this report are suitable for the decontamination of BWR primary circuits and for the dissolution of loose, low chromium content, PWR oxides. Development of LOMI reagents is continuing with the aim of obtaining a system which will also dissolve the high-chromium grown-on oxide layers from LWR surfaces in a low concentration, single stage process.

Section 1

INTRODUCTION

The accumulation of radiation dose with time at LWRs has been reviewed by Shaw (1979). In early life the dose rate on PWR primary circuit pipework increases at a rate of 50 mR h^{-1} $EFPY^{-1}$ and appears to saturate at a few hundred mR h^{-1} after $\sim$6 years. The dose rates in steam generators are considerably higher in the range 5-30 R h^{-1}, values achieved after only 1-2 years operation in some cases. The picture for BWRs is different. The rate of increase of dose rate on recirculation pipework is in the range 50-150 mR h^{-1} $EFPY^{-1}$ and this shows little tendency to level off with time. However, there are a number of BWRs - notably Japanese and Swedish plant - where dose rates are very much lower than the BWR average. The geometric mean annual doses for both PWR and BWR are shown in Fig. 1. This shows that the effect of the above dose rates is to give an exposure commitment of about 500 Man Rem y^{-1} per plant on a PWR after 5-6 years operation if the plant operates routinely. Very much higher commitments occur if extensive non-routine maintenance is required, such as steam generator repairs. Historically occupational doses of this size have been accommodated by dose-sharing procedures, but with the new attitudes to radiation exposure set out in ICRP-26 (1977)* this practice will be less convenient.

The main sources of the radiological doses are radiation fields associated with the coolant circuit. The dominant contributors to these fields are activated corrosion products, with the gamma-ray emitting isotopes ^{58}Co and ^{60}Co being mainly responsible. Because of its five year half-life, ^{60}Co is expected to become the dominant γ-source later in plant life. The processes that result in out-of-core radiation fields are summarized in Fig. 2. These radiation fields from the primary circuits of reactors build up for several years after the start of operation, and it is anticipated that there will be growing emphasis on radiation control in the future.

Radiation exposure can be reduced by improving layout and shielding, the adoption of remote inspection and maintenance methods and more rigorous operator training.

---

* Recommendations of the International Commission on Radiological Protection. Annals of the ICRP Vol.I No. 3, 1977 Pergamon Press.

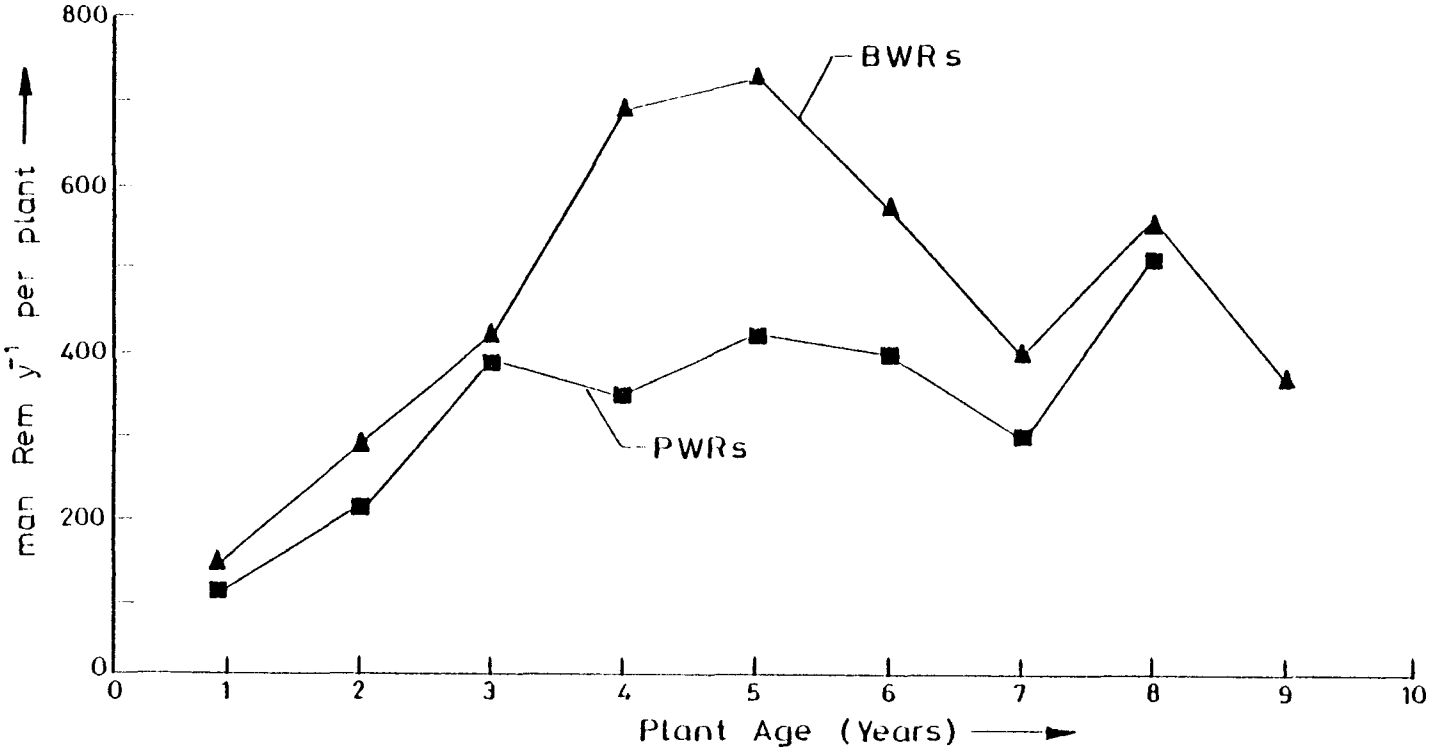

FIG. 1. Water Reactor Doses — EPRI Plant Survey Data. (Geometric means of U.S. nuclear power plant annual exposures)

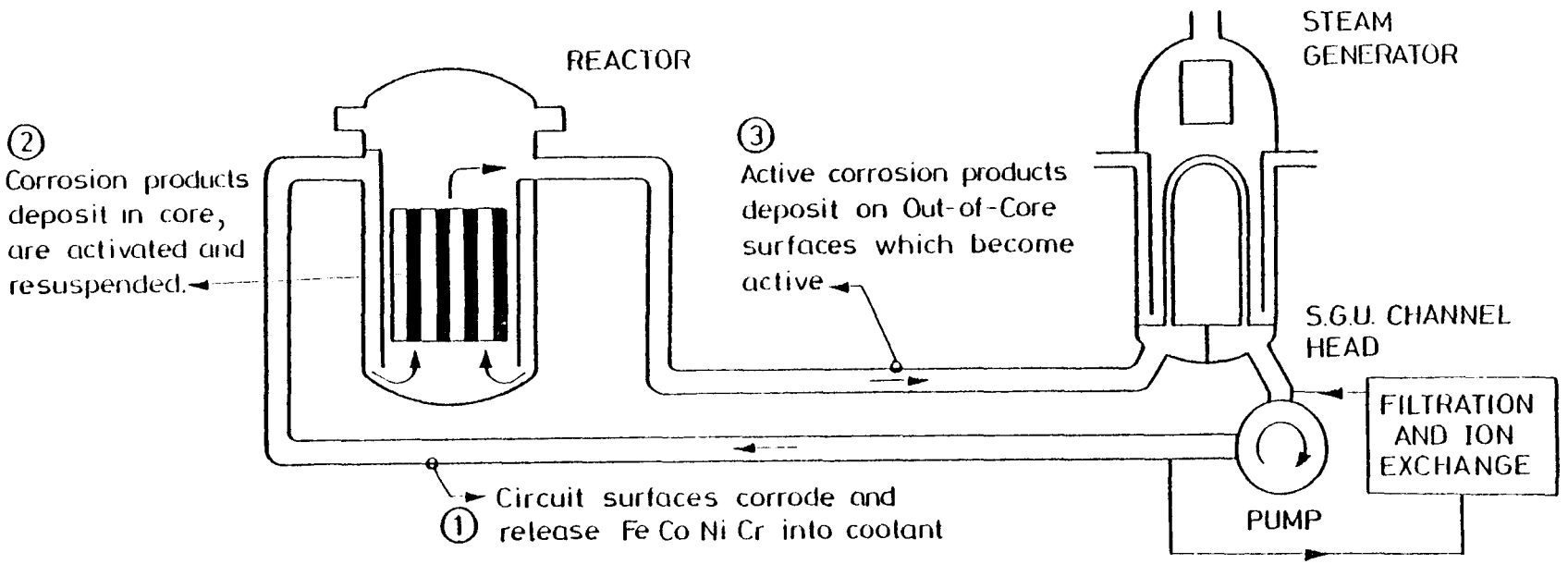

FIG. 2. Source of Plant Radiation Fields

However, the reductions that can be achieved by these methods are limited, and in order to minimise doses it is necessary to reduce the radiation fields on out-of-core coolant circuit surfaces. EPRI have a wide-ranging programme aimed at radiation control, including improved chemical control of the primary circuit, replacement of high-cobalt alloys, high temperature filtration and chemical decontamination. This programme includes a collaborative project between CEGB and EPRI on the development of an improved method of chemical decontamination, which is the subject of this report.

The main body of this report consists of an overview of the entire project, with full details being contained in the Appendices. Theoretical considerations are given in Appendix 1, experimental details in Appendix 2, and results and discussion in Appendix 3. Appendix 4 deals with the radiolytic stability of the decontamination reagents, and application to reactor decontamination is discussed in Appendix 5. This format will allow the general reader to grasp the essential requirements for a reactor decontamination reagent and the way in which the new LOMI reagents fulfil these needs, without having to digest the detailed physical chemistry of the LOMI process which is covered in the Appendices.

Section 2

DECONTAMINATION EXPERIENCE

Traditional descaling methods have been applied to water reactor decontamination and give worthwhile dose reductions. A two-stage treatment with 12% alkaline permanganate followed by a 6% mixture of oxalic and citric acids will decontaminate most LWR surfaces (Ayres 1970). However, this high-concentration chemical method has two major drawbacks. First it leads to very large volumes of radioactive effluent which require a sizeable facility for their handling. Second, because it employs high concentrations of agressive chemicals, there are considerable materials compatibility uncertainties. Ideally, these problems could be overcome if a reagent was found which could be used at much lower concentration. An example of this approach is the Candecon treatment (Pettit 1974) which employs low concentrations (0.1%) of complexing organic acids to dissolve the activity and relies on reagent regeneration on an ion-exchange column to provide adequate capacity. The big advantage of this method is that the radioactive waste is concentrated onto a few cubic meters of ion-exchange resin. The drawback is that these dilute solutions of conventional boiler cleaning reagents dissolve BWR crud only slowly and PWR crud hardly at all (Johnson et al. 1979). There is thus a requirement to develop reagents which are efficient crud dissolvers when used at low concentration to reduce corrosion and waste handling problems. Figure 3 summarises the situation on decontamination reagents at the start of this project, and the direction taken to overcome the problems.

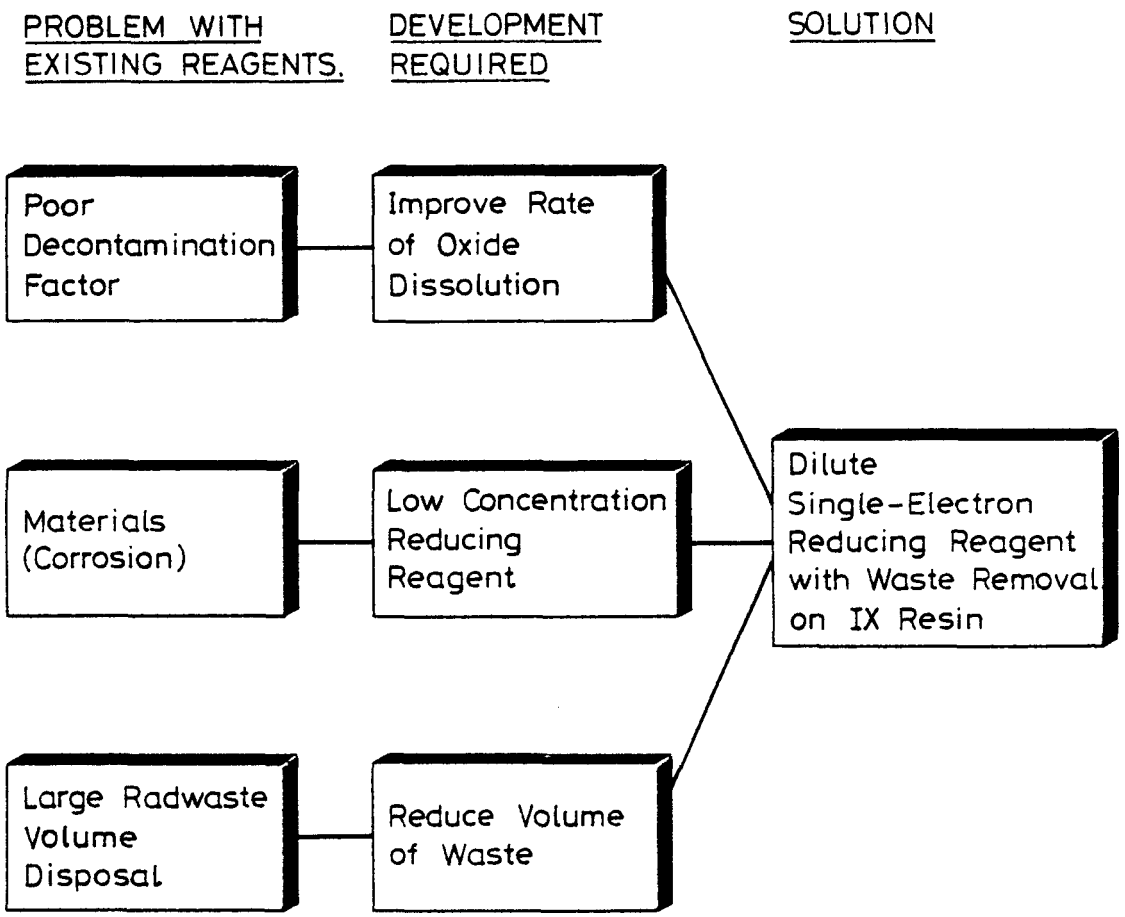

FIG.3. The Main Problems Associated with Existing Decontamination Methods and the Development Required to Overcome Them

Section 3

DECONTAMINATION REAGENT DEVELOPMENT

There are two approaches to reagent selection for decontamination. That which has most often employed is essentially empirical and relies on testing a wide range of candidate reagents for their ability to decontaminate either specimens removed from actual reactor circuits or else material which has been oxidised under conditions similar to those in the reactor circuit, but without the radioactivity. This approach relies on the selection of a wide and diverse range of reagents and even then the chance of identifying an efficient oxide dissolution mixture is small. A better approach is to attempt to understand the chemistry of the decontamination process so that reagent development can proceed on a technically logical basis.

3.1 SOURCE OF RADIATION DOSE

The radioactive nuclides are present in the oxide layers which form on all the surfaces in the water circuit. This oxide may be subdivided into two main categories :

i) deposited oxide

ii) grown-on oxide

These two types exist in all water reactor systems but the relative amounts of each very considerably between BWRs and PWRs and even between different plants of the same type. Figure 4 summarises the oxide types which have been found on surfaces in BWRs and PWRs. Deposited radioactive oxide may form on fuel and on out-of-core surfaces by several mechanisms: it may arise as a result of precipitation from solution or from the deposition of coolant-borne particles. The particles and precipitates may be radioactive because they are formed from material which has resided in core. Once they have been deposited as oxide they may pick up additional activity by ion-exchanging dissolved activity from the coolant. Grown-on oxide arises from the in-situ corrosion of the circuit surfaces. It stays where it is formed, and does not itself become radioactive by residing in core. Instead grown-on oxide absorbs active species from solution as it grows and incorporates them into its structure.

Corrosion of primary circuit materials is very low ($\sim 0.1 \rightarrow 1$ mg dm^{-2} $month^{-1}$)

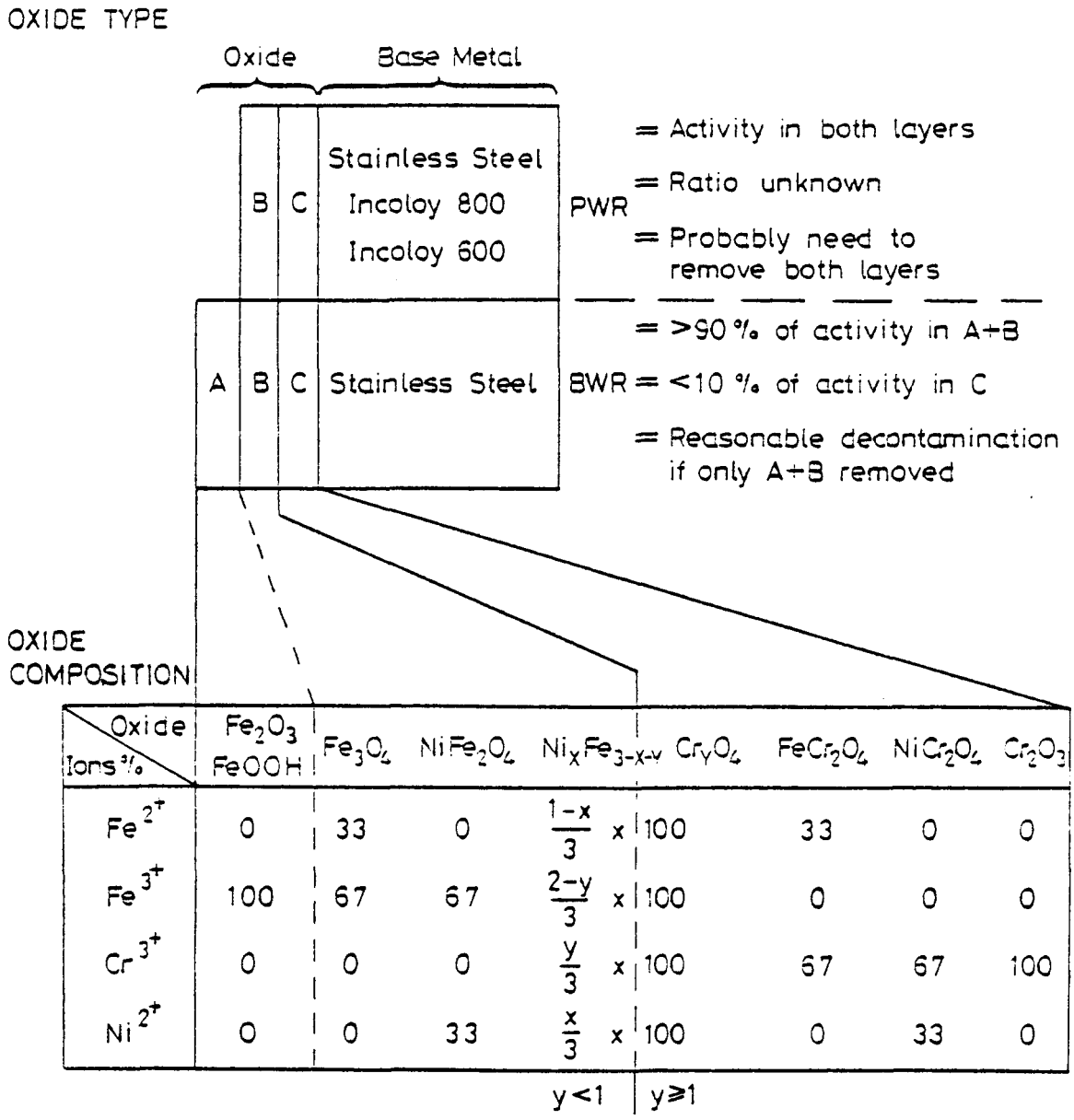

FIG. 4. Nature of Oxides in LWR Primary Circuits

for AISI 304, Inconel 600, etc.) and grown-on corrosion layers would be expected to be quite thin. In the case of a PWR, where all the corrosion products arise within the primary circuit, the relative quantities of deposited and grown-on oxide will be related to the ratio of corrosion/release rate for the alloys concerned. With release rates in the range 30 - 60% the total quantities should be about equal. In the case of BWRs, the major source of corrosion product input is from the feed train and hence deposited oxide will exceed grown-on material by a significant amount. The specific activity of the various oxide types will be different, because of the differences in the way radioisotopes are incorporated and differences in the rates of material exchange with in-core material. Depending on the relative quantities of deposited and grown-on oxides and their specific activities it may be sufficient to remove only the deposited oxides to achieve a significant reduction in radiation dose. An example of this is afforded by specimens removed from the primary circuit of the Winfrith Steam-Generating Heavy Water Reactor (a BWR) where the quantity of deposited oxide was much greater than that of grown-on oxide and it also contained > 97% of the radioactivity (Brookes - Private Communication). In other plants, particularly PWRs, the grown-on oxide may contain a higher proportion of the total activity, requiring the removal of both oxide types to achieve a good decontamination.

3.2 OXIDE TYPES

Composition data is available for corrosion products found on fuel in both BWR and PWR and also for loose oxide found on out-of-core surfaces and in the coolant. Less data is available on the composition of grown-on oxide for either system.

3.2.1 Deposited Oxides

Loose crud found on PWR surfaces, in the coolant and scraped from fuel is generally close in composition to nickel ferrite ($NiFe_2O_4$) (Sandler, 1978). The ferrite is seldom found in its chemically stoichiometric form and is usually described as $Fe_{3-x-y}Ni_xCr_yO_4$ (i.e. a mixed ferrite/chromite). Excess nickel above the spinel stoichiometry is sometimes accommodated as NiO. In the case of BWRs which run with oxygenated primary circuit chemistry the loose oxide may consist of more than one layer. Typical BWR crud has an outer layer of iron oxide in the highest oxidation state as either Fe_2O_3 (α-haematite) or FeOOH (goethite or lepidochrocite). Under this is a layer of Fe_3O_4 (magnetite) which may be partially substituted with Ni or Cr and resembles the loose oxide found in PWRs (Romeo, 1978). The delineation between layers is not always precise and elemental composition probably changes with depth within a particular layer.

3.2.2 Grown-on Oxide

The small amount of data available on the composition of the inner, grown-on oxide layers suggests that these tend to be rich in chromium in both BWR and PWR. The composition will be a stronger function of the base metal composition than is that of deposited material, and iron and nickel chromites are likely to be major constituents on stainless steel and Inconel respectively. Table (1) and Figure 4 set down the various oxide types together with their cationic composition. The deposited oxides are characterised by Fe^{3+} always being the predominant iron cation. It is likely that Cr^{3+} is the predominant chromium cation in grown-on oxides.

Since deposited oxides have been better characterised than grown-on material, the dissolution work described in this report has concentrated on studying the basic dissolution chemistry of these oxides. Further work to develop dissolution techniques may be required for grown-on oxide, but this has been deferred until these are better characterised.

TABLE 1

Water Reactor Oxide Types and Composition

Cation % \ Oxide	FeO.OH Goethite	Fe_2O_3 Haematite	Fe_3O_4 Magnetite	Fe_2NiO_4 Nickel Ferrite	NiO Nickel Oxide	$Fe_{3-x-y}Ni_xCr_yO_4$ Mixed Ferrite Chromite	$FeCr_2O_4$ Iron Chromite	$NiCr_2O_4$ Nickel Chromite	Cr_2O_3 Chromia
Fe^{2+}	0	0	33.3	0	0	$\frac{1-x}{3}$ x 100	33.3	0	0
Fe^{3+}	100	100	66.6	66.6	0	$\frac{2-y}{3}$ x 100	0	0	0
Ni^{2+}	0	0	0	33.3	100	$\frac{x}{3}$ x 100	0	33.3	0
Cr^{3+}	0	0	0	0	0	$\frac{y}{3}$ x 100	66.6	66.6	100
	Deposited Oxide					y<1	y≥1	Grown-On Oxide	

Section 4

DEVELOPMENT OF DISSOLVING REAGENTS FOR DEPOSITED OXIDES

As pointed out above, the predominant cation in the lattices of deposited oxides is always Fe^{3+}, irrespective of whether the oxide has been formed in the oxidising chemistry of a BWR or the reducing chemistry of a PWR. This suggests that the oxide might be destabilised by attacking it with a strong reducing agent and this may be a more efficient way of dissolving the deposit than relying on attack by protons as in conventional acid cleaning techniques.

The first test of this hypothesis was reported by Bradbury (1977) when it was found that the reducing agents thioglycollic acid and sodium dithionite dissolved α-haematite much more rapidly than strong acids. The present study has extended this work to investigate a number of redox systems. The rates of oxide dissolution were greatest for the one-electron reductants V^{2+}, Cr^{2+}, $HSCH_2COOH$ and $Na_2S_2O_4$ irrespective of redox potential, indicating that the dissolution process was sensitive to the kinetic mechanism rather than the thermodynamic reducing power. One-electron reductants are those which, in carrying out an electron-transfer reaction, reach a stable state where they have donated one electron only, for instance Cr^{2+} donates one electron to become Cr^{3+} which is then stable in solution. For the reduction with chromium to go further would then require the removal of three more electrons before the stable Cr^{6+} ion was produced. This is unfavourable on thermodynamic grounds except in the presence of a very powerful oxidant. The preference for single electron reductants to dissolve Fe^{3+}-bearing oxides occurs because the reduction process Fe^{3+} (oxide surface) → Fe^{2+} (oxide surface) requires just one electron per site. Multi-electron redox systems only attack multiple Fe^{3+} sites and are not therefore as rapid.

These studies have concentrated on a comparison of one-electron reducing agents with conventional cleaning reagents for the dissolution of a selection of synthetic oxide powders typical of the deposited material in LWRs. The most suitable reagents for further development have been identified and this has been undertaken by cleaning radioactive specimens removed from the Winfrith BWR. Techniques have been developed for the large scale application to a reactor primary circuit.

4.1 EXPERIMENTAL PROGRAM WITH SYNTHETIC POWDERS

The principal synthetic oxides studied were α-Fe_2O_3, Fe_3O_4, $Fe_{3-x}Ni_xO_4$ ($x = 0.4 \rightarrow 1$) and $Fe_{2.35}\ Cr_{0.15}\ Ni_{0.5}\ O_4$. Dissolution experiments were undertaken with HCl, H_2SO_4, Citric/Oxalic acids and EDTA as representing a cross-section of conventional reagents based on strong or complexing acids. The dissolution kinetics in these experiments were compared with those for a number of one-electron reductants:- V^{2+}, Cr^{2+} and thioglycollic acid. In the case of the low oxidation-state metal ions (LOMI) Cr^{2+} and V^{2+}, these would only remain in solution at low pH in the presence of such counter ions as Cl^-, SO_4^{--} and ClO_4^-. Since such acid anions are not acceptable for reactor use complexes of the chromium and vanadium were produced so that the pH could be raised without precipitation occurring. Complexing the Cr^{2+} and V^{2+} has the effect of changing the reagent redox potential. Some complexing agents lower the redox potential to such an extent that the reagent reacts rapidly with water thereby destroying itself by a simple thermal reaction. 2,2'-bipyridyl and picolinic acid were chosen as complexing agents for V^{2+} and Cr^{2+} because these were among the simplest ligands having adequate complexing ability which, however, did not lead to rapid thermal reagent decomposition.

The dissolution of the oxides followed a cubic rate law, i.e. proportional to surface area of spherical particles, and the relative rates for the reagents are shown as histograms in Figures (5) and (6). Without exception the reducing agent systems dissolve the oxides more rapidly than reagents which rely on proton attack or strong complexation alone. In the case of the V^{II}/2,2'-bipyridyl system dissolution rates are up to four orders of magnitude greater than with the conventional citrox reagent even when used at one hundredth the concentration. This clearly indicates that the key to the rapid dissolution of deposited oxide is attack by an efficient reducing system.

4.2 RADIATION STABILITY

The most promising reagents from the oxide powder dissolution experiments have been subject to further investigation. If a reagent is to be used in the radiation field of a reactor primary circuit it must have adequate radiation stability. The radiolysis of candidate reagents has therefore been examined using γ-radiation from a ^{60}Co source. The most efficient dissolving reagents identified were Cr^{II} bipyridyl, V^{II}bipyridyl and V^{II} picolinate. On irradiation at the dose rates of 0.5×10^6 rads h^{-1} typical of the core of a shutdown reactor, 2,2'-bipyridyl polymerised after a short exposure and can only be considered for use in out-of-core regions or for component decontamination. Picolinic acid, on the other hand,

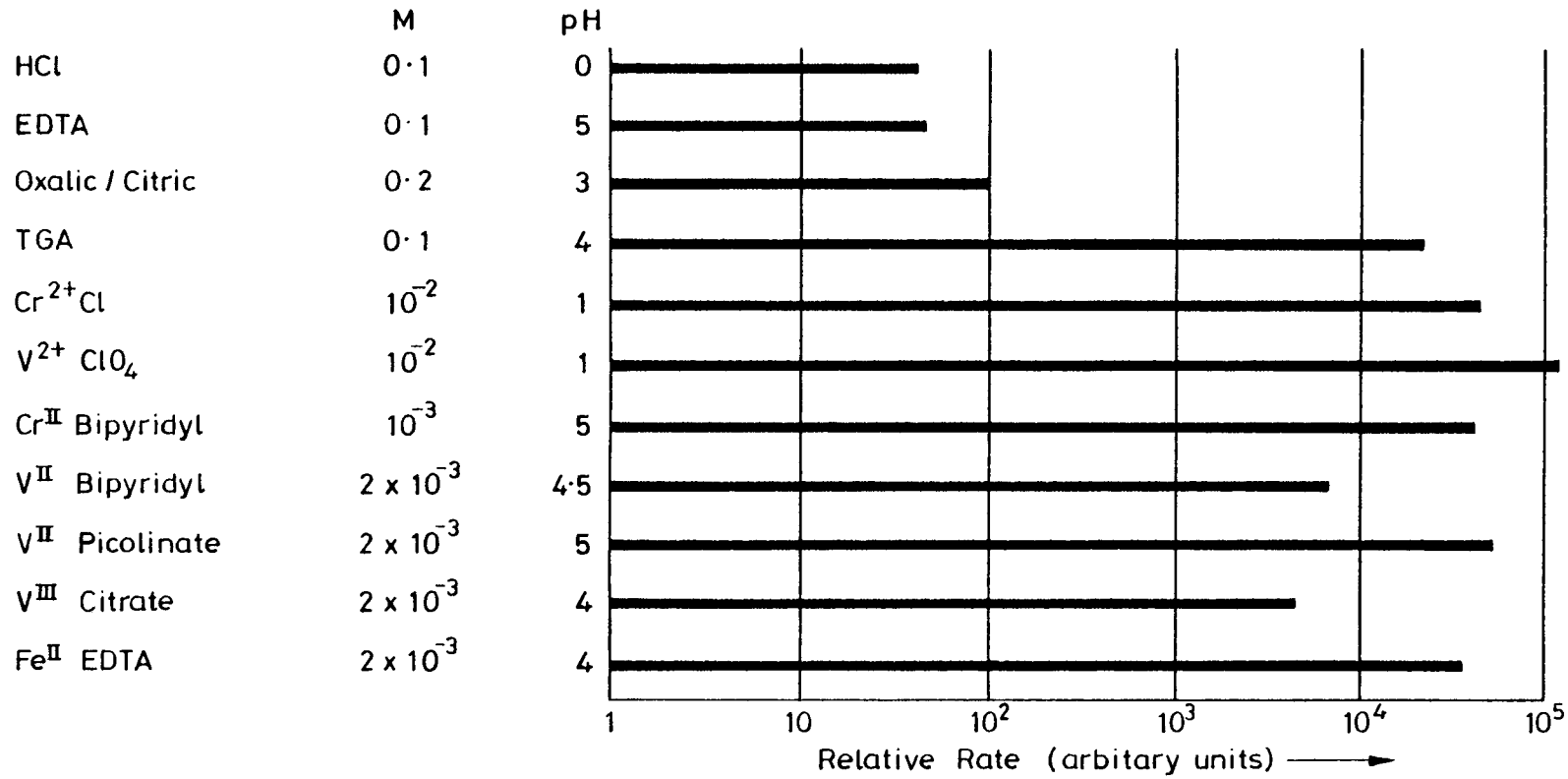

FIG. 5. Dissolution of Simulated Reactor Oxide Powders – Haematite

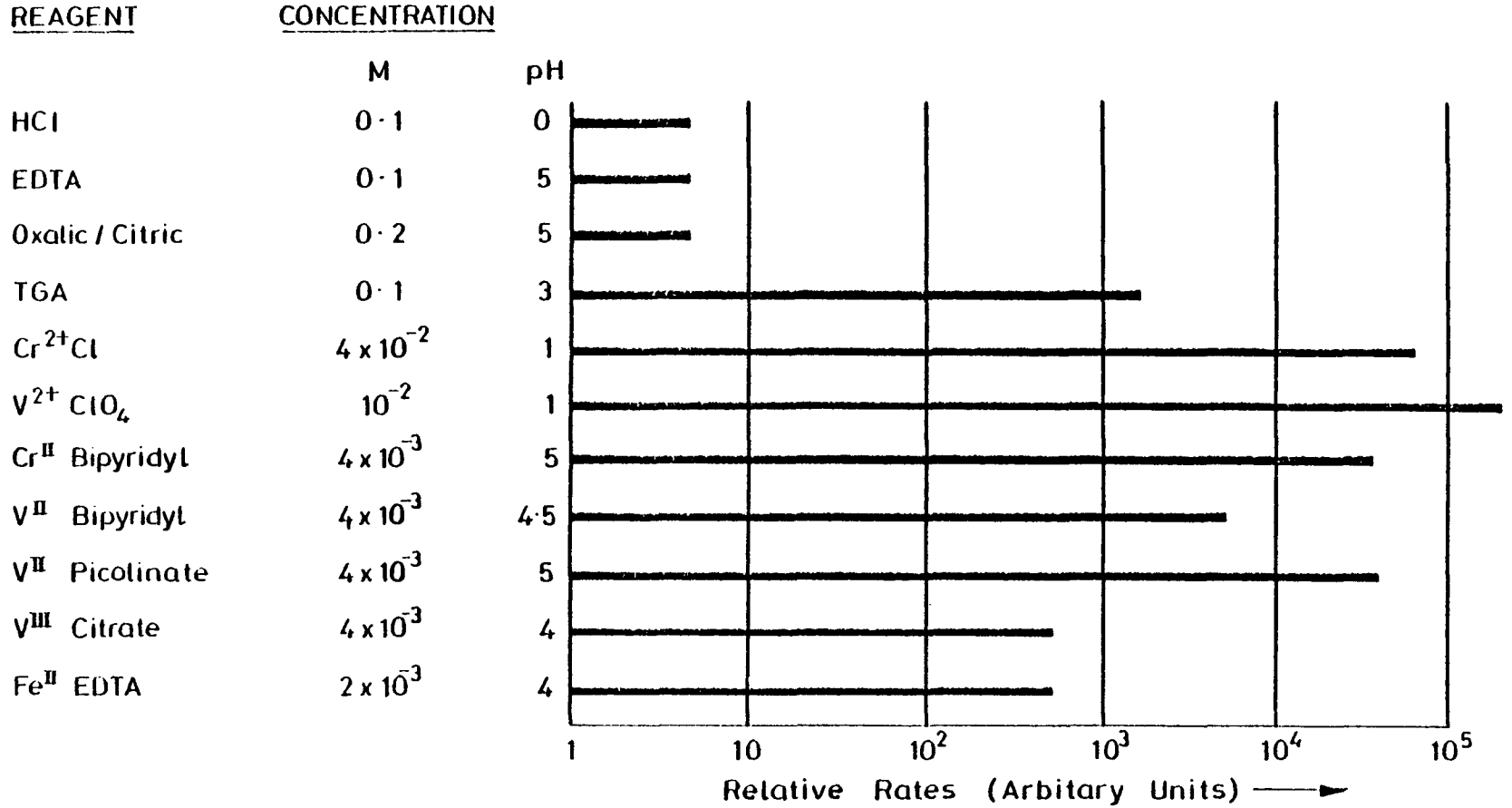

FIG. 6. Dissolution of Simulated Reactor Oxide Powders – Nickel Ferrite

had a half life of 10 - 20h at the high dose rate. This compares well with the half-lives of such reagents as EDTA and NTA which have been used for a whole circuit decontamination. In addition to decomposition of the complexing agent, the oxidising species formed from water radiolysis (e.g. $H^{\cdot}, OH^{\cdot}, HO_2^{\cdot}, H_2O_2$) also attack the low oxidation state-metal ion. It has been discovered that the V^{2+} metal ion can be protected from oxidising attack by the addition of an excess of formate. This scavenges the oxidising radicals in reactions such as:

$$OH^{\cdot} + HCOO^{-} \rightarrow CO_2^{-} + H_2O$$

The CO_2^{-} will then reduce any V^{III} in the system to regenerate the low oxidation

$$V^{III} + CO_2^{-} \rightarrow V^{II} + CO_2 \uparrow$$

state, V^{II}. Thus no matter whether the V^{II} is oxidised to V^{III} as a result of water radiolysis or by reacting with Fe^{III} oxide to reduce and dissolve it, in the presence of sufficient formate ion the LOMI reagent V^{II} is regenerated.

Because the V^{II} picolinate/formate system gave rapid dissolution of deposited oxide types at low concentration (0.1% total reagent) and displayed adequate radiation and thermal stability with the added advantage that the oxide-attacking component V^{II} could be radiolytically regenerated in the core of the reactor, further development concentrated on this reagent. A variety of other complexing agents were tried with the V^{II} reductant, but only one, histidine, gave comparable dissolution rates. Others were either thermally unstable or reacted slowly with the oxide. Histidine has not been pursued further at this stage because the additional benefits from its use are outweighed by the large program of radiation chemistry and corrosion testing required before reactor use.

4.3 DECONTAMINATION OF METAL SAMPLES

The vanadous picolinate reagent $\left[V^{II}(pic)_3\right]^{-}$ has been used to remove the oxide from three types of steel specimen. Two types were contaminated as a result of exposure in a reactor circuit. The first type consisted of specimens of AISI 321 stainless steel cut from the S21 riser at Winfrith SGHWR. The second type was mild steel samples which had been exposed to PWR primary circuit conditions in a reactor loop. The third type was inactive. The latter were samples of 9%Cr Advanced Gas-cooled Reactor boiler tube which had been oxidised in high pressure reducing chemistry

typical of the steam circuit of that plant. Typical conditions for the decontamination are shown in the following table :-

V^{II}	$2 - 4 \times 10^{-3}$ M
Picolinic Acid	$1 - 2 \times 10^{-2}$ M
Formate	$1 - 2 \times 10^{-2}$ M
pH	4 - 5
Temperature	$80^{o}C$

In the case of samples containing chromium, the oxide was removed down to the thin chromium-rich layer adjacent to the metal surface. In the case of the S21 specimens from SGHWR-BWR this inner chromium rich grown-on layer contained only $\simeq$ 4% of the activity so decontamination factors up to 35 were achieved. The vanadous picolinate LOMI reagent was compared with the TURCO 4521 process traditionally employed to decontaminate the Winfrith reactor. The results of parallel cleans of S21 riser samples are shown in Figure 7. The LOMI reagent used $\sim$ 0.1% concentration produced a more rapid and more complete decontamination than TURCO 4521 used at 6% concentration.

4.4 MATERIALS COMPATIBILITY

The vanadous picolinate reagent has been screened for compatibility with circuit materials. Because its oxide dissolving action is rapid, its concentration low and its redox potential close to the immunity region for iron dissolution, corrosion of circuit materials would be expected to be minimal. Corrosion tests have been summarised in Table 2. For most alloys uniform corrosion rates were too low to measure.

However, significant corrosion was found with AISI 410 and mild steel. In the case of AISI 410 corrosion rates in the LOMI reagent were at least an order of magnitude smaller than in 6% TURCO 4521, this alloy being well known for its corrosion sensitivity, Figure 8. Corrosion of mild steel (EN2) only occurs when the reducing capacity of the reagent has been exhausted, i.e. when all the V^{2+} has been converted to V^{3+}. At this stage a decontamination would normally be terminated, but if the reagent is left in the system, mild steel will corrode at a rate comparable to that in 6% TURCO 4521.

Incoloy 800, Inconel 600 and Zircaloy-2 were not corroded by the LOMI reagent. A small number of weld specimens have also been tested, including AISI 410/321,

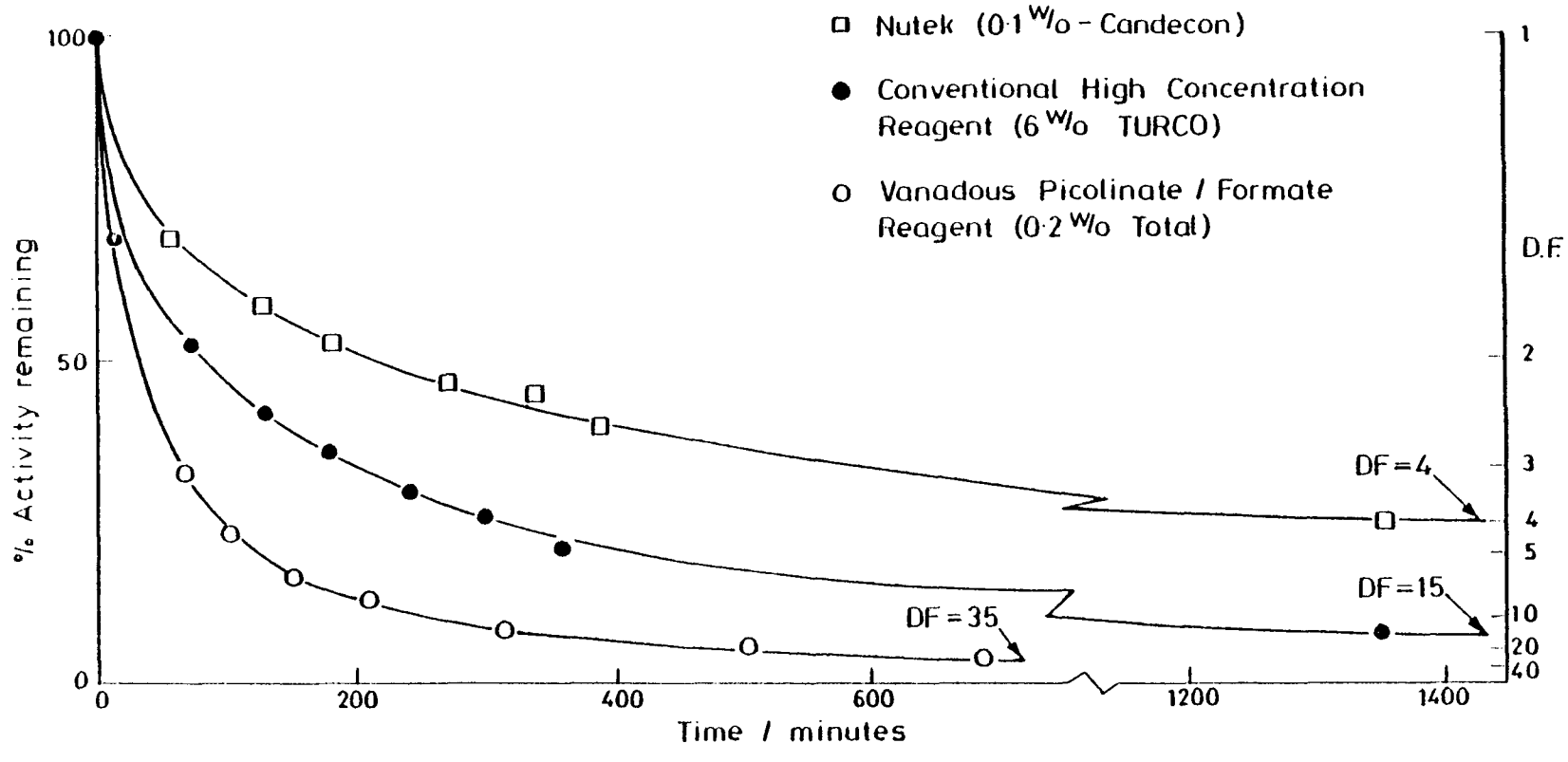

FIG. 7. Decontamination of AISI 321 Stainless Steel from WSGHWR S 21 Riser Pipework — Comparison of Vanadous Picolinate, 6% TURCO 4521 and 0·1% Nutek L106 (Candecon)

TABLE 2

Materials Corrosion in LOMI Reagents

Metal	Area/cm^2	wt. loss/mg	Penetration/μm	Rate μm/hr
AISI 410	10	13.9	1.5	0.47
	10	13.5	1.5	0.47
	10	19.0	2.1	0.66
EN 2 Carbon S	10	18.3	2.0	0.62*
	10	9.3	1.0	0.31*
	10	20.7	2.7	0.72*
AISI 321	10	0	0	0
	10	0	0	0
	10	0	0	0
AISI 304	10	0	0	0
Inconel 600	8	0	0	0
Incoloy 800	10	0	0	0
Zircaloy-2	11	0	0	0
AISI 321/410	-	0.1	0.01	0.002
AISI 321/EN 2 Weld	-	0.1	0.02	0.004

Conditions : $[V^{II}] \cong 2 \times 10^{-3}$ M (initially)

[Pic] 1.7×10^{-2} M

pH 5.0 - 5.3

Temperature 80°C

Run time 3.2 hour

*Corrosion of EN 2 occurs only when the V^{II} is exhausted; corrosion rate quoted is the average for the whole experiment.

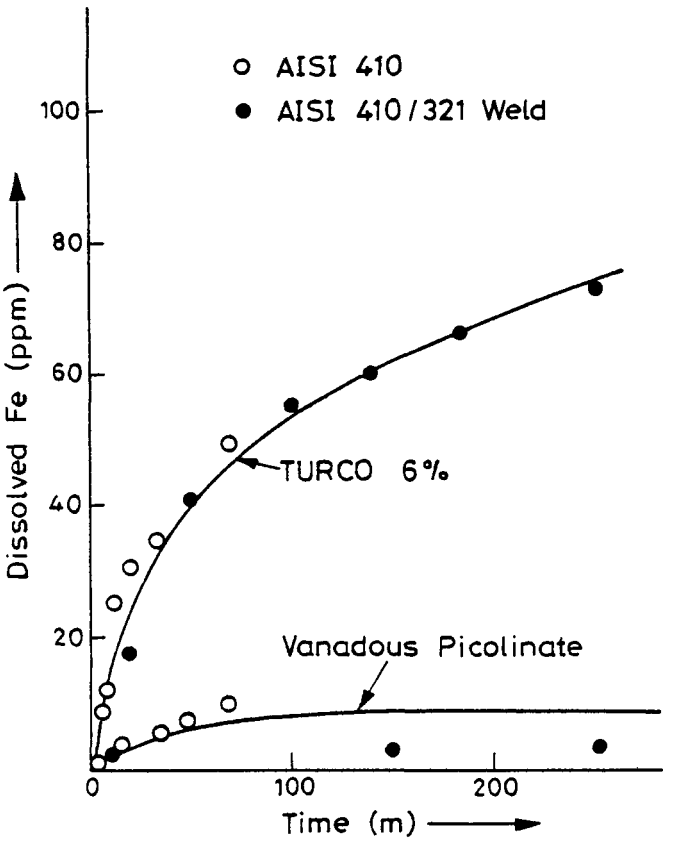

FIG. 8. Corrosion of AISI 410/321 Weld and AISI 410 Coupon in TURCO 4521 and Vanadous Picolinate. In Case of the Weld all the Corrosion was on AISI 410

AISI 321/316, AISI 316/316 and AISI 316/Mild Steel. Only in the case of mild steel was any corrosion detected and this took the form of slight pitting which, by analogy with the foregoing results, probably occurred in exhausted reagent. Again the corrosion was insignificant compared with what occurs in TURCO.

4.5 REAGENT PREPARATION AND REACTOR APPLICATION

Methods have been developed for the manufacture of reagents on a scale up to that necessary to clean the 40,000 kg primary half circuit of WSGHWR which involves the removal of 20 - 25 kg of iron oxide and its associated activity.

The LOMI reagent is air sensitive and its decomposition is catalysed by certain clean metal surfaces. For these reasons the circuit to be decontaminated must be degassed and the reagent stored in plastic or glass. The application method adopted for loop experiments will probably be suitable for reactor application. The circuit is first filled with a degassed solution of picolinic acid and alkali (to adjust pH) and circulated at $80^{o}C$. A concentrated solution of vanadous formate is then injected to achieve a final vanadium content equal to the amount of iron in the oxide to be dissolved. After circulation for a time sufficient to complete the decontamination the flow is diverted through a mixed ion-exchange bed which will remove both the reagents and the dissolved activity. The reagent is unaffected by the presence of boric acid which would be present in a PWR for reactivity control. If advantage is to be taken of radiolytic regeneration of the low oxidation state, a bleed of formic acid into the system may be required together with a method of removing the CO_2 reaction product.

The low oxidation-state chemical is not available "ex stock" and has to be manufactured shortly before the decontamination exercise. This is done by electrochemical reduction of a higher oxidation state. There are two possible routes for this preparation. One starts with vanadyl sulphate $VOSO_4$. This is electrolysed in the following cell :

$$- \text{ Pb Sheet}/VOSO_4 : H_2SO_4 \;//\; H_2SO_4 \;/\; \text{Pt gauze.}$$

This yields VSO_4 at concentrations upto 2M. The sulphate ion is then replaced by formate by anion exchange to yield $V^{2+}(HCOO^{-})_2$. The alternative route avoids anion exchange by electrolysing a slurry of V_2O_5 in formic acid in the cell :

$$- \text{ Pb Sheet}/V_2O_5 : \; HCOOH \;//\; HCOOH \;/\; \text{Graphite.}$$

This gives $V(HCOO)_2$ directly at concentrations up to 0.4M and avoids any possibility of contamination by sulphate. A schematic process flow sheet for a reactor decontamination is shown in Figure 9.

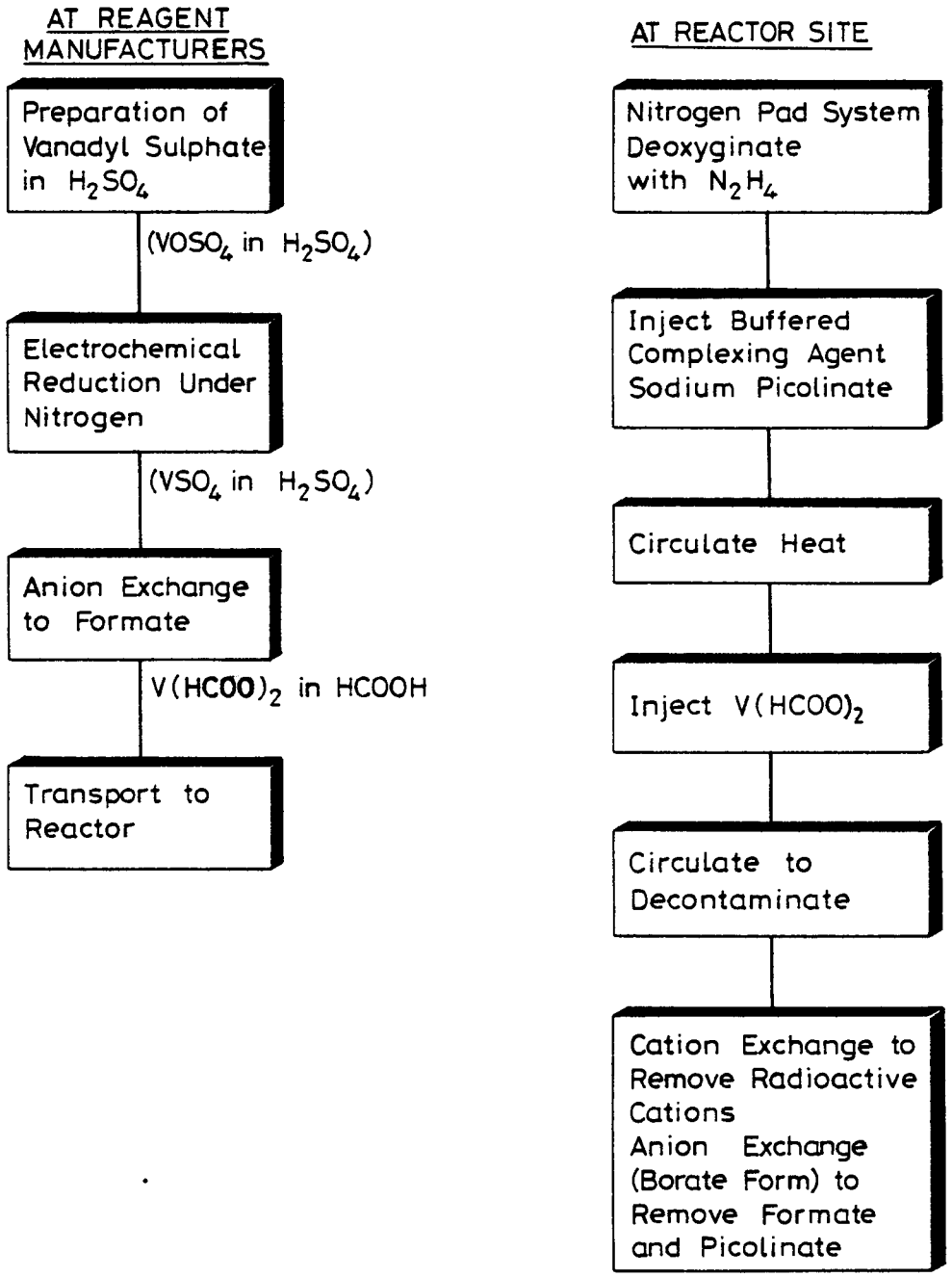

FIG. 9. Stages in Reactor Decontamination

Section 5

DISSOLUTION OF GROWN-ON OXIDE

At the inception of this project grown-on oxides were poorly characterised and only limited studies of their dissolution have been undertaken. More recent data shows that they contain a large proportion of Cr^{III} in the lattice. Although leaving this layer intact has advantages in that the base metal remains passivated, it will probably be necessary to dissolve this layer to achieve decontamination factors greater than 2 in a PWR.

As the proportion of Cr^{III} in the oxide increases, (and that of Fe^{III} falls), the vanadous picolinate reagent becomes less effective. This is because the redox potential of the V^{II}/V^{III} picolinic acid system is not low enough to reduce $Cr^{III} \rightarrow Cr^{II}$. To dissolve grown-on oxide there are two lines of development. One is to modify the reducing system so that the redox potential is adequate to reduce Cr^{III}. The other is to develop a low concentration oxidising system and to attack the oxide lattice by oxidising Cr^{III} to Cr^{VI}.

Experiments have been conducted with Cr_2O_3 (100% Cr^{III}) in an attempt to develop a reducing dissolving agent. Limited success has been achieved with LOMI reagents based on Cr^{II} EDTA. The reagents tend to be unstable and further developments are being pursued to find a metal ion/complexing agent pair which gives usable dissolution rates.

It is known that low concentration oxidising treatments based on acidic solutions of Mn^{VII} (acid MnO_4^-) are capable of dissolving some chromium-rich oxides. Later in the programme efforts will be made to identify other high oxidation-state metal ions (HOMI) which may be capable of dissolving grown-on oxide layers.

One of the most important aspects of future studies will be to obtain representative samples of grown-on oxides from water reactors so that they may be characterised, thereby allowing the reagent characteristics to be matched to the material whose removal is desired.

Section 6

DECONTAMINATION STATUS

The LOMI reagents based on V^{II} are capable of dissolving all the deposited oxides which have been found in LWRs. Dissolution is both complete and rapid leading to a minimal amount of suspended particulate in the fluid. The reagent has adequate radiolytic and thermal stability for whole circuit cleaning and is capable of radiolytic regeneration. A combination of short process times, low concentration and low redox potential result in good materials compatibility. Both the reagent and the radioactive isotopes can be cleaned up by ion exchange to give waste in a form convenient for disposal. In many BWR's the bulk of the circuit activity is contained in the deposited oxides and V^{II} LOMI reagents will therefore provide a good decontamination. BWR decontamination can also be achieved with dilute reagents such as modified Candecon and dilute oxalic acid. LOMI has the advantage over these methods of producing complete dissolution of crud (thereby avoiding problems of redeposition) and also of speed, very low base metal corrosion and radiolytic regeneration.

Out of core PWR crud contains a proportion of deposited oxides and the V^{II} picolinate reagent will dissolve these. However, PWR crud probably contains a higher proportion of chromium-rich grown-on oxide than does BWR crud. V^{II} picolinate based LOMI reagents become ineffective once the chromium content exceeds 20% because the reagent redox potential is too high to reduce Cr^{III}. It is therefore necessary to develop dilute decontamination techniques further in order to identify either a LOMI reagent which attacks Cr^{III} efficiently, or else a dilute oxidising treatment to convert Cr^{III} into Cr^{VI}. Ideally either process should be capable of ion exchange clean-up. Early investigations indicate that reagents based on Cr^{II} EDTA are capable of dissolving high-chromium cruds by a reductive mechanism and research on this aspect is continuing.

Section 7

CONCLUSIONS

7.1 A study of the types of oxide present in LWRs has identified two classes of material which exhibit significantly different dissolution chemistry.

7.2 The better characterised oxide is the loose deposited material which is found on fuel, in the coolant and as the outer layer on both PWR and BWR out of core surfaces. This decontamination reagent development program has concentrated on the dissolution of this material. Deposited oxide is the major contributor to dose in BWR and a significant contributor in PWR. In PWR a proportion of the activity is incorporated in the second oxide type which consists of a chromium-rich grown-on layer.

7.3 The dissolution of oxides by conventional reagents is not limited by inadequate thermodynamic solubility. The problem is one of kinetics and it is on this aspect of the dissolution process that the current research has concentrated. Reagents have been sought which provide rapid dissolution pathways. When a sufficiently rapid reagent is used its concentration can be reduced to be stoichiometrically equivalent to the quantity of oxide to be dissolved.

7.4 A detailed study of the dissolution chemistry of deposited oxide has lead to the development of efficient, low concentration decontaminating reagents based on reducing agents. The most rapid dissolution was obtained with low oxidation state metal ion (LOMI) reductants and these were found to dissolve deposited oxides at rates up to four orders of magnitude faster than conventional reagents, such as citrox, even when the latter was present at 100 times the concentration.

7.5 The radiation and thermal stability of LOMI reagents is adequate. Indeed the present preferred reagent vanadous picolinate/formate is regenerated by a radiation field.

7.6 Corrosion of the major LWR circuit materials by vanadous picolinate/formate is negligible, as would be expected for a reducing system.

7.7 The LOMI reagent, vanadous picolinate/formate, produces a solution containing radio-isotopes and spent reagent in a form which is readily treated by ion exchange to yield a compact solid waste.

7.8 Vanadous picolinate formate is suitable for the rapid decontamination of BWRs with negligible circuit corrosion and convenient waste handling. Partial decontamination of PWR is also practical.

7.9 LOMI reagents are being developed further to provide a system which will also dissolve the high-chromium, grown-on layers which are more important contributors to dose in PWR chemistry.

Section 8

REFERENCES

1) Ayres, J.A., 1970. Decontamination of Nuclear Reactors and Equipment. J.A. Ayres, Ed. The Ronald Press Co., N.Y.

2) Johnson, A.B., Griggs, B. and Dillon, R.L., 1979, Candidate Reagents for Activity Reduction in BWR and PWR Primary Systems. ANS Conf. on Decontamination and Decommissioning of Nuclear Facilities, Sun Valley, ID., Sept., 1979.

3) Pettit, P.J., 1974. Decontamination of CANDU Primary Coolant System, AECL 5113.

4) Romeo, G., 1978. Characterisation of Corrosion Products on Recirculation and Bypass Lines at Millstone-1. EPRI Report NP 949.

5) Shaw, R.A., Naughton, M.D. and Miller, A.D., 1979. Radiation Exposure, Radiation Control and Decontamination. ANS Conference on Decontamination and Decommissioning of Nuclear Facilities, Sun Valley, ID., Sept., 1979.

6) Sandler, Y.L., 1978. Structure and Solubility of PWR Primary Circuit Corrosion Products, Corrosion 78, Paper No. 158, Houston, U.S.A.

CONTENTS OF APPENDIXES

APPENDIX A1

1.0 THEORETICAL CONSIDERATIONS

The ultimate aim of this study is the development of a reagent system capable of rapidly dissolving active crud from LWR primary circuits, ideally at a concentration much lower than that required for the reagents in current use for decontamination and steam generator cleaning. Low concentrations of reagents are very desirable (i) for the ease of introduction into the reactor circuit and (ii) for the ease of treatment of the resulting, active, waste water. The latter is the most serious consideration. If the reagent dissolves oxide rapidly, then only stoichiometric quantities will be required.

We have therefore undertaken an investigation of the fundamental chemistry of oxide dissolution, to determine what properties are important in determining the ability of a reagent or system to dissolve oxides at an appreciable rate. We have studied the rate of dissolution in a series of experiments in which the nature of the oxide, the reagents used to dissolve it, and the conditions of reaction were all varied. Most of the oxides used were prepared specifically for this study, and include magnetite (Fe_3O_4), haematite (Fe_2O_3), nickel ferrite ($NiFe_2O_4$) and a chromium-containing "synthetic crud" ($Ni_{0.6}Cr_{0.15}Fe_{2.25}O_4$). Reagents included acids, chelating agents (e.g. EDTA) and reducing agents, and the conditions varied were pH, temperature and concentration.

A secondary part of this study has been to investigate the radiation chemistry of candidate reagents. High-intensity γ- and pulse radiolysis have been used to investigate the stability of several reagents to radiation. Clearly the system chosen for reactor decontamination must not degrade too rapidly in the fields encountered in primary circuits.

Important aspects of the complete project which do not primarily fall within the scope of this study are : (i) corrosion studies - reagents used must not materially corrode or weaken the structure of a LWR circuit and (ii) testing of reagents on actual LWR materials - although we have carried out a few experiments on samples of corroded steel. It is the intention that the most promising reagents will be

TABLE A1

Water Reactor Oxide Types and Composition

Cation % \ Oxide	FeO.OH Goethite	Fe_2O_3 Haematite	Fe_3O_4 Magnetite	Fe_2NiO_4 Nickel Ferrite	NiO Nickel Oxide	$Fe_{3-x-y}Ni_xCr_yO_4$ Mixed Ferrite	$FeCr_2O_4$ Iron Chromite	$NiCr_2O_4$ Nickel Chromite	Cr_2O_3 Chromia
Fe^{2+}	0	0	33.3	0	0	$\frac{1-x}{3} \times 100$	33.3	0	0
Fe^{3+}	100	100	66.6	66.6	0	$\frac{2-y}{3} \times 100$	0	0	0
Ni^{2+}	0	0	0	33.3	100	$\frac{x}{3} \times 100$	0	33.3	0
Cr^{3+}	0	0	0	0	0	$\frac{y}{3} \times 100$	66.6	66.6	100
	Deposited Oxide					$y<1$	$y>1$	Grown-On Oxide	

tested on LWR tubing samples in the once through test facility (OTTF) at Battelle Pacific North West Laboratory as part of a separate EPRI contract.

1.1 APPROACH

The major metallic component of all the oxides under consideration is iron. Although high-nickel alloys are used in the primary circuit of PWRs, the deposited crud found in such reactors is generally an Fe/Ni/Cr spinel containing roughly $Fe_{2.26}Ni_{0.6}Cr_{0.14}O_4$ (Sandler 1978); the activity is mostly due to chemically insignificant amounts of Co-60. Even under the completely reducing conditions of a PWR primary circuit, the iron is mostly in the +3 oxidation state. The ionic composition of the major oxides of interest is set out in Table A1 where it is seen that Fe^{3+} is also the major species formed by oxidation of stainless steels, where Fe_3O_4, not FeO, predominates.

There is considerable evidence that oxides of Fe(III) can be made to dissolve by a process of reduction, which releases the iron into solution as Fe(II). Pryor and Evans (1950) and Rantell, Jones and Furlong (1976) have shown that the base metal can perform this reduction, being itself corroded by the overall reaction

$$Fe^{o} + 2Fe^{III} \rightarrow 3Fe^{II}$$

Valverde (1978) found that the dissolution rates of haematite and magnetite increased as the solution redox potential became more negative (i.e. reducing). Bradbury (1977) investigated the dissolution of haematite in the presence of a variety of reducing agents and found that the rate increased in the order oxalic acid ($E_{SHE} = -0.49$) < thioglycollic acid ($E_{SHE} = -0.23$) << sodium dithionite ($E_{SHE} = -1.40$). Here the rate did not follow the redox potential exactly and it appears that the reduction mechanism, and hence the reaction kinetics, is important, the single-electron reducing agents being the most rapid. Pitzer (1961) and Margulova (1965) also report increased oxide dissolution in the presence of reducing agents.

Previous work in the field of decontamination has centred on the use of strong chelating ligands (EDTA, citrate, etc.) which increase the thermodynamic solubility of metal ions enormously. That dissolution rates with these reagents are often modest (Johnson et al., 1978) is further evidence that it is the kinetics and mechanism of the reaction which are important and that little is to be gained by further increases in thermodynamic solubility.

For the above reasons the present study has concentrated on the kinetics and mechanisms of oxide dissolution by reducing agents. It is convenient if the reducing agent is well characterised when investigating the mechanism by which it dissolves oxides and we have therefore worked with reagents which have been the subject of previous studies in solution redox chemistry. This field embraces a considerable body of literature with well established principles to guide the experiments. In particular, electron-transfer reactions between metal ions in solution, often including Fe(III), have been extensively studied. We have drawn on our knowledge of this field in the choice of reagents for investigation, and in the interpretation of results.

In this Appendix we shall present the solution redox chemistry background in some detail, as it is a considerable help in explaining the work presented. This is followed by the main body of the experimental work, with an exposition of the experimental methods used for the preparation and dissolution of oxides, (Appendix 2), and discussion of the results obtained from these experiments, (Appendix 3). We draw preliminary conclusions from these results as to what sort of reagent system in general, and which reagents in particular, are likely to be the most suitable for decontamination work, having regard to the rate of dissolution of the appropriate oxide types under suitable conditions for reactor use. The radiation chemistry of certain of these systems is then presented, (Appendix 4), and the implications for a reactor clean discussed. This is followed by a general discussion on the applicability of these laboratory results to a full-scale reactor system (Appendix 5).

1.2 BACKGROUND TO THE REACTIONS AND REAGENTS

1.2.1 Electron-transfer Reactions in Solution

Since this report is concerned largely with reductions of iron(III) to iron(II), we shall discuss the reactions of these ions in solution: many studies have been made of such reactions, although cobalt(III) has been the most popular subejct of kinetic investigation by solution chemists.

When iron(III) is reduced by another metal ion in a low oxidation state, such as chromium(II), we can consider two possible mechanisms.

a) Inner sphere, in which the two ions are bound together by the co-ordination of a ligand to both metals. In the reduction of Fe^{III} by

Cr^{II} in dilute HCl, for example, the major pathway involves the following sequence (Taube and Myers, 1954; Dulz and Sutin, 1964) :

$$Fe^{3+} + Cl^{-} \rightleftharpoons FeCl^{2+}$$

$$FeCl^{2+} + Cr^{2+} \rightleftharpoons [Fe^{III} - Cl - Cr^{II}]^{4+} \quad (1)$$

$$[Fe^{III} - Cl - Cr^{II}]^{4+} \rightleftharpoons [Fe^{II} - Cl - Cr^{III}]^{4+} \quad (2)$$

$$[Fe^{II} - Cl - Cr^{III}]^{4+} \longrightarrow Fe^{2+} + CrCl^{2+} \quad (3)$$

In this reaction, we say that chloride is the bridging ligand, the intermediate (1) is the precursor complex, and the immediate product of the electron-transfer step is the successor complex (2), which breaks up to form the primary reaction products. These may subsequently undergo further reactions such as hydrolysis. The factors controlling the observed rate of reactions are the stability of the precursor complex and the rate of the electron transfer itself, since we can treat the system as a pre-equilibrium followed by rate-determining electron transfer. In a few cases, principally when the reductant is V^{II} (see below), the rate-determining step is the formation of the precursor complex, in which case the rate of the actual reduction step is not measurable.

b) Outer sphere, in which there is no binding of the two metal ions together. This will occur (i) if no suitable bridging ligand is present, (ii) if electron transfer can take place more rapidly than the formation of a bridged intermediate, or (iii) if one or both of the ions is very strongly bound by other ligands which prevent binding of the bridging ligand. An example of the third category is the reduction of the phenanthroline complex $Fe(phen)_3^{3+}$ by Mn^{III}, (Diebler and Sutin, 1964).

When the reducing agent is not another metal ion, the possibility exists of direct binding of reductant to oxidant. For example, thioglycollic acid reduces Fe^{III} in solution, via an intermediate complex (Lappin and McAuley, 1975) :

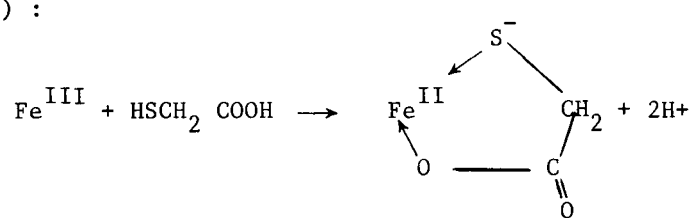

Hydroquinone also reduces ferric ions, as it easily undergoes one-electron reactions, but no intermediate complex is formed (Baxendale et al., 1951). This is therefore an outer-sphere reaction.

A number of theoretical treatments of outer-sphere reactions have been published, but inner-sphere ones are not susceptible to a general theoretical approach (see e.g. Basolo and Pearson, 1967, p. 454-466). The theory of Marcus (1969) has received the most attention, and in general the equations derived by him have been in good agreement with experimental results. There are three basic terms contributing to the activation energy of an outer-sphere reaction: (i) the energy required to bring the reagents together before reaction, (ii) the re-arrangement of the co-ordination shells of the ions to the configuration required for electron transfer (the Frank-Condon barrier), which is a result of the slow movement of atoms compared with electrons, and (iii) the overall free energy change of reaction. In the special case where (i) and (ii) are essentially constant, which occurs only in very similar complexes, Marcus theory predicts a linear relation between the free energy of activation ($\Delta G^{\ddagger}$) and the overall thermodynamic free energy (ΔG^{o}), with a slope of one-half. Alternatively, when two different reducing agents are reacted with a series of oxidants, a linear free-energy relation with a slope of unity is predicted. Many such relations have been found experimentally, though the slope does not always agree with the predicted value.

With inner-sphere processes, a great many studies have been made with a variety of metal ions (e.g. Taube 1970; Sykes, 1967). Although a theoretical prediction of reaction rates is not possible, there is now a general understanding of the factors which determine reaction rates and the features which affect the ability of an ion or molecule to act as an inner-sphere bridging ligand. The work of Gould, in particular, on organic ligands has been most illuminating (e.g. Taube and Gould, 1969). Nevertheless, there are important questions still to be answered in this field; it is not yet clear for instance, why the "normal" order of reactivity of halide complexes is I > Br > Cl > F, but with a few systems the order is reversed.

1.2.2 Reagents Used

Our work has concentrated largely on the use of two metals, chromium and vanadium. In the +2 oxidation state, both are strong one-electron reducing

agents, and their reactions with a wide variety of oxidants have been studied. This section contains a brief outline of the solution chemistry of these two metal ions, and the products formed on oxidation, with special regard to the features affecting their role as reducing agents.

(a) Chromium. The aqueous ion, Cr^{2+}, is six-coordinate, with a high-spin d^4 electronic configuration. This means that three of the 3d electrons are in the lower-energy, non-bonding t_{2g} orbitals, and the fourth is in a higher-energy, anti-bonding e_g orbital. The redox potential of the $Cr^{2+/3+}$ couple is -0.41 V, which means it is a very strong reducing agent, thermodynamically capable of reducing water at pH < 7. Fortunately, the rate of this reaction is immeasurably slow. There are two important consequences of the electronic configuration: (i) the ion is very labile to substitution, which allows the very rapid exchange of ligands, and hence rapid formation of bridged intermediates in inner-sphere reactions, and (ii) there is a very high Franck-Condon barrier to electron transfer, arising from the fact that the electron to be transferred is in an anti-bonding orbital and therefore strongly influences the bond lengths of the complex. Thus the major features of the redox chemistry of the aqueous Cr^{2+} ion are a strong tendency to inner-sphere mechanisms where possible, and only slow outer-sphere reactions where no inner-sphere pathway is available. The product, chromium(III), is also generally octahedral, and has only three d-electrons, which must therefore occupy singly the t_{2g} orbitals. This leads to great stability of complex with respect to substitution. Thus the product of an inner-sphere process (e.g. $CrCl^{2+}$ in the example given in reaction 3 above) can be readily isolated and identified.

Like other highly-charged metal ions, Cr^{3+} is not stable in solution except in acid. The hydroxide precipitates when the pH is raised much above 3. We therefore consider the use of ligands which form complexes stable in solutions at higher pH levels. To prevent participation of $Cr(OH)_3$ and related species, strong complexing is required, and so we use chelating ligands with two or more groups binding to the metal ion. There is, however, one drawback to the use of ligands which form very strong complexes with Cr(III): unless they bind to Cr(II) as strongly as to the oxidised form, the electrode potential of the complex is even more negative, and reduction of water can become a problem, especially at elevated temperature. This

occurs with EDTA, for example, where for Cr(III) log K ≃ 23, while for Cr(II) log K = 13.6, giving an electrode potential of about -1 volt; the Cr(II) complex is stable in water only for minutes at room temperature (Pecsok et al., 1964). Other ligands of the same type, with high negative charge and many oxygen donor atoms, also stabilise the higher oxidation state. Thus citrate, for example, which gives a redox potential of approximately - 0.8 V for the Cr(II)/Cr(III) couple (Pecsok and Lingane, 1950) is also rather unstable.

The ligand most suitable for our purpose appeared to be 2,2'-bipyridyl:

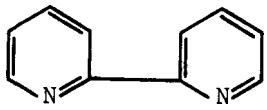

As a neutral, N-donor ligand, this does not cause the problems discussed above; in fact, it stabilises the lower +2 oxidation state because it is a π-acceptor, that is a ligand which binds not only by the donation of electrons from the donor atoms to the metal ion but also by the back-donation of electron density from occupied metal d-orbitals. This raises the redox potential of the $[Cr(bipy)_3]^{2+/3+}$ couple to -0.26 V (Baker and Melita, 1965). However, the π-acceptor nature of the ligand also changes the electronic structure of the Cr(II) from high- to low-spin, resulting in a lowering of the Franck-Condon barrier to electron transfer. Delocalisation of the electron density over the aromatic bond system of the ligands also helps to make the complex a very rapid outer-sphere reducing agent (Zwickel and Taube, 1960; Candlin et al., 1964; Beattie and Basolo, 1967).

(b) Vanadium. The V^{2+} ion is also octahedral in aqueous solution. The d^3 electronic structure makes this ion a more rapid reducing agent for outer-sphere reactions than Cr^{2+}, although it is a weaker reductant thermodynamically (E^o = -0.255 V). Generally V^{2+} is some fifty times faster than Cr^{2+} when both reactions are outer-sphere (Toppen and Linck, 1971). In inner-sphere reactions, however, the rate is limited by the rate of formation of the precursor complex,

since V(II) is rather inert to substitution, as it is iso-electronic with Cr(III). Inner-sphere reactions of V^{II} are generally recognisable by the fact that their rates and activation parameters lie within a narrow range, typical of substitution reactions of this ion. The product of one-electron oxidation, V(III) is more labile to substitution, so the mechanism cannot usually be determined by examination of the products.

Unlike Cr(III), V(III) acts as a reducing agent, and the oxidation to V(IV) is observed with mild oxidants. Thus V^{3+} or complexes of this ion can also be used as reducing agents, or the V(II) may act as a two-electron reductant. This may occur in a single step, e.g. $V^{2+} \rightarrow VO^{2+} + 2e$, but successive one-electron steps are more usual in solution chemistry (e.g. Basolo and Pearson, 1967, p. 473).

As with chromium, chelating ligands are required to prevent the precipitation of vanadium(III) hydroxide at pH values above 3. With ligands such as EDTA, the higher oxidation state is greatly stabilised with respect to the lower, and again the problem of water reduction arises (Schwarzenbach and Sandera, 1953). We have also found that addition of citrate to V^{II} solutions yields complexes of V(III). Bipyridyl forms a stable complex with V(II); the stability constants for the ion $V(bipy)_3^{2+}$ have been measured (Crabtree et al, 1961) and a few electron-transfer reactions studied (Bennett and Taube, 1968). As this ligand raises the electrode potential of the V(II)/V(III) couple considerably, this is a slower reducing agent than $Cr(bipy)_3^{2+}$ in solution reactions. Unfortunately, the vanadium(III) complex is not very stable, and this ligand does not prevent the precipitation of V(III) hydroxide at elevated pH. We have found that a mixture of bipyridyl and citrate is satisfactory: the former binds strongly to V^{2+}, while the latter binds to the V^{3+} product and keeps it in solution. The requirement for a ligand capable of binding to vanadium in either oxidation state is met by picolinate, which

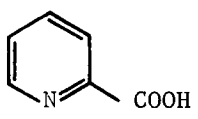

combines the features required for strong binding to both V^{2+} and V^{3+}. The overall stability constants for complexation are log β_3 = 12.8

and log β_3 = 15.4 respectively, where :

$$\beta_3 = \frac{[ML_3]}{[M]\,[L^-]^3} \qquad M = V^{2+},\ V^{3+},\ L = \text{picolinic acid.}$$

(Mercier and Paris, 1964; Mercier, Bonnet and Paris, 1965). From these stability constants we can calculate an electrode potential of -0.41 V for the couple. By Marcus theory, this would make the complex $V(pic)_3^-$ around ten to a hundred times faster than V^{2+} in outer-sphere electron-transfer reactions, if the ligand has no other major effects on the metal ion. Unfortunately no such reactions have been studied until now to confirm this prediction.

A number of other chelating ligands containing similar nitrogen and/or oxygen donor groups have also been tested with V^{II}. The vanadous complexes were screened for rate of reaction with oxides, and rate of oxidation by water. According to these criteria, no ligand tested is significantly better than picolinate. These tests are reported in Appendix 3.4.

(c) $Fe^{II}(EDTA)^{2-}$. The stabilisation of the +3 oxidation state, which creates difficulties in the use of EDTA with Cr^{II} or V^{II}, turns the Fe^{II} into a good reducing agent (E^o = -0.12V) (Phillips and Williams, 1966). The chemistry of the complex is complicated by hydroxide binding and/or dimer formation, depending on pH, but it can be used as an outer-sphere reducing agent in solution. The very great lowering of redox potential results in its rapid oxidation by air.

1.2.3 Counter Ions

Clearly, whenever an ionic reagent is used, some ion of opposite charge must also be present. Lithium or sodium are the most commonly used cations in the laboratory, as they rarely interfere in reactions, and perchlorate (ClO_4^-) is the most commonly used anion. The latter is one of the few readily available anions that only complexes metal ions very weakly, if at all. Unfortunately, it is a strong oxidising agent, although this is rarely a problem as it generally reacts only very slowly. For example, $V(ClO_4)_2$ solutions decay slowly at room temperature over a few weeks, even in quite strong solutions (e.g. $[ClO_4^-] > 1$ M) and Cr^{2+} lasts for months under the same conditions. At high temperatures, however, we have found ClO_4^- reduction to be a problem with

some of the reactive reducing agents under consideration. Sulphate is a satisfactory substitute for laboratory work, but it does form a complex with V^{3+}. In the presence of strong complexing agents this is not significant. For use in a reactor, however, sulphur-containing anions are ruled out by the risk of materials corrosion, as are halides. An obvious choice of a common, non-aggressive anion is acetate; this was used as the buffer in many experiments. For buffering at lower pH (i.e. 4 - 4.5) formate was used, and this is greatly favoured as a result of its radiation chemistry (see Appendix 4). The manufacture of vanadous formate, free of aggressive anions, is discussed in Appendix 5.2.

APPENDIX A2

2.0 EXPERIMENTAL

2.1 REAGENTS

Stock solutions of Cr^{3+} were prepared either direct from commercial salts (sulphate) or by reduction of CrO_3 with H_2O_2 in acid (perchlorate). Electrolytic reduction was carried out in a cell shown in Figure A1. Typical conditions were 70 mls. of 0.8 M Cr^{3+} in ca.1 M $HClO_4$, with 1 M $HClO_4$ in the anode compartment, electrolysed at 10 V, 1 Amp for 5 hours. $VOSO_4$ was either dissolved directly in H_2SO_4, or, to obtain perchlorate solution, loaded onto a cation-exchange column (Amberlite IR 120 H), washed with water and eluted with 2 M $HClO_4$. These solutions were reduced, typically at 6 V, 0.5 A, with $[VO^{2+}] \sim 0.2$ M in 1 N acid. Solutions of V^{3+} were prepared by the reaction of equimolar amounts of V^{2+} and VO^{2+} under Argon.

Solutions of Cr^{2+} were analysed for total [Cr] by oxidation in alkaline H_2O_2 and spectrophotometric determination of CrO_4^{2-} at 372 nm (ε = 4.82×10^3 M^{-1} cm^{-1}).

Residual Cr^{3+} was determined directly from spectrophotometric measurement of the stock at 408 nm (ε = 14.8), and hence $[Cr^{2+}]$ found. Total anion concentration and hence $[H^+]$, was found by loading 1 ml aliquots on a cation-exchange column in the H^+ form, washing with water, and titrating the released protons vs. NaOH. For V^{2+} solutions, total [V] was determined as the peroxo-vanadium(V) complex (ε_{450} = 281, ε_{400} = 205); V^{3+} in the reduced stock directly at 400 nm (ε = 8.3, $\varepsilon(V^{2+})$ = 0.9), and $[H^+]$ as above.

2.2 PREPARATION OF FERRITES

The object of the ferrite preparation portion of the programme was to prepare a set of nickel ferrites with a variety of iron-to-nickel ratios, and a further requirement was to produce a ferrite bearing a small proportion of chromium similar in composition to PWR crud.

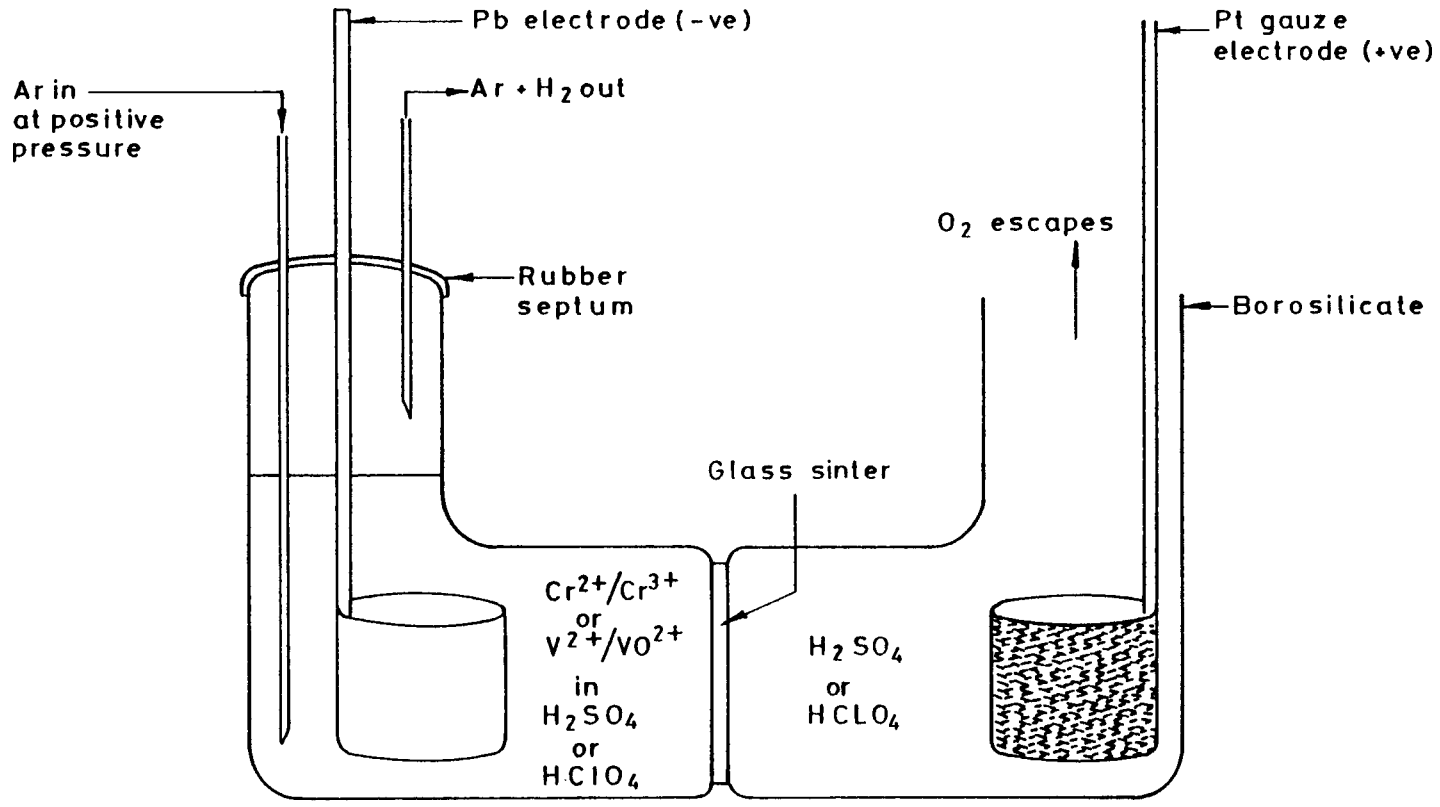

FIG.A1. Electrochemical Cell for the Reduction of Cr^{3+} and VO^{2+} on a Laboratory Scale

The iron/nickel ratios chosen were as shown below, intended to cover the majority of PWR oxide compositions (Sandler, 1978).

	Fe	Ni	Cr	O
1	2.6	0.4	0	4
2	2.4	0.6	0	4
3	2.2	0.8	0	4
4	2.0	1.0	0	4
5	2.25	0.6	0.15	4

2.2.1 Nickel Ferrites

The simplest method available in the literature was the oxalate method (Wickham, 1967). In this method ferrous and nickel acetates are precipitated with oxalic acid to give a combined ferrous nickel oxalate precipitate. Although the method was not reported to give non-stoichiometric precipitates there seemed to be no reason why this should not be possible. Indeed, no iron or nickel was detected in the filtrate when non-stoichiometric iron:nickel ratios were used. Ratios 1 - 4 above were prepared by this method. Unfortunately, the method is not suitable for preparing chromium-bearing ferrites since it relies on each of the elements having an insoluble oxalate salt. The oxalate precipitate once prepared and filtered was washed, dried and calcined. In the calcining stage the oxalates lose CO_2 and CO to give the appropriate ferrite.

$$2Fe\ (COO)_2 + Ni\ (COO)_2 \xrightarrow{heat} NiFe_2O_4 + 2CO + CO_2$$

The most useful analytical technique applicable to the ferrite was I.R. spectroscopy (Sandler, 1978) Figure A2. From the spectrum it was possible to deduce the presence of ferrite, and any impurities showed clearly as extra bands in the region 470 cm^{-1}. Sandler (1978) states that a band at 470 cm^{-1} is due to the presence of NiO in the sample. In the stoichiometric sample ($NiFe_2O_4$) it was found that a good ferrite spectrum was obtained after calcining at 1,000°C. As the proportion of nickel was lowered, however, the samples showed an increasing absorption at 470 cm^{-1}. This seemed inconsistent with the presence of NiO, which would be expected to be stronger in the 'higher nickel' samples. Furthermore, examination of spectra of NiO and Fe_2O_3 suggested that the band in the ferrite samples was closer (λ_{max}) to Fe_2O_3 than NiO, though the difference in wavelength is rather small (about 15 cm^{-1}). Further confirmation came from examination of X-ray diffraction patterns (Figure A3) which showed a

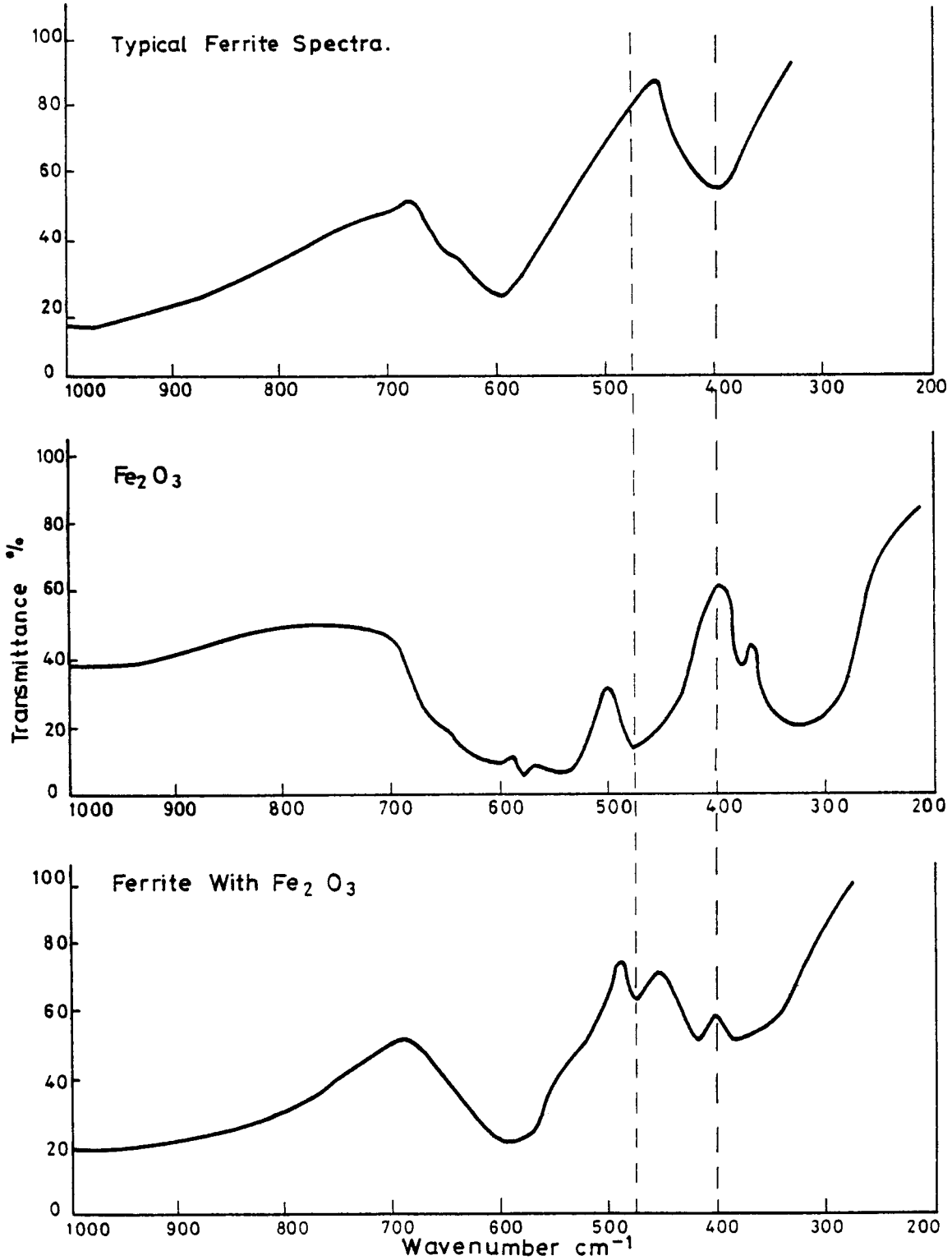

FIG. A2. Nickel Ferrite and Haematite Infra-red Spectra

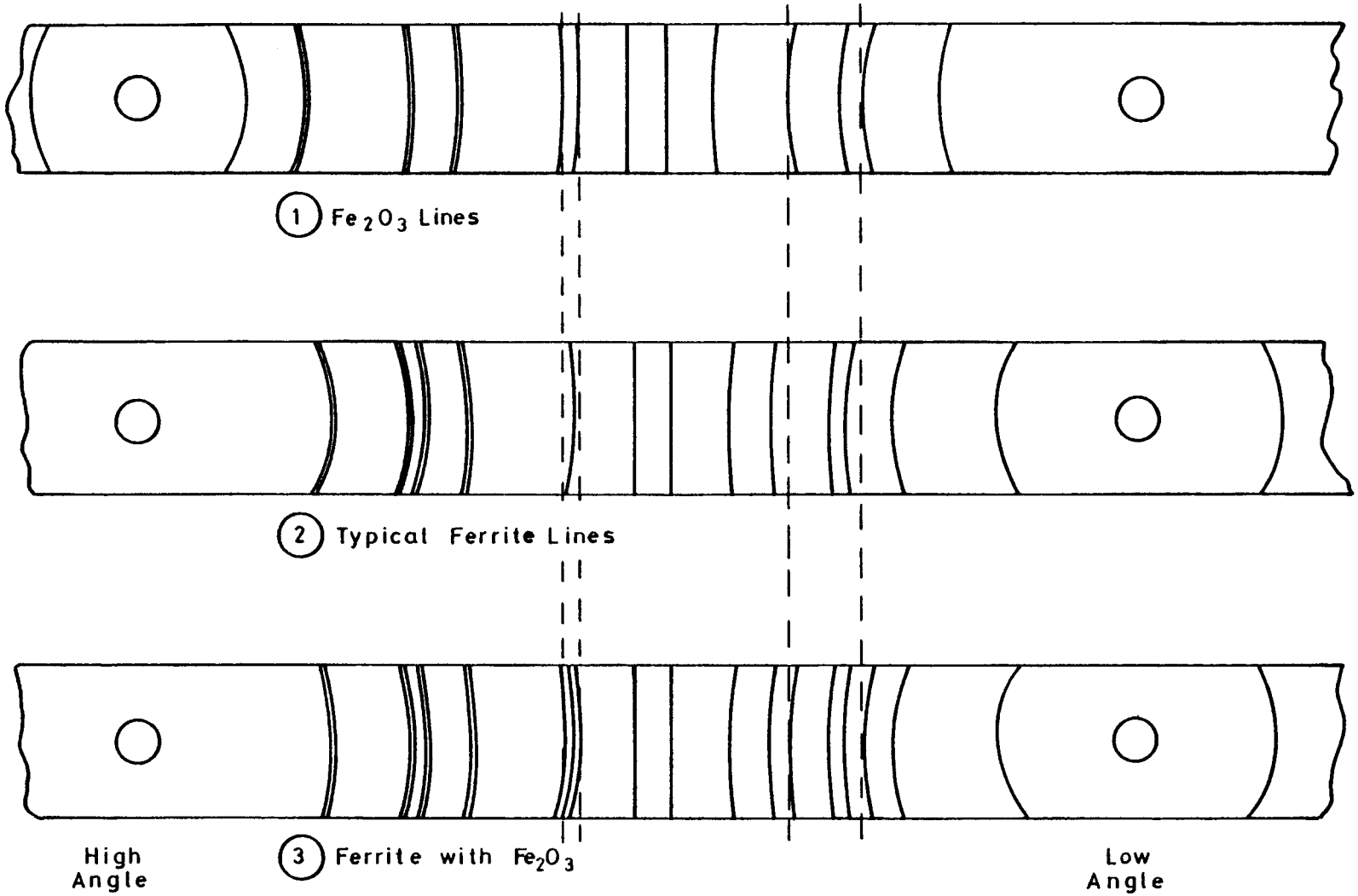

FIG. A3. Nickel Ferrite / Fe_2O_3 X-ray Diffraction Lines

correlation between lines ascribable to Fe_2O_3 in samples with the extra 470 cm^{-1} band. In samples where the band was absent, only ferrite X-ray diffraction lines were observed. It thus seems more likely that the non-stoichiometric samples had a higher oxygen content that the true ferrite, leading to a micro-inclusion of Fe_2O_3 within the sample.

Energy dispersive X-ray analysis of individual particles indicated little variation of Fe/Ni ratio between one particle and another in a given ferrite sample, within the experimental accuracy of the technique ($\sim \pm$ 10%).

The calcining of the sample is very important, since at very high temperatures (1400°C) the true ferrite stoichiometry is the stable phase in air, but at lower temperatures higher oxygen content is possible. Higher temperatures lead to excessive sintering of the sample, and a balance has to be struck between obtaining a representative surface area and proper stoichiometry.

Because of the inability of the oxalate method to produce a chromium-bearing ferrite, an alternative route was also developed. This involved the precipitation of iron, nickel and chromium hydroxides (Sandler and Kunig, 1977). In order to compare the ferrites from the two sources, a full range of stoichiometries was prepared by the second method.

The required amounts of iron, nickel and chromium nitrates were dissolved in 0.1 N nitric acid, and a solution containing an equivalent amount of sodium carbonate was added slowly. Immediately a thick brown precipitate of iron/nickel/chromium hydroxide was formed

$$Fe(NO_3)_3 + 3Na_2CO_3 + 3H_2O \rightarrow Fe(OH)_3 + 3NaNO_3 + 3NaHCO_3$$

The precipitate was very fine, making it difficult to filter. A coarser precipitate was formed by heating the two solutions to near boiling before adding the carbonate solution. The precipitate was washed free of sodium until the filtrate from washing was found to contain less sodium than 0.05% of the amount of iron, nickel and chromium originally added. The precipitate was then dried at 120°C for 48 hours before being calcined.

A sample of material produced by this method was calcined for 6 hours at 1000°C and analysed by IR spectrometry. It was found to contain the

TABLE A2

Surface Area and Calcining Histories of Metal Oxide Samples

Oxide	Method of prep-aration	Calcining History	Size/μm (by Sieving)	Specific Surface Area/$m^2\ g^{-1}$
Fe_2O_3	$FeCl_3$+OH^-	4h at 350°C	<150	37
"	a	800°C	<150	6.7
Fe_3O_4	a	?	?	7.4
$NiFe_2O_4$	Oxalate	6h at 1000°C	<150	1.2
"	Carbonate	6h at 1400°C	< 53	0.14
"	Carbonate	6h at 1400°C	53 - 75	ca 0.08
"	Carbonate	6h at 1400°C	75 - 106	<0.04
$Ni_{0.4}Fe_{2.6}O_4$	Carbonate	6h at 1400°C	<150	0.11
$Ni_{0.6}Fe_{2.4}O_4$	Carbonate	6h at 1400°C	< 53	0.45
$Ni_{0.6}Fe_{2.4}O_4$	Carbonate	6h at 1400°C	53 - 150	0.04
$Ni_{0.8}Fe_{2.2}O_4$	Carbonate	6h at 1400°C	<150	0.10
$Ni_{0.6}Cr_{0.15}Fe_{2.25}O_4$	Carbonate	6h at 1400°C	<150	0.06
$CoFe_2O_4$	b	?	< 53	0.44
"	b	?	53 - 150	0.24

a) Commercial material obtained from 'British Drug Houses'.

b) Commercial material obtained from Ventron.

Fe_2O_3 absorption lines found in the specimens prepared by the oxalate method. In an attempt to get rid of this Fe_2O_3, the sample was recalcined at 1400°C for a further 6 hours, which resulted in little improvement. More tests were done on other specimens by varying the time at full temperature but again little effect was noted. It appeared that whilst Fe_2O_3 was probably being destroyed on heating, it was reformed on cooling in air. A sample was calcined for 6 hours at 1400°C and cooled to laboratory temperature under a steady stream of argon. When analysed by IR spectrometry, it was found that this specimen gave a clean ferrite spectrum and the absence of Fe_2O_3 was confirmed by X-ray diffraction. This calcining procedure was used subsequently for all samples produced by this method.

Before carrying out a particle size analysis, samples were ground and sieved with a 100 mesh sieve (150 μm). The resulting distributions are shown in Figures A4 and A5.

Sandler has shown that the lattice parameter of non-stoichiometric nickel ferrite varies as an almost linear function of composition from Fe_3O_4 through to $NiFe_2O_4$ and this was used to check the composition of the specimen.

Lattice parameters were measured by X-ray diffraction using a Debye-Scherrer powder camera and chromium characteristic radiation. ($K_{\alpha 1}$ = 2.28962 Å, $K_{\alpha 2}$ = 2.29351 Å, weighted average = 2.29092 Å.) The results of these measurements, Figure A6, show a relationship similar to that obtained by Sandler (1978).

All samples were examined in a scanning electron microscope fitted with Kevex analysis facility to check the homogeneity of the specimens and their geometry. The particles were more or less spherical in shape, and in a number of cases showed distinct stepped structures on their surfaces. Some typical micrographs are shown in Figure A7.

The surface areas of the samples were measured using a Perkin-Elmer type 212D Sorptometer by the BET single point method, and are summarised in Table A2. With material calcined at 1400°C the values are close to the theoretical geometric surface areas calculated on the basis of particle sizes as determined by sieving or using a Coulter counter. Some increase

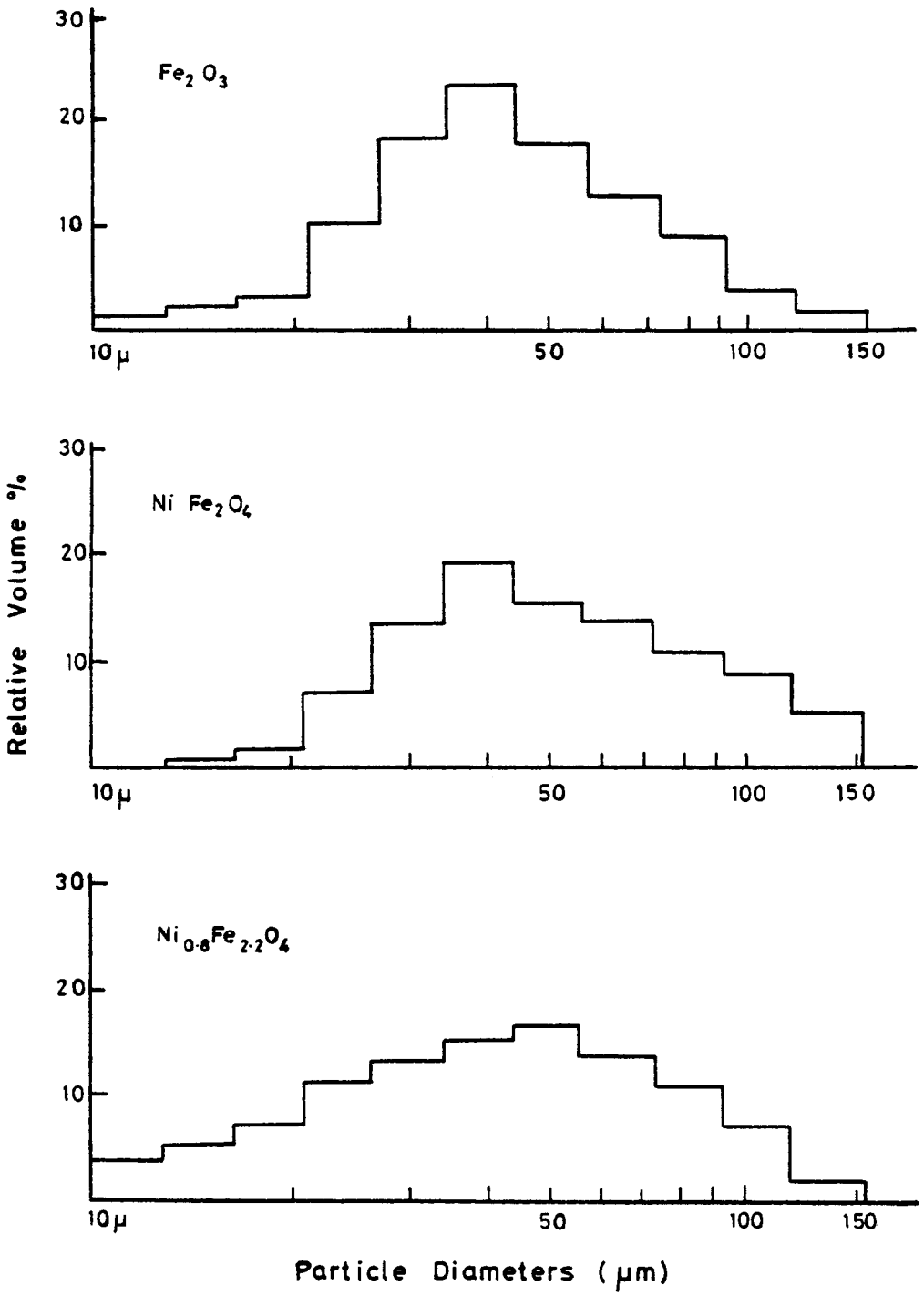

FIG.A4. Ferrite and Fe_2O_3 Particle Size Distributions

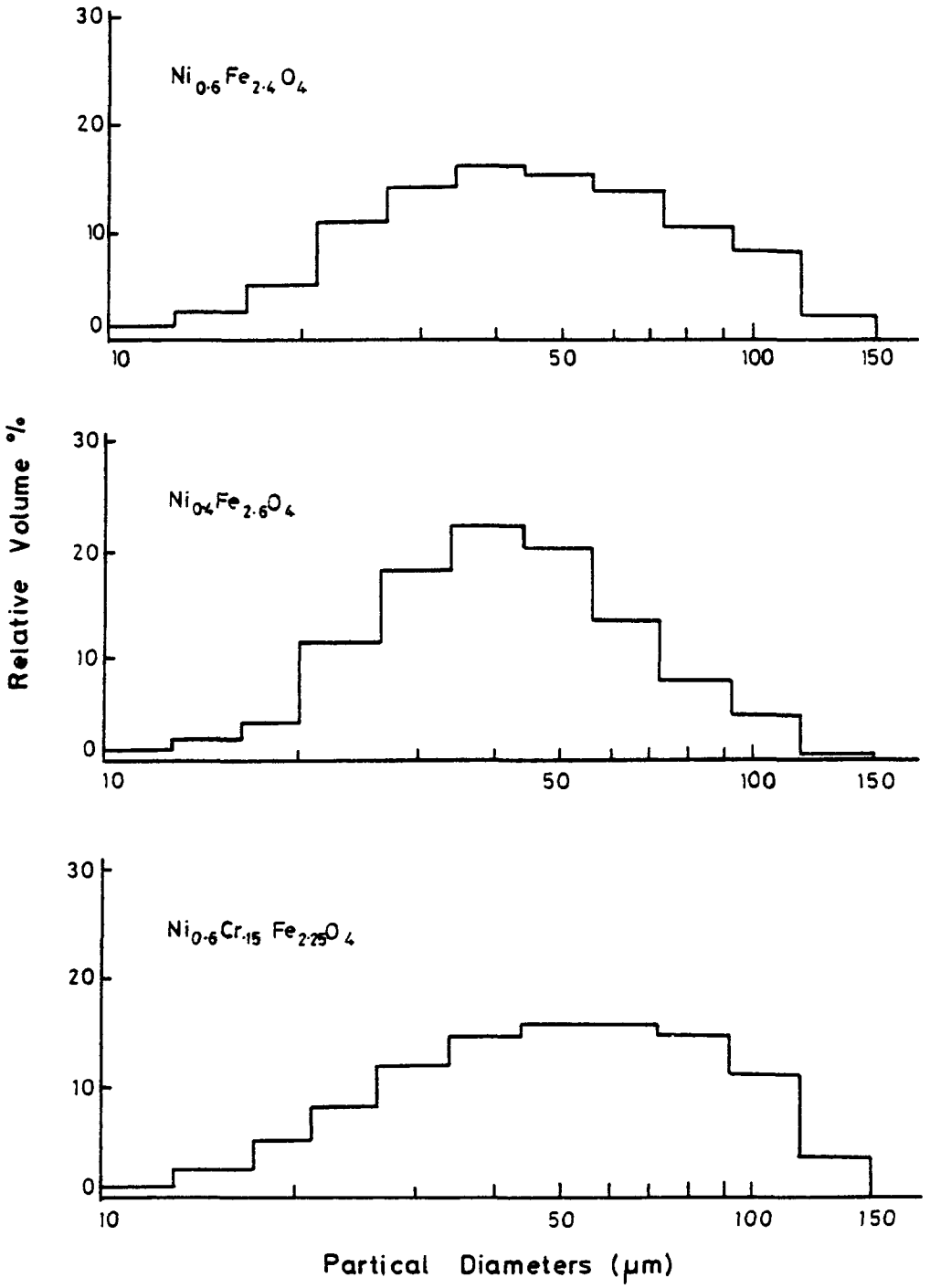

FIG.A5. Ferrite Particle Size Distributions

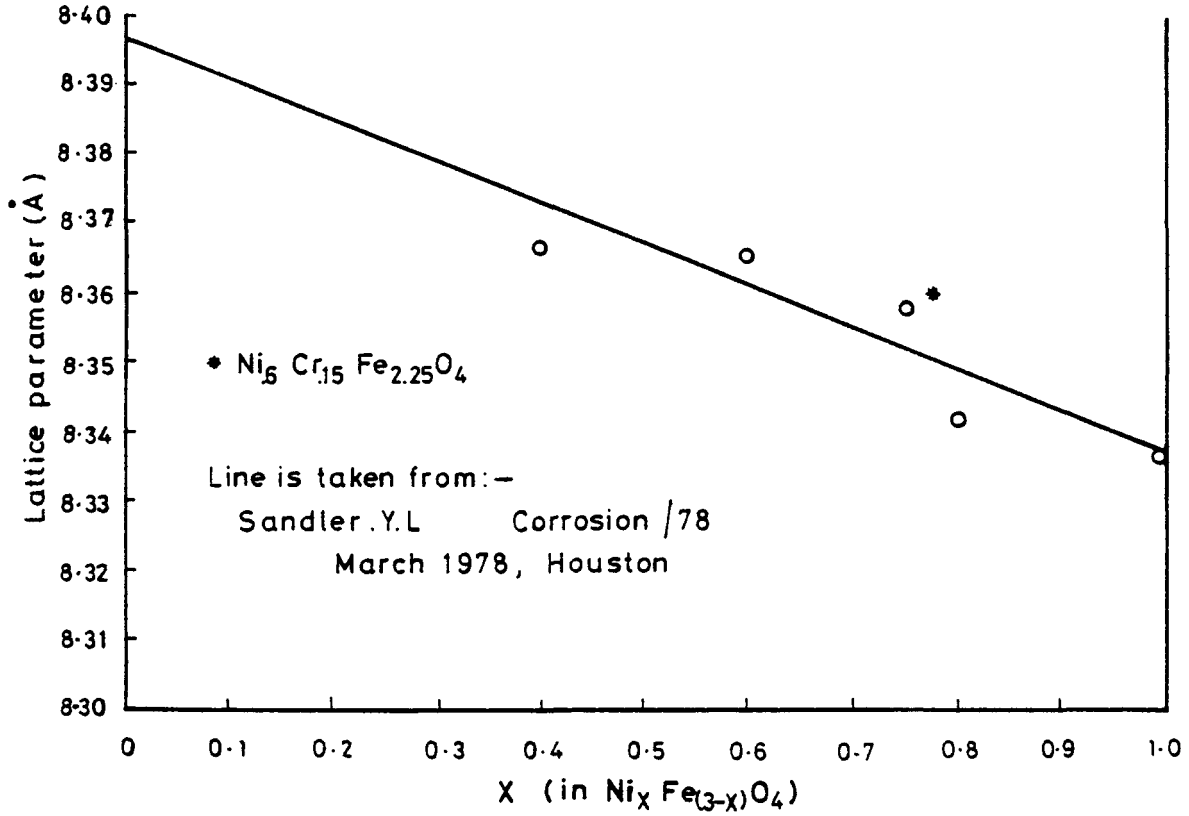

FIG.A6. X-ray Diffraction Lattice Parameter as a Function of Nickel Content in Nickel Ferrites

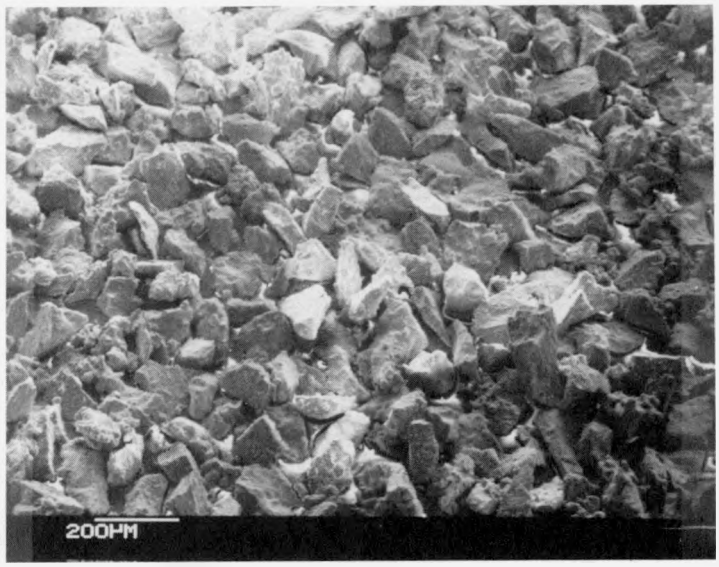

(a) $NiFe_2O_4$ prepared by the carbonate method, and calcined for 6h at 1400°C.

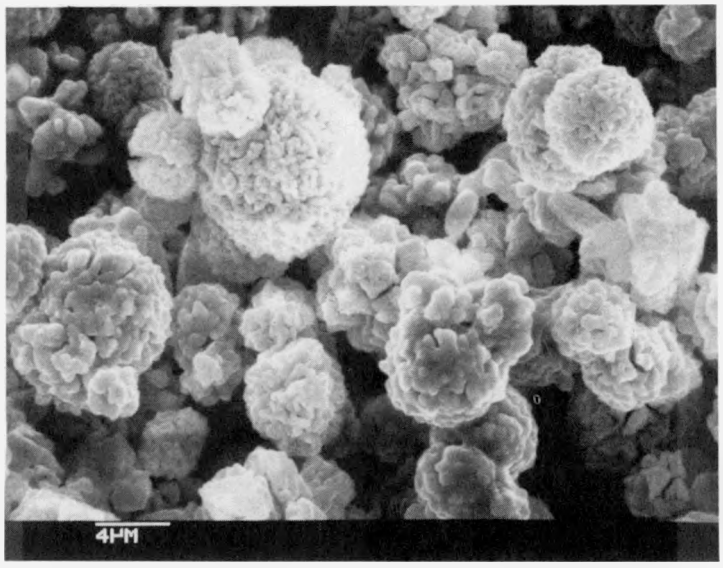

(b) $NiFe_2O_4$ prepared by the oxalate method, and calcined for 6 h at 1000°C.

Fig. A7. Scanning Electron Micrographs of $NiFe_2O_4$ particles

in specific surface area is apparent as the calcining temperature is reduced, although the temperature range over which this could be measured was limited - at the lower end by the temperature (ca. 800°C) required to form the spinel phase, and at the upper end by the materials of construction of the furnace.

2.2.2 Haematite Preparation

Haematite was prepared by precipitation of $Fe(OH)_3$ from $FeCl_3$ solution followed by drying and calcination. The procedure used was as follows. Ferric chloride was dissolved in water and aqueous ammonia added to precipitate $Fe(OH)_3$. The ferric hydroxide was washed copiously with water until washings showed no further chloride present ($AgNO_3$, visual test). The precipitate was then dried at 120°C for 1 week.

In order to approximate to the oxides found in-reactor a calcining temperature of 350°C in air was chosen. This was intended to be equivalent to a much longer period in-reactor at a slightly lower temperature.

After calcination for 4 hours the sample was sieved, the 50 - 150 mesh fraction being collected.

Examination of the oxide by scanning electron microscopy showed the particles to be essentially spherical, but highly porous (see Figure A8). The latter was borne out by the high specific surface area measured by N_2 adsorption (Table A2). In addition, the marked dependence of specific surface area on calcining temperature is to be noted, and is indicative of extensive sintering as the temperature increases. The surface areas found are similar to those reported by Kametani and Azuma (1968).

Commercially available haematite (calcined at 800°C) was supplied to BDH Ltd., and was used without further purification or treatment.

Magnetite (Fe_3O_4) was the standard laboratory grade supplied by BDH Ltd., and was used without further purification. The particle size distribution for haematite is shown in Figure A4.

2.3 KINETICS

Runs were generally carried out in the jacketed reaction vessel shown in

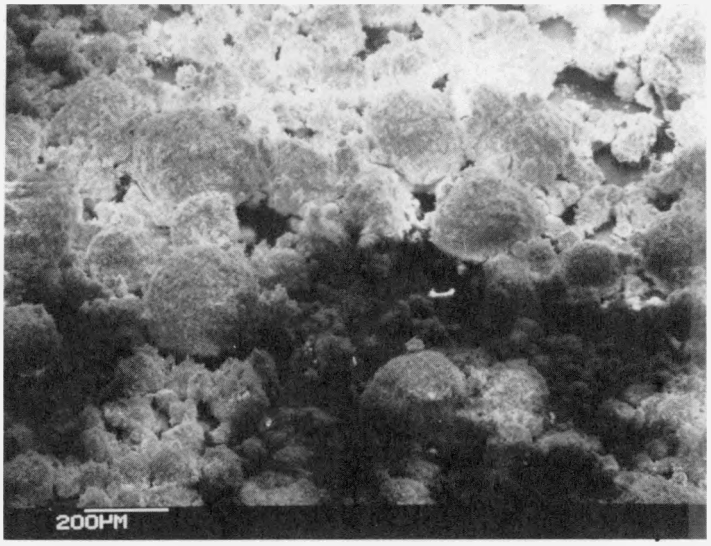

Fig. A8. Scanning Electron Micrograph of Fe_2O_3 particles

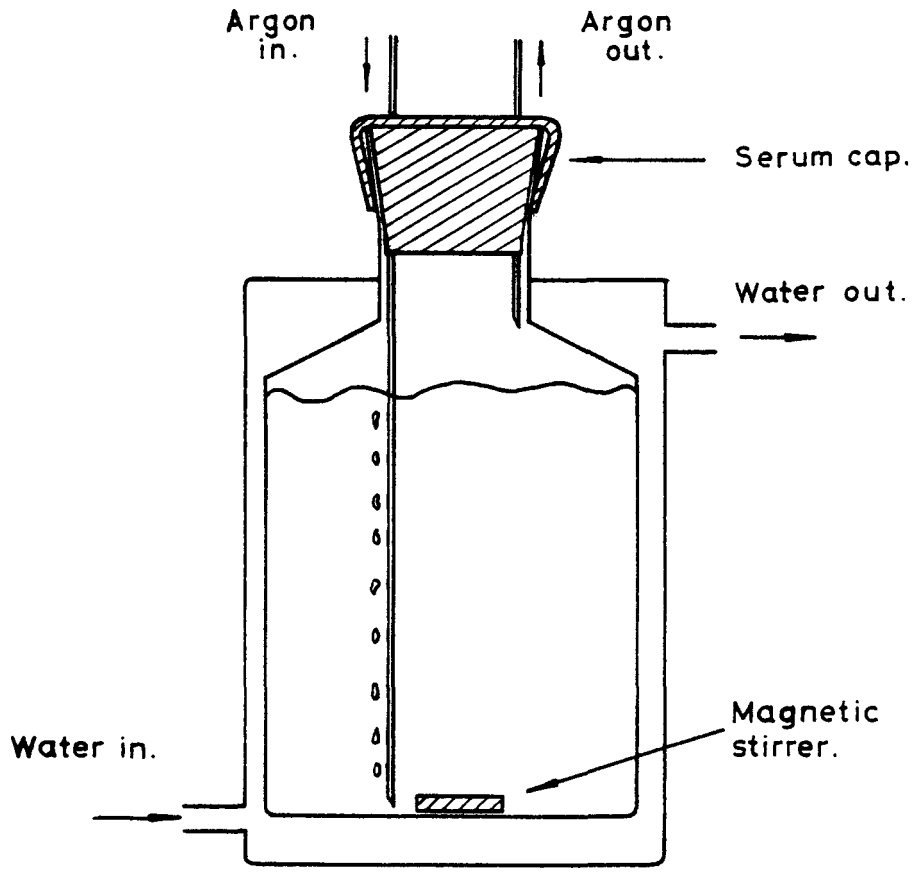

FIG.A9. Jacketed Reaction Vessel for Kinetic Experiments

Figure A9. The required amount of oxide was weighed into the vessel, together with any ligand, and other reagents such as buffer, acid or base. Water was added such that the final volume was 100 ml, and the vessel closed with a serum cap. This mixture was then de-aerated with argon, and equilibrated at the required temperature. Stirring was by a magnetic stirrer, and the thermostatting water pumped either from a Gallenkamp water circulator or a Grant water bath. The appropriate volume of stock of the reduced metal ion was injected after 30 - 45 minutes degassing. Samples for analysis were withdrawn at suitable intervals, diluted as appropriate and filtered through a 0.45 μm filter before analysis by Atomic Absorption Spectrometry. Runs with mixed metal oxides were analysed for each component. Reactions were carried out under pseudo-first-order conditions, that is with a large excess of reducing agent over oxide.

Some reactions, in which no air-sensitive reagent was present, such as with acids or chelating agents alone, were carried out in a Grant water-bath with a shaker attachment. Appropriate amounts of oxide and other reagents were measured into a 25 ml conical flask, which was then closed with a rubber bung and the reaction rapidly brought to temperature in the bath. Many runs could be carried out simultaneously using this technique, but stirring was less effective than by a magnetic stirrer.

2.4 LARGE SCALE RUNS

Decontamination trials on metal coupon sections were performed in a 5-litre scale rig (Figure A10). The rig was used in three configurations. For inactive runs the coupons were inserted into the main vessel and the solution mechanically agitated. Alternatively, whole pipe sections were incorporated into a loop, the solution being withdrawn from the reservoir pumped through the pipe section and returned to the reservoir. For active runs (using artefacts) the pumping method was employed but the coupon section was placed in a separate vessel in the external loop (Figure A11).

Metal ion reagents were prepared electrochemically as described in 2.1 above. The reduced metal in solution was then passed through an anion exchange column to replace aggressive counter-ions (e.g. sulphate) with a less aggressive ion (e.g. acetate). From thence the solution was mixed with the bulk volume, consisting of de-oxygenated water and the appropriate complexing agent.

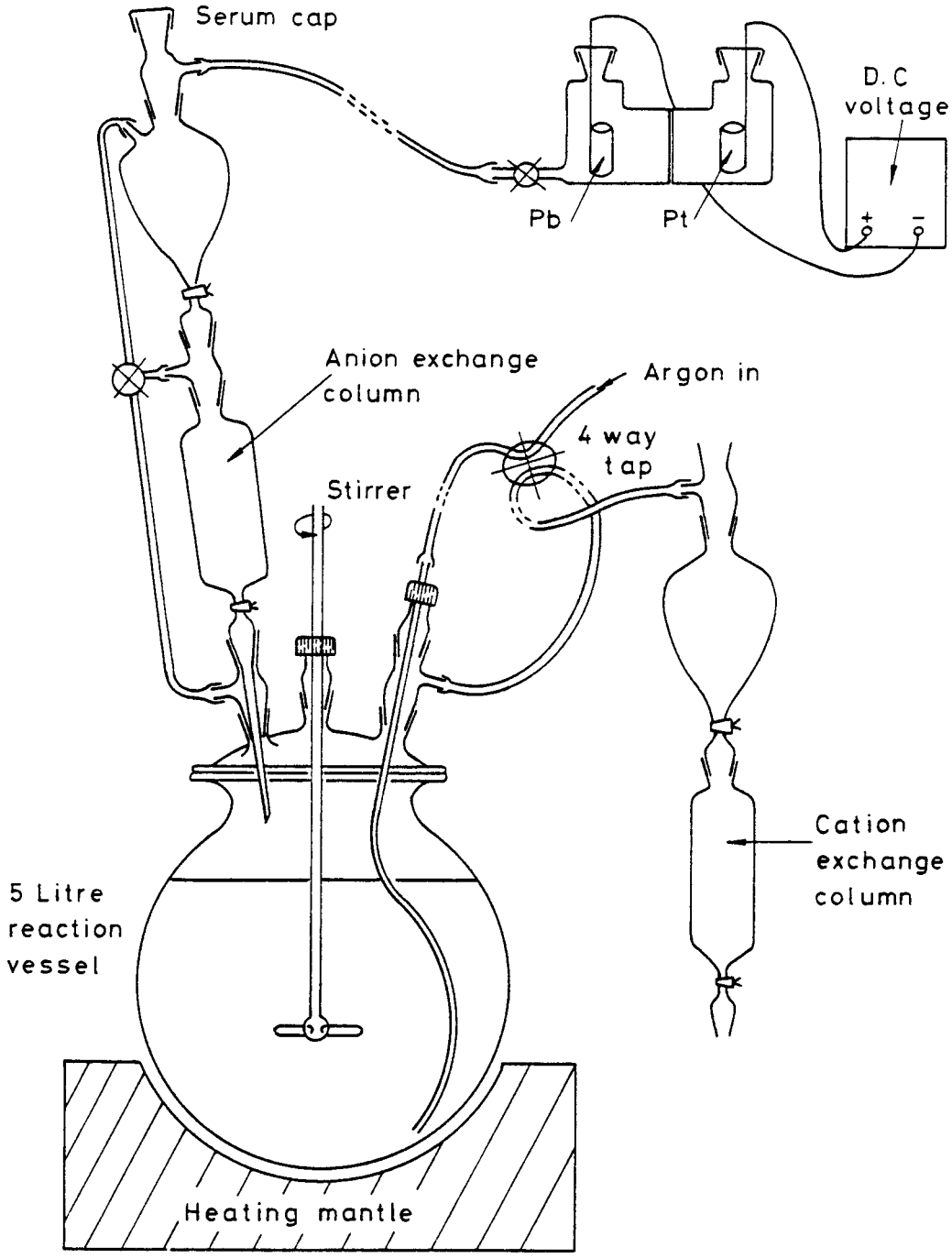

FIG.A10. 5 Litre Scale Decontamination Apparatus

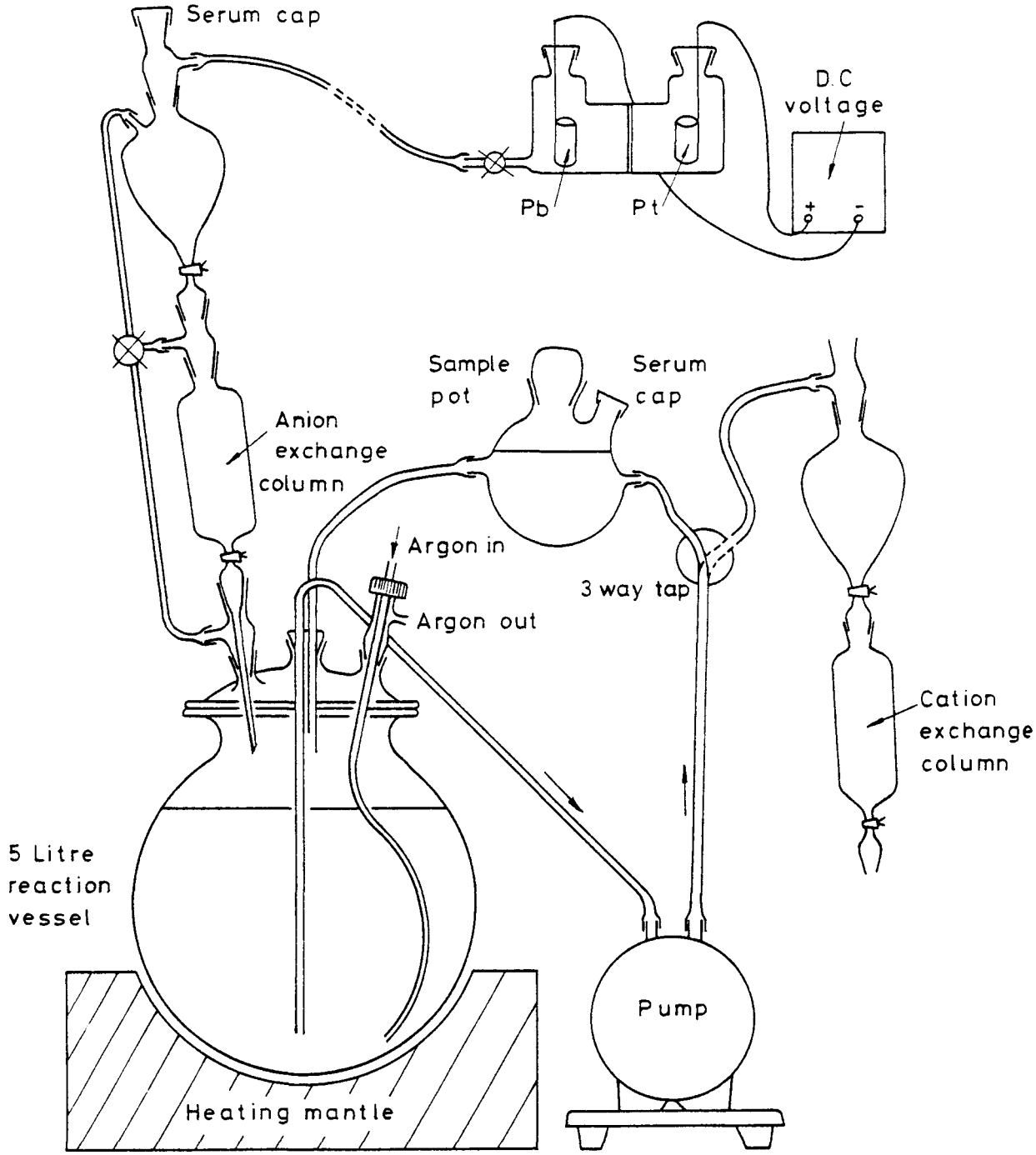

FIG.A11. 5 Litre Decontamination Apparatus with Recirculation

Sampling of the solution was achieved by withdrawal and filtration of a measured volume in the case of inactive runs. In active runs no filtration was employed. Analysis of the samples was achieved by atomic absorption spectrometry and by γ-counting employing a sodium iodide scintillation counter for routine use or GeLi γ-spectrometry.

Coupon samples used for inactive runs were 9-chrome ferritic steel which had been exposed to reducing chemistry in water for 1,000 hours at 350^{o}C.

For active runs coupon samples were obtained from a section of austenitic channel riser from the Winfrith SGHWR*. Also employed were some mild steel coupons that had been exposed to reducing chemistry for an unknown period in a reactor loop at AERE Harwell.

On the 9-chrome samples the oxide consisted of a duplex structure of magnetite overlaying an iron-chromium spinel. On the SGHWR samples the oxide consisted of haematite overlaying magnetite, possibly with some chromium content. The mild steel samples had been out of reactor for several months and significant activity was confined to ^{60}Co. Metallographic examination of specimens consisted of mounting in a suitable medium, grinding and polishing. Samples were examined by optical and electron microscopy and electron microprobe analysis. Energy dispersive X-ray analysis was used to examine the elemental proportions of the samples.

At the end of each decontamination, the decontaminant solution was passed down a cation column and the resulting solution analysed. The ion exchange was normally performed at 80^{o}C.

---

* This reactor is a heavy-water-moderated pressure tube type BWR, that operates in the neutral oxygenated chemical regime.

APPENDIX A3

3.0 RESULTS AND DISCUSSIONS

3.1 THE RATE LAW

To a first approximation, a suspension of fine particles of oxide can be treated as a uniform distribution of spheres. We define :

- N number of particles,
- R_o initial radius,
- M_o initial mass of solid present,
- ρ density of oxide
- V volume of solution.

If it is assumed that the reaction occurs at the surface of each particle, at a rate proportional to the available surface area at any instant,

$$\frac{dM}{dt} = - kA \qquad (4)$$

where M is the instantaneous mass of solid in the reaction, and k is a rate constant in units of mass/area/time, e.g. g cm^{-2} min^{-1}. Then

$$\frac{dM}{dt} = - 4\pi N k R^2 \qquad R = \text{instantaneous radius}$$

but $M = \frac{4}{3}\pi\rho N R^3$

$$\therefore \quad \frac{dM}{dt} = - \left(\frac{36\pi N}{\rho^2}\right)^{1/3} k M^{2/3}$$

which, on integration, yields

$$M_o^{1/3} - M^{1/3} = \left(\frac{4\pi N}{3\rho^2}\right)^{1/3} kt \qquad (5)$$

where M_o is the mass at t = 0.

Experimentally it is the concentration of a metal ion in solution, usually Fe, which is measured (C).

$$C = \frac{X(M_o - M)}{V}$$

where X is the weight fraction of metal in the oxide, and the final concentration is given by

$$C_\infty = \frac{XM_o}{V}$$

when all oxide has dissolved.

Substitution into (5) above, gives

$$(C_\infty - C)^{1/3} = -\left(\frac{4\pi NX}{3\rho^2 V}\right)^{1/3} kt + C_\infty^{1/3}$$

which rearranges to give

$$\left(1 - \frac{C}{C_\infty}\right)^{1/3} = 1 - \left(\frac{k}{R_o\rho}\right)t \qquad (6)$$

Thus a plot of the left hand side of this equation versus time should yield a straight line with intercept at $t = 0$ of 1, and slope of $-\frac{k}{R_o\rho}$, a direct measurement of the rate of reaction of the oxide with the particular reagent under consideration. Since R_o and ρ are constants for any single batch of oxide, we can call this slope the observed rate constant, k_{obs}. It is convenient to use the reciprocal of this, which gives the time to complete dissolution :

$$t_\infty = \frac{1}{k_{obs}} = \frac{R_o\rho}{k} \qquad (7)$$

Since the real oxides used do not have a uniform particle distribution, this cubic rate law does not yield a true straight line. It is possible to calculate the shape of the function $\left(1 - \frac{C_t}{C_\infty}\right)^{1/3}$ with time for non-uniform distributions. The results of such a calculation are shown in Figure A12, where we have arbitrarily chosen a situation of equal masses of particles of initial radius, a, 2a, 3a, 4a and 5a, which corresponds approximately to the distribution found with the oxides prepared in the laboratory. Although there is considerable curvature over long times, the plot is quite linear to 60% dissolution $\left(\left(1 - \frac{C_t}{C_\infty}\right)^{1/3} = 0.73\right)$, and the intercept is close to the value of t_∞ we should obtain if all the particles had the same, average, initial radius. Figure A.13 shows the results obtained in

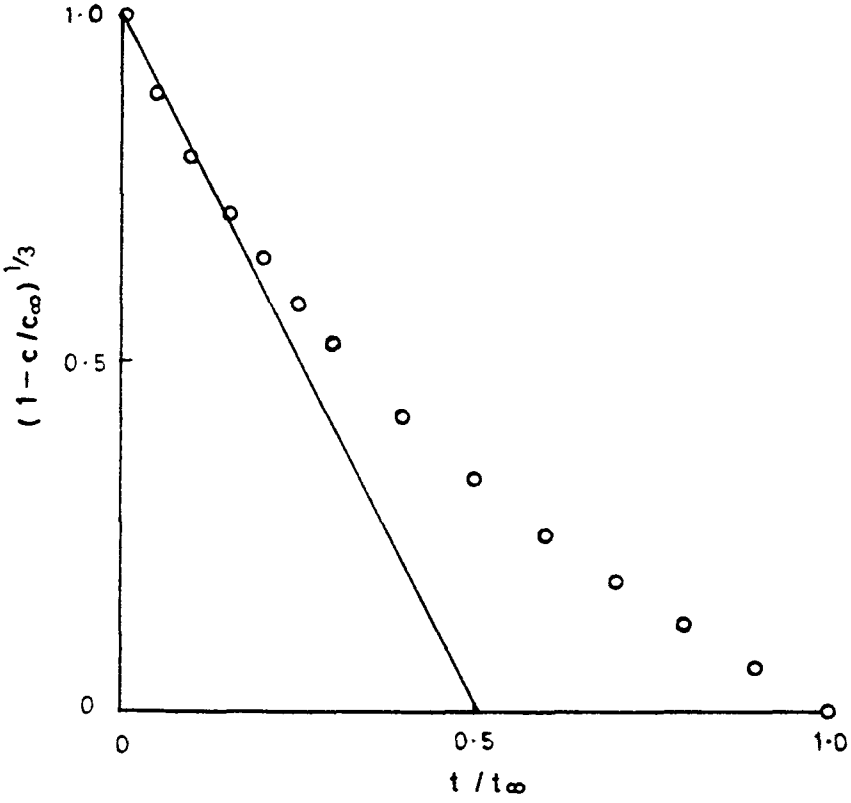

Fig.A12. Cubic Rate Law Plot Calculated for a Non-Uniform Size Distribution

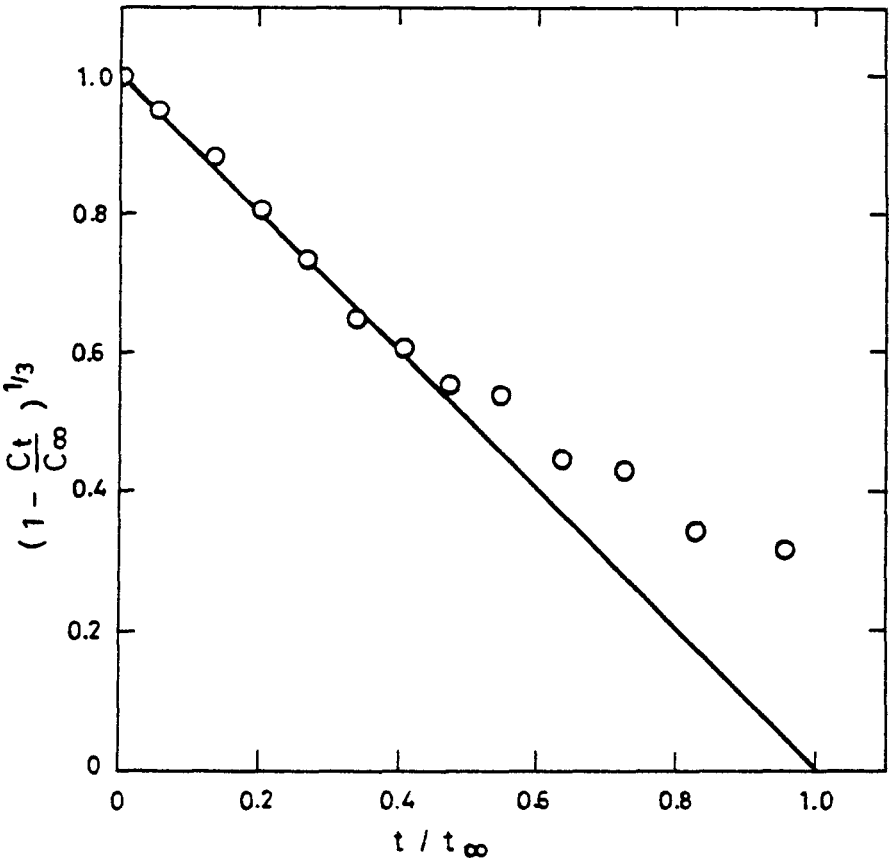

FIG. A13. Cubic Rate Law Plot for the $V(pic)_3^-$ Dissolution of Nickel Ferrite Sample with Broad Particle Size Distribution. Data Measured in Solutions Containing 3.2×10^{-3} M $V(pic)_3^-$ + 0.03 M Free Picolinate + 0.1M HCO_2^- + 20 ppm Triton X-100, pH 4.3, 80°C. t_∞ = 220 min

a typical experiment, in this case the dissolution of $NiFe_2O_4$ by $V(pic)_3^-$. Linearity was observed to ca.75% dissolution. When the experiment was repeated using a $NiFe_2O_4$ sample sieved to give a very narrow particle size distribution (53-75μm) a plot of $\left(1 - \frac{C_t}{C_\infty}\right)^{1/3}$ v. time was linear to ca. 95% completion as shown in Figure A.14 for the case of dissolution in $V(pic)_3^-$.

The validity of Eqn. (6) [and (7)] has also been investigated by measuring k_{obs} as a function of particle diameter (d). For this purpose a sample of nickel ferrite was sieved into size fractions, and the dissolution kinetics in the presence of $V(pic)_3^-$ measured under otherwise constant conditions. The results are shown in Figure A15. There is clearly an inverse relationship between k_{obs} and d. The line shown in the figure is drawn according to Eqn. (7) with $k/\rho = 7 \times 10^{-8}$ m min^{-1} and gives a reasonable fit to the data. Plotting k_{obs}^{-1} v. d yields a straight line, but with intercept k_{obs}^{-1} = ca. 300 min, when d = 0 indicating some agglomeration of smaller particles, no doubt because nickel ferrite is magnetic.

The cubic rate law of Eqn. (6) provides then the framework within which we have interpreted the kinetic results. When reaction was sufficiently rapid, observed values of C_∞ were used in the calculations; otherwise they were based on the weight of oxide added initially. For very slow reactions (generally $t_\infty > 10^3$ min) a cubic rate law was assumed, and values of t_∞ or k_{obs} were estimated from the initial dissolution rate.

3.2 COMPARISON OF OXIDE DISSOLUTION BEHAVIOUR OF VARIOUS LOMI REDUCING AGENTS AND OTHER REDUCTANTS

3.2.1 Results

The principal aim of these experiments was to compare the dissolution rates with different reagents on a constant batch of a particular oxide. Although the results indicate that some reductive dissolution may be insensitive to oxide history (see below), the non-reductive dissolutions were very sensitive and for this reason a number of experiments were conducted with acids and chelating agents in the absence of reducing agents to provide comparative data with some oxide batches rather than relying on literature data for material of unknown history.

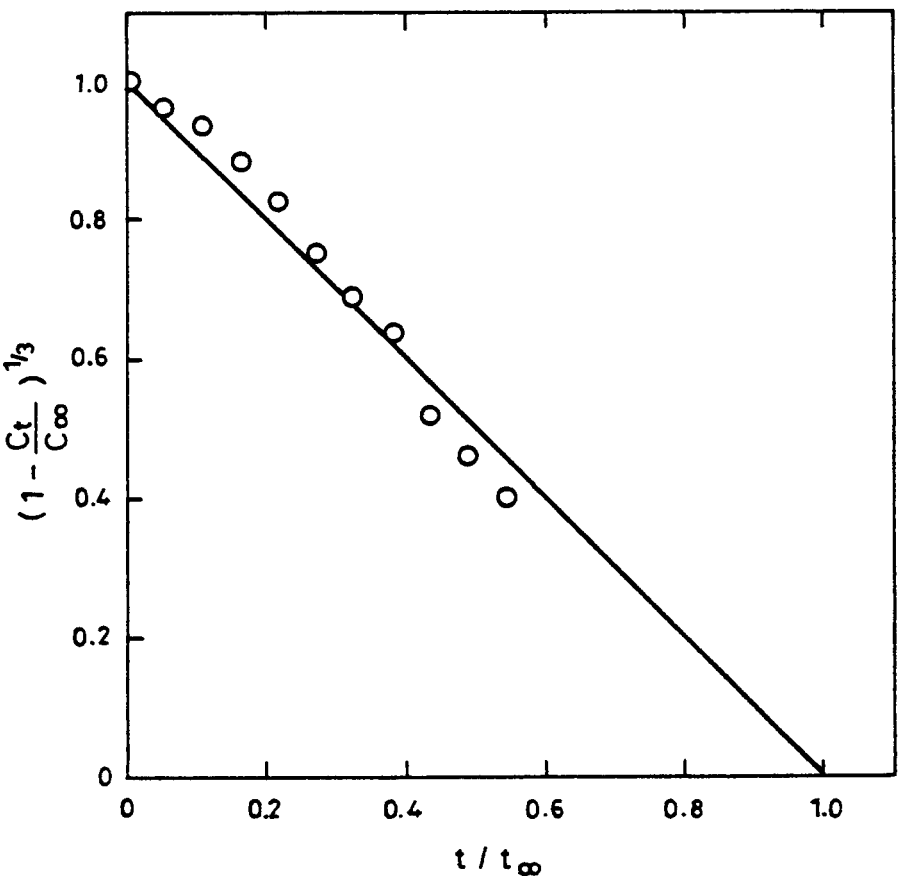

FIG. A14. Cubic Rate Law Plot for the $V(pic)_3^-$ Dissolution of Nickel Ferrite Sample with Narrow Particle Size Distribution. Reagents and Conditions as for Fig. A13; t_∞ = 1100 min

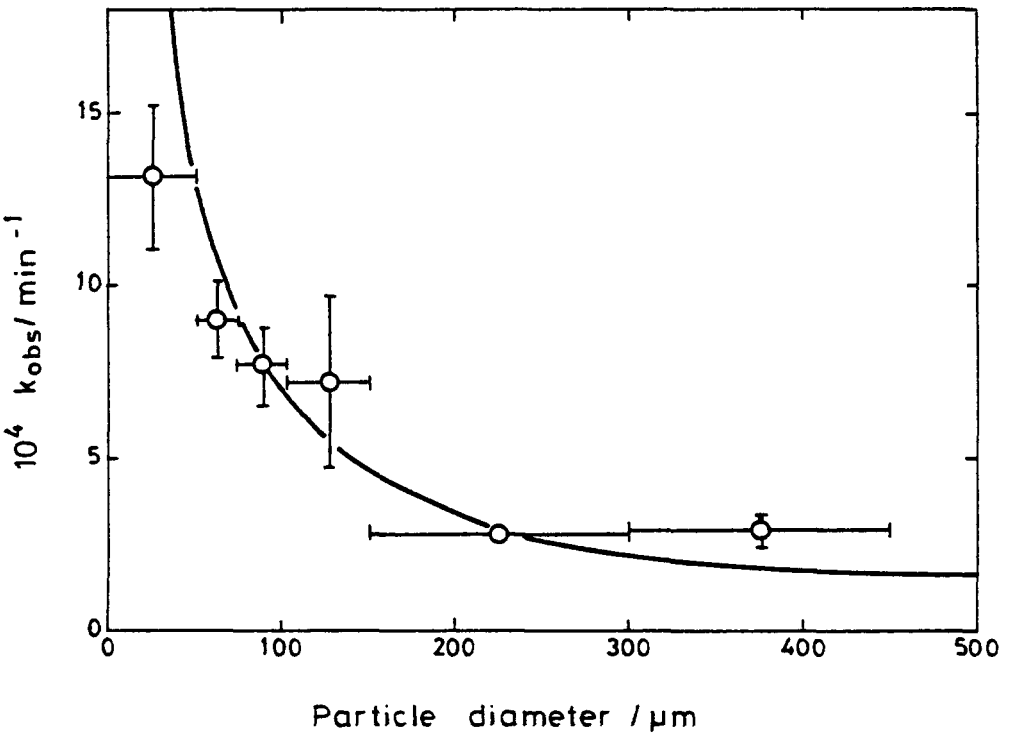

FIG. A15. Effect of Particle Size on the Dissolution of $NiFe_2O_4$ by $V(pic)_3^-$
Line Drawn for $k_{obs} = \frac{a}{d}$, with
$a = 7 \times 10^{-8}$ m min^{-1}
Vertical Error Bars are ± Mean Deviation;
Horizontal Error Bars Show Range of Particle Sizes

Equally, the dissolution rate differences between Fe_2O_3, Fe_3O_4 and $NiFe_2O_4$, although indicative of the broad qualitative variation between oxide types, is unlikely to be reproduced quantitatively when the same oxides are formed by different routes. It is stressed that identical dissolution times are unlikely to be found with reactor oxides.

The results are shown as follows: Table A3, oxide dissolution with acids and chelating agents alone. Table A4, oxide dissolution with the addition of reducing agents. Slow reactions ($t_\infty \geq 10^3$ min) were generally followed for only a small part of the reaction, and so the values of t_∞ quoted are only reasonable approximations. Faster runs, where regular sampling over 50% or more of the total dissolution could be carried out, are more accurate.

One system was investigated in greater detail. Figures A16 and A.17 show the effects of temperature and pH, respectively, on the rate of reaction of Fe_2O_3 with $Cr(bipy)_3^{2+}$. From the former we calculate an activation enthalpy of 7 kcal mol^{-1}, a figure not inconsistent with the suggestion that electron transfer is the rate-determining step. (We have also obtained a rough estimate of around 10 kcal mol^{-1} from the system $NiFe_2O_4/Cr^{2+}/Cl^-$.) Figure A.18 shows the dependence of rate on the concentration of reductant, which is clearly first order over this range.

3.2.2 Discussion

The most striking observation is made by comparison of the figures for Fe_2O_3(350) in Tables A.3 and A.4. In the absence of reducing agents, the most rapid dissolution obtained with chelating agents gave $t_\infty \simeq 10^4$ min. Every figure for Fe_2O_3(350) in Table A.4 is faster than this, in many cases using the reagents ten to a hundred times more dilute. The same observation applies to the dissolution of $NiFe_2O_4$, the 'insoluble' ferrite, and also to Fe_3O_4 in all cases except for quinol (which is only marginally reducing to Fe_3O_4). There can be no doubt that reduction of Fe^{III} to Fe^{II} in the oxide provides the key to rapid dissolution, whereas the increase in metal-ion solubility by addition of chelating agents is not sufficient to overcome the kinetic barriers to dissolution. In particular, the most rapid dissolution is obtained by use of the reagents known for their ability to reduce rapidly Fe^{III} in homogeneous aqueous solution. The most marked increase in dissolution rate in the presence of an efficient reducing agent is provided with 350°C calcined Fe_2O_3 which dissolved completely in

TABLE A3

Oxide Dissolution with Acids and Chelating Agents Only

Reagent	Concentration (M)	$[H^+]$ (M)	T °C	Dissolution time t_∞ (min)			
				Fe_2O_3(350)	Fe_2O_3(800)	Fe_2NiO_4	Fe_3O_4
EDTA	0.1	10^{-7}	60	3×10^5	-	-	-
EDTA	0.1	10^{-5}	60	1.5×10^4	-	$\geq 2 \times 10^6$	2×10^4
EDTA	Sat.	10^{-3}	60	10^4	-	-	-
Citrate/ Oxalate	Both 0.1	$10^{-6.5}$	60	$> 10^6$	-	-	10^5
Citrate/ Oxalate	Both 0.1	10^{-5}	60	3.5×10^5	-	$\geq 2 \times 10^6$	-
Citrate/ Oxalate	Both 0.1	10^{-3}	60	10^4	-	-	2.5×10^3
Citrate	0.5	$10^{-3.5}$	80	-	-	5×10^4	-
Bipyridyl	0.01	$10^{-2.5}$	60	$> 4 \times 10^5$	-	-	-
Catechol	0.1	10^{-3}	80	10^4	-	-	-
H_2SO_4	2.15	4.3	60	360	1.3×10^4	6×10^5	-
HCl	0.1	0.1	60	1.7×10^4	2.0×10^5	$\geq 2 \times 10^6$	10^4
HCl	1.0	1.0	60	240	2.3×10^4	8×10^5	10^3
HCl	4.0	4.0	60	-	1.4×10^3	-	-

TABLE A4

Oxide Dissolution with Reducing Agents

Reductant	Conc. (M)	Other Reagent	Conc. (M)	$[H^+]$ (M)	T °C	Dissolution time t_∞ (min)				
						Fe_2O_3(350)	Fe_2O_3(800)	Fe_2NiO_4	Fe_3O_4	$Ni_{0.6}Cr_{0.15}Fe_{2.25}O_4$
Cr^{2+}	0.01	Cl^-	0.24	0.2	23	-	100	-	-	-
Cr^{2+}	0.01	Cl^-	0.1	0.1	40	40	-	-	-	-
Cr^{2+}	0.02	Cl^-	0.1	0.1	23	-	-	-	800	-
Cr^{2+}	0.001	Bipyridyl	0.005	10^{-3}	23	50	-	-	-	-
Cr^{2+}	0.002	Bipyridyl	0.02	10^{-6}	60	70	-	-	-	-
Cr^{2+}	0.004	Bipyridyl	0.02	$10^{-5.2}$	80	-	-	500	-	-
Cr^{2+}	0.04	ClO_4^-	0.23	0.15	23	5×10^3	-	-	-	-
Cr^{2+}	0.04	Cl^-	0.24	0.12	23	-	-	$>3 \times 10^4$	-	-
Cr^{2+}	0.04	Cl^-	0.24	0.12	50	-	-	3×10^3	-	-
Cr^{2+}	0.04	Cl^-	0.56	0.44	80	-	-	120	-	-
V^{2+}	0.01	ClO_4^-	0.04	0.025	23	10	24	-	-	-
V^{2+}	0.01	ClO_4^-	0.12	0.10	23	-	-	-	12	-
V^{2+}	0.01	ClO_4^-	0.12	0.1	80	-	-	80	-	-
V^{2+}	0.02	ClO_4^-	0.5	0.20	80	-	-	-	-	300
V^{2+}	0.002	Bipyridyl	0.01	$10^{-4.5}$	80	150	-	-	-	-
V^{2+}	0.004	Bipyridyl	0.02	$10^{-4.6}$	80	-	-	2.3×10^3	-	-
V^{2+}	0.002	Picolinate	0.01	$10^{-4.1}$	60	25	-	-	-	-
V^{2+}	0.0017	Picolinate	0.01	$10^{-5.1}$	80	-	-	300	-	-
V^{2+}	0.0017	Picolinate	0.01	$10^{-5.6}$	80	-	-	-	≤ 10	3000
V^{3+}	0.02	SO_4^{2-}	0.5		23	330	-	-	-	-
V^{3+}	0.002	Citrate	0.01	$10^{-4.6}$	60	210	-	-	600	-
V^{3+}	0.004	Citrate	0.02	$10^{-3.2}$	80	-	-	1.5×10^4	-	-
Fe^{2+}	0.002	EDTA	0.005	$10^{-3.8}$	80	80	-	-	-	-
TGA	0.1	-	-	10^{-4}	80	80	-	-	-	-
TGA	0.1	-	-	10^{-3}	80	-	-	6×10^3	-	-
Quinol	0.1	-	-	0.2	60	-	-	2×10^6	-	-
Quinol	0.1	-	-	10^{-3}	80	10^3	-	-	$\leq 3 \times 10^6$	-

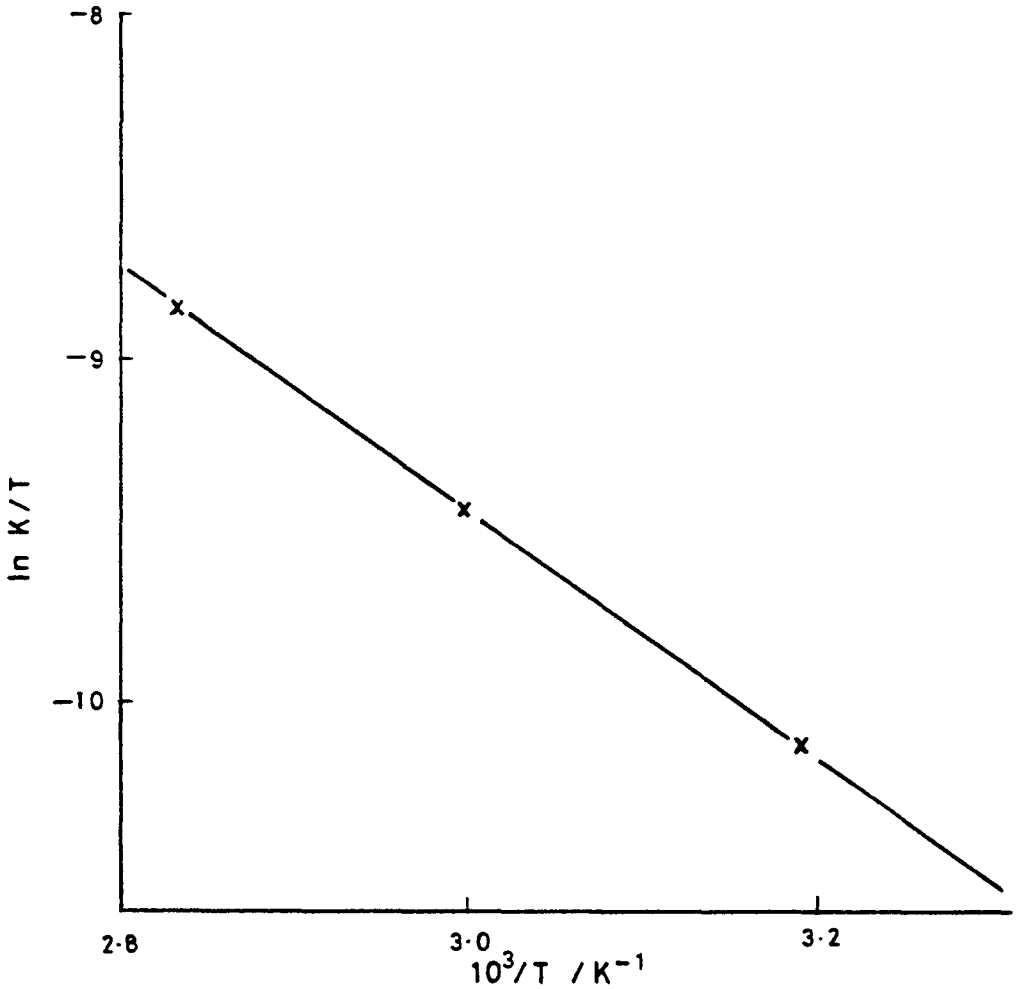

Fig.A16. Activation Plot for the Reaction Fe_2O_3+Cr(bipy)$_3^{2+}$

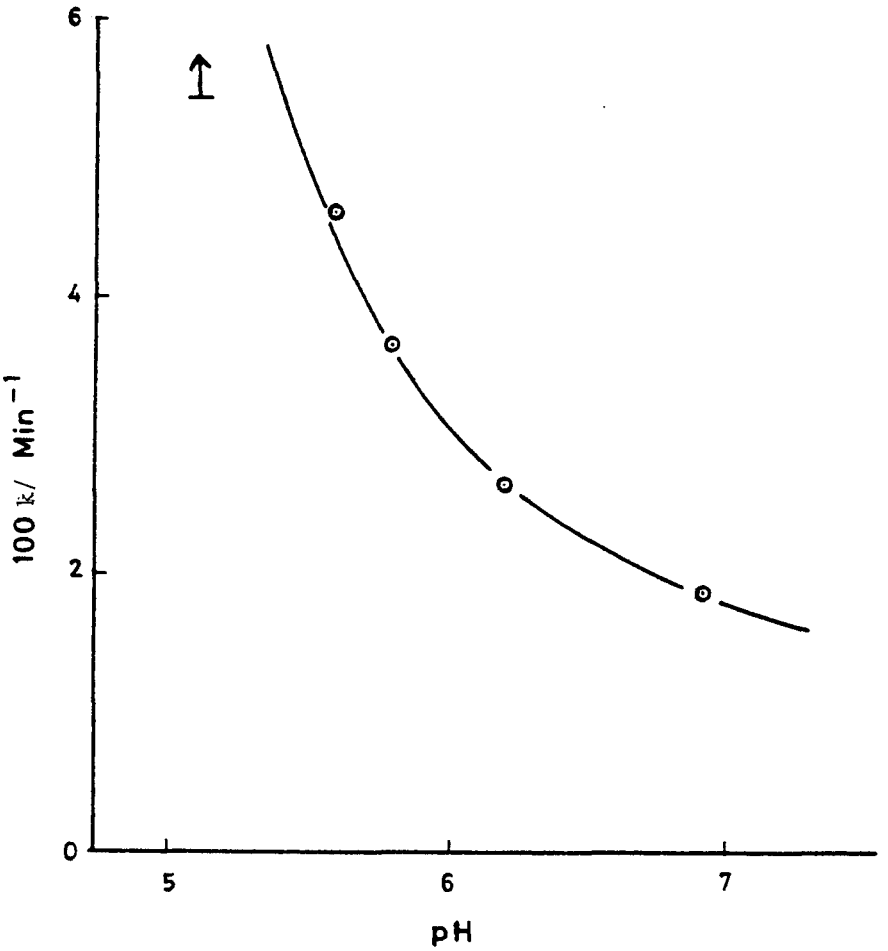

Fig.A17. pH Dependence of the Reaction $Fe_2O_3 + Cr(bipy)_3^{2+}$

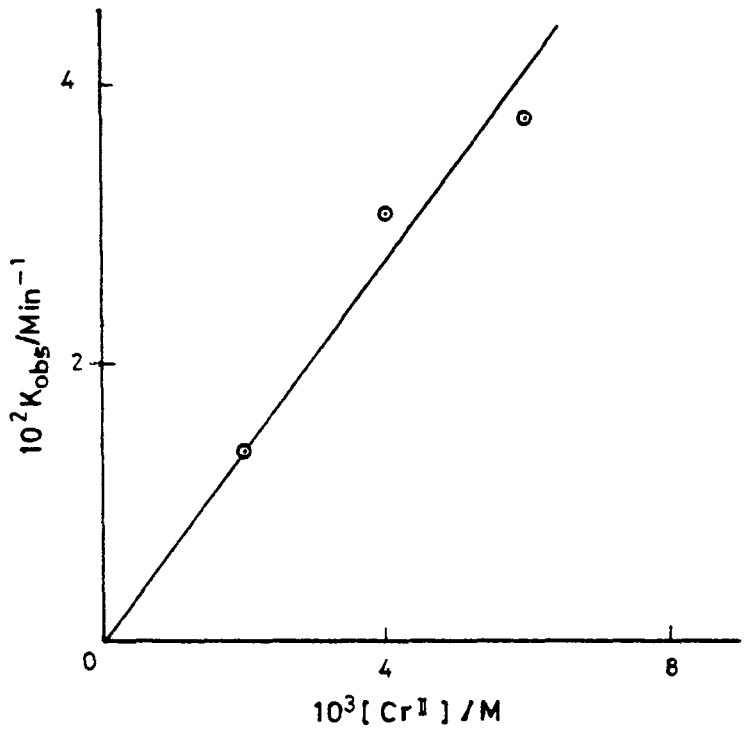

Fig .A18. Dissolution of Fe_2O_3 in $Cr(bipy)_3^{2+}$ Influence of Reagent Concentration on Rate

$\sim$ 10 min. at room temperature in 0.01 M V^{2+}. This rate is approaching the diffusion-controlled limit predicted by Rodliffe (1978a). The rate for this reagent with Fe_3O_4 is comparable.

With all the reductants shown in Table A.4, we can consider the mechanisms of the dissolution reactions by analogy with those of homogeneous electron-transfer reactions in solution. If we consider first the organic reagents thioglycollic acid and quinol, each of these can act as a one-electron reductant, forming the thiol and semiquinone radicals respectively. The reaction of quinol with Fe^{3+} in solution is probably outer-sphere (Baxendale et al., 1951), with TGA the inner-sphere intermediate has been identified (Lappin and McAuley, 1975). In heterogeneous reactions with a solid metal oxide, the process analogous to inner-sphere reaction would involve binding of the reductant to the surface of the oxide as a requirement for reaction. If this were the case, then the presence of other non-reducing, chelating agents might event turn out to lower the rate of reaction by competing for binding sites (Matijević and Rubio, 1978).

Direct evidence for an inner-sphere mechanism is obtained from the reaction of Fe_2O_3 with Cr^{2+} in dilute HCl. Here, the rate of dissolution depends on the concentration of chloride, and the chromium(III) product is $CrCl^{2+}$, identified by ion-exchange and UV - visible spectroscopy. This proves that Cl^- is bound to the Cr^{2+} ion in the transition state, so we can confidently deduce its function as a bridging ligand. In the absence of chloride, the reaction is very much slower; it is not clear whether an inner-sphere mechanism operates, involving binding of Cr^{2+} to oxide or hydroxide ions, or if an outer-sphere one applies, with no bridging between Fe^{3+} and Cr^{2+}.

In the presence of an excess of bipyridyl, the reducing agent is $Cr(bipy)_3^{2+}$; as explained in Appendix 1, this is limited to outer-sphere mechanisms, but is a very rapid reductant. Rapid dissolution of both Fe_2O_3 and $NiFe_2O_4$ is obtained with this reagent, and the $Fe_2O_3/Cr(bipy)_3^{2+}$ system was chosen for more detailed investigation, as it is suitable for operations at near-neutral pH values and does not require the presence of aggressive anions [e.g. Cl^-] for dissolution. Three variables were studied: i) concentration, which showed the expected first-order dependence of rate on $[Cr^{II}]$; ii) temperature, from which a linear Eyring plot was obtained, yielding a value of $\Delta H^{\ddagger}$ of 7 kcal mol^{-1}; iii) pH, which showed a significant increase

in rate with decreasing pH at both 40°C and 60°C. We deduce that only a single mechanism operates over the temperature range studied (40 - 80°C) and that the rate-determining step is almost certainly electron transfer. Since the reductant is unaffected by pH over the range 5 → 7, the variation in rate must be due to different degrees of protonation of the oxide surface. Binding of bipyridyl molecules to the surface may also affect the dissolution rate, as it is established that ligands of this type also raise both the electrode potential and the reactivity of Fe^{III} in solution (Nord et al., 1978; Eichler and Wahl, 1958; George and Irvine, 1957).

It is probable that V^{2+} also reacts by an outer-spere mechanism. It dissolves Fe_2O_3 and other oxides much faster than Cr^{2+}, in the absence of chloride, while the reverse is normally found in inner-sphere reactions. (It is interesting that a ratio of 50:1 for outer-sphere reductions by V^{2+} and Cr^{2+} is generally observed in solution reactions (Toppen and Linck, 1971) while $Cr(bipy)_3^{2+}$ is some 10^5 times faster than V^{2+} under similar circumstances (Candlin et al., 1964)). Clearly these quantitative relationships which follow from the Marcus theory, do not hold for the heterogeneous reactions considered here.

When ligands such as bipyridyl or picolinate are present, we can be sure that reaction is outer-sphere. $V(bipy)_3^{2+}$ dissolves Fe_2O_3 and $NiFe_2O_4$, both a little slower than $Cr(bipy)_3^{2+}$, which is consistent with the results obtained in solution reactions (Bennett and Taube, 1968). The addition of citrate, to keep the vanadium(III) product in solution, does not affect the rate of reaction. The complex $V(pic)_3^-$ (pic = picolinate) is a rapid reducing agent, as expected, and gives very encouraging dissolution times with Fe_2O_3, $NiFe_2O_4$, and even the chromium-bearing ferrite, $Ni_{0.6}Cr_{0.15}Fe_{2.25}O_4$. As with V^{2+} alone, this latter ferrite dissolves with the appearance of all three metal ions in solution. The concentration of chromium in solution, however, is only about 70% of the calculated value. This could be due either to the presence of small inclusions of insoluble Cr_2O_3 in the oxide, or to a deficiency in the composition of the material, which has not been analysed.

A few runs were carried out with V^{III} as the reductant. Both in acid solution, and complexed by citrate buffers, this dissolves Fe_2O_3 rapidly. The complex dissolves Fe_3O_4 also, but does not give a good rate with

$NiFe_2O_4$. Any reduction of oxides by V^{III} in a reactor clean using V^{II} lowers the amount of reagent required.

$Fe(EDTA)^{2-}$ also dissolves Fe_2O_3 very rapidly but has little effect on $NiFe_2O_4$. The dissolution of Fe_2O_3 is catalytic, as the product includes one $Fe(EDTA)^{2-}$ for each one consumed. This reagent can therefore dissolve an unlimited amount of oxide, without exhausting the reducing agent, given enough EDTA for complexation. This suggests the possibility of an autocatalytic mechanism for the dissolution of, for example, Fe_3O_4 by EDTA alone. We can envisage a sequence of this type :

$$Fe_3O_4 + EDTA^{4-} \xrightarrow[2H^+]{\text{SLOW}} Fe(EDTA)^{2-} + H_2O + Fe_2O_3$$

$$\tfrac{1}{2}Fe_2O_3 + Fe(EDTA)^{2-} + EDTA^{4-} \xrightarrow[3H^+]{\text{FAST}} Fe(EDTA)^{-} + Fe(EDTA)^{2-} + \tfrac{3}{2}H_2O$$

and possibly

$$Fe_3O_4 + 2Fe(EDTA)^{2-} + EDTA^{4-} \xrightarrow[8H^+]{\text{FAST}} 3Fe(EDTA)^{2-} + 2Fe(EDTA)^{-} + 4H_2O$$

Even in oxygenated solution, a local concentration of $Fe(EDTA)^{-}$ could build up at the oxide surface to carry on reaction.

On the basis of these results, a number of reagents suggest themselves as suitable for reactor application, as rapid dissolving agents for oxides at near-neutral pH and high temperature. $Cr(bipy)_3^{2+}$, $V(bipy)_3^{2+}$, $V(pic)_3^{-}$ and V^{III} (citrate) are all worthy of consideration. Some of these were therefore used in large-scale laboratory experiments, to test their efficacy in removing oxide from steel specimens and also the ion-exchange removal of unwanted anions before use and of dissolved metal ions after reaction.

3.3 DETAILED STUDY OF THE DISSOLUTION OF NICKEL FERRITE BY $V^{II}(pic)_3$

We have seen in the previous section how the presence of reductant, particularly one based on a low oxidation-state metal ion, can dramatically increase the dissolution rates of Fe^{III}-containing oxides over reagents containing only acids and/or chelating agents. Although there are many parallels between the reaction of LOMI-type reagents with Fe^{III}-containing oxides and Fe^{3+} in homogeneous solution, and much data for the latter on

which to draw, we considered that it would be of value to study one of these dissolution reactions in detail. For this purpose the $V^{II}(pic)_3^-$ + nickel ferrite system was chosen. The results of this study are presented in this section. The work was performed in two parts; in the first, described in the following section, stoichiometric nickel ferrite was used, and in the second, (Section 3.3.2) various non-stoichiometric oxides were used.

3.3.1 Dissolution of Stoichiometric Nickel Ferrite by $V^{II}(pic)_3$

Results : The rate constants measured in the dissolution of stoichiometric nicel ferrite by $V^{II}(pic)_3$ are summarised in Tables A5 and A6. In general solutions contained an excess of picolinate to ensure that all V^{2+} was present as the 1:3 complex, although in a few runs a significant amount of the 1:2 complex was present. Corrections have been made to the calculated free picolinate concentrations shown to allow for picolinate complexed to the small amount of V^{III} present as an impurity in the V^{II} solutions. Most solutions contained also a surfactant to aid dispersion of the oxide, and a buffer to keep the pH constant. The concentration of each additive was varied in turn to elucidate the dependence of rate on concentration. The results obtained can be summarised as follows :

(i) Using formate as buffer (80°C) a good linear dependence on $[V^{II}]$ was found (Fig. A.19) for $[V^{II}] = (2 - 13) \times 10^{-3}$M, with no evidence for any pathway independent of $[V^{II}]$. With acetate as the buffer (60°C) a linear dependence on $[V^{II}]$ was again found (Fig. A19) for $[V^{II}] = (0.9 - 7) \times 10^{-3}$M. Here however there was some indication of a $[V^{II}]$- independent pathway. A dependence of the form given in Eqn. (8), gives

$$k_{obs} = a + b[V^{II}] \qquad (8)$$

a good description of the data, and a linear regression of $[V^{II}]$ on k_{obs} gives $a = 3 \times 10^{-4}$ min^{-1}, and $b = 0.4$ M^{-1}min^{-1}. These experiments have, however, a relatively large experimental error (ca.15%). The intercept is thus within the experimental error of measurements, and in no sense do they establish the existence of a $[V^{II}]$- independent pathway. Other interpretations of the data are possible, for instance that the reaction becomes less than first

TABLE A5

Effect of Buffer on the $V(pic)_3^-$ + $NiFe_2O_4$ Reaction[a]

Buffer		pH	$k_{obs}/[V^{II}]^b$
Conc./M	type		M^{-1} min^{-1}
0.1	HCO_2^-	4.3	1.6
0.2	HCO_2^-	4.6	1.8
0.5	HCO_2^-	4.9	1.2
0.1	$CH_3CO_2^-$	4.4	2.2

a Measurements made in solutions containing also ca. 3×10^{-3} M $V(pic)_3^-$ + 2.9×10^{-2} M free picolinate + 20 ppm Triton X-100; T = 80°C.

b Rate constants based on the amount of iron dissolved in the reaction.

TABLE A6

Effect of Surfactant on the $V(pic)_3^-$ + $NiFe_2O_4$ Reaction[a]

Surfactant		$k_{obs}/[V^{II}]$
Conc./ppm	type[b]	$M^{-1}\ min^{-1}$
0	-	1.6
20	T	1.6
100	T	1.5
100	NaLS	1.2
100	H	2.5

a Measurements made in solutions containing also ca. 3×10^{-3} M $V(pic)_3^-$ + 2.9×10^{-2} M free picolinate + 0.10 M HCO_2^-; pH 4.4, T = 80°.

b T = Triton X-100; NaLS = Sodium lauryl sulphate, H = Hyamine 1622.

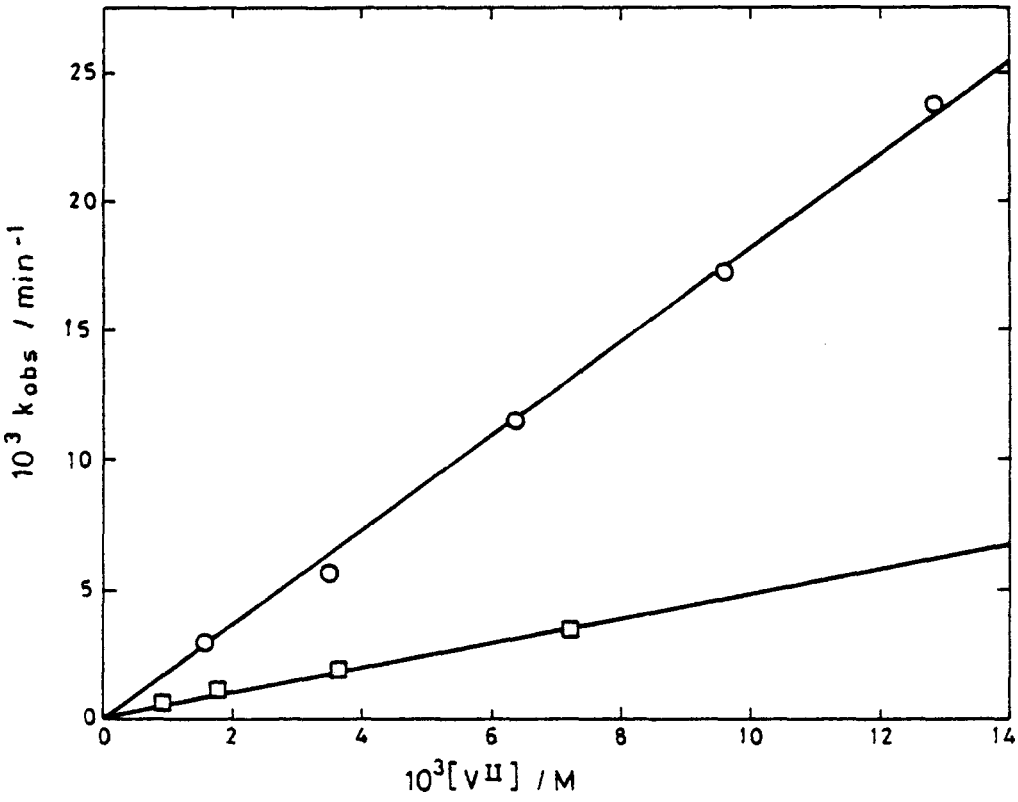

FIG. A19. Dependence of k_{obs} on $[V^{II}]$ in the Dissolution of $NiFe_2O_4$ by $V(pic)_3^-$ Measurements Made in Solutions Containing ca. 3×10^{-2} M Free Picolinate + 20 ppm Triton x-100 pH 4·4 and (o) 0·10 M HCO_2^- at 80°C or (□) 0·10 M Acetate at 60°C

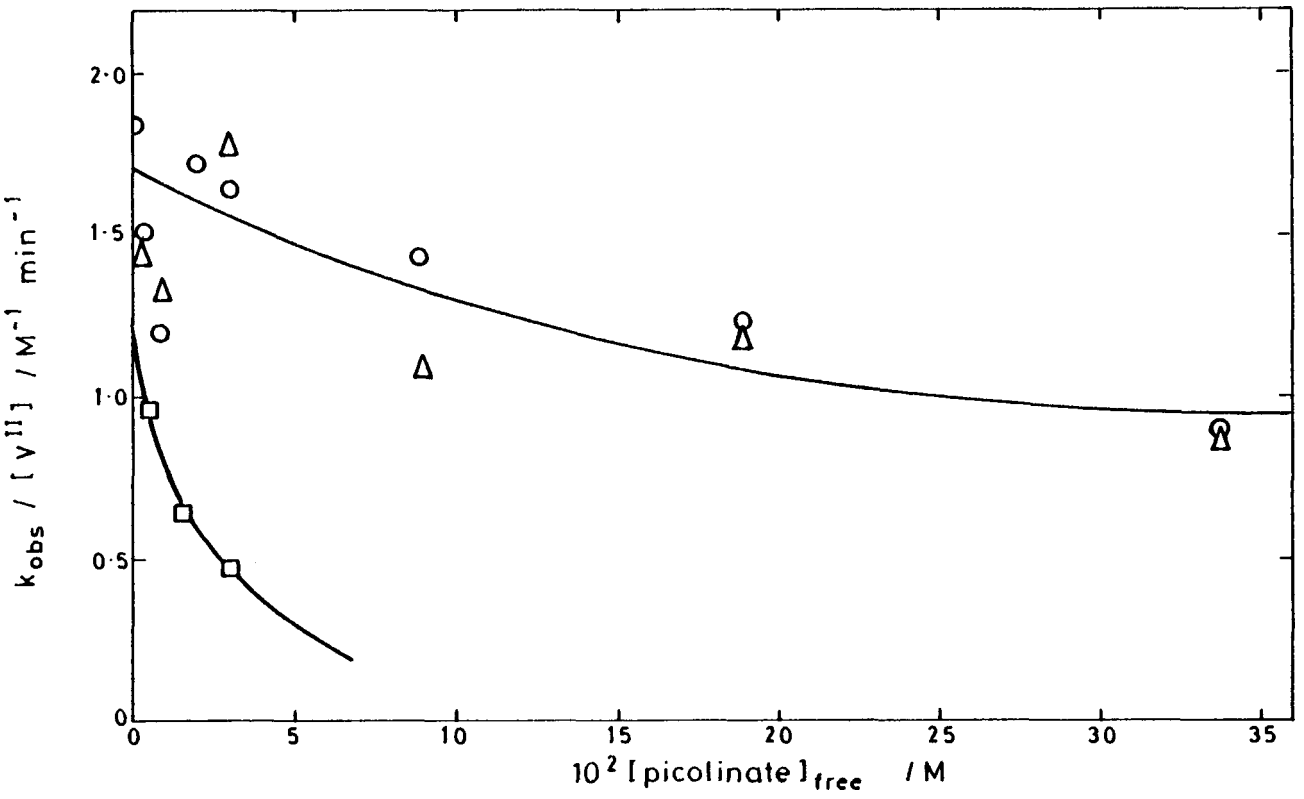

FIG. A20. Dependence of k_{obs} / [V^{II}] on Free Picolinate Concentration in the Dissolution of $NiFe_2O_4$ by $V(pic)_3^-$. Measurements Made in Solutions Containing ca. 3×10^{-3} M $V(pic)_3^-$ + 20ppm Triton X-100, pH 4·4, and (o,Δ) 0·10 M HCO_2^- at 80°C or (□) 0·10 M Acetate at 60°C. (o) and (□) Based on Amount of Iron Dissolved, (Δ) on Nickel Dissolved

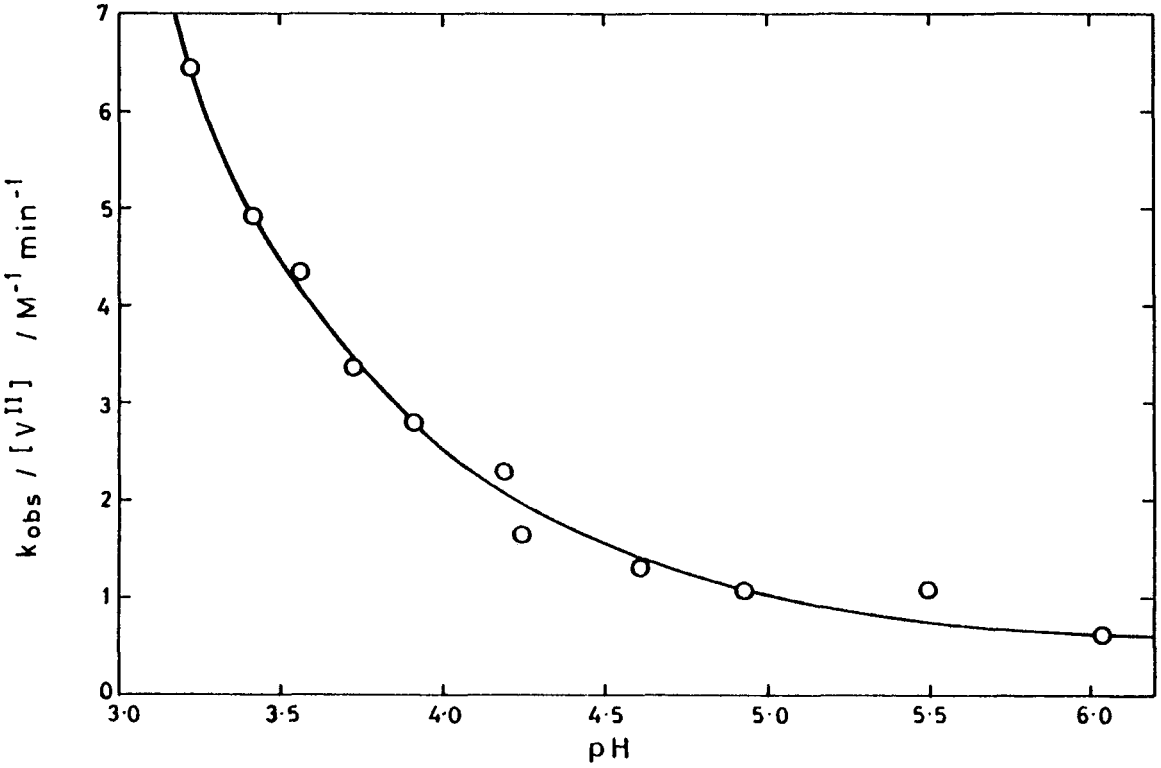

FIG. A21. Dependence of k_{obs} / $[V^{II}]$ on pH in the Dissolution of $NiFe_2O_4$ by $V(pic)_3^-$. Measurements Made in Solutions Containing ca. 3×10^{-3}M $V(pic)_3^-$ + $2{\cdot}9 \times 10^{-2}$ M Free Picolinate + 0·10M HCO_2^- + 20ppm Triton X-100, 80°C

order in $[V^{II}]$ at high $[V^{II}]$, but they provide no good evidence for pathways other than that involving direct reaction with V^{II} at the rate-determining step.

(ii) Picolinate

Only a weak dependence on [picolinate] was found, the rate falling by a factor of ca. 2 on increasing the free picolinate concentration from ca. 0 to 0.35M in the presence of formate buffer (80°C) or ca. 0 to 0.03M with acetate buffer (60°C), as shown in Fig. A20.

(iii) pH

A marked increase in the rate was found on decreasing the pH. With formate buffer (80°C) the rate increased 20-fold in the pH range 6 to 3.2 (Fig. A21). Less extensive data are available for the acetate system (60°C), but the trend was similar.

(iv) Surfactant

Varying the concentration of the surfactant Triton X-100* had essentially no effect on the rate even under conditions where the surface was completely covered. Within experimental error there was no change in rate on omitting the surfactant altogether, and only minor changes on substituting an anionic surfactant, sodium lauryl sulphate, or a cationic one, Hyamine 1622†.

(v) Buffer

With formate as the buffer the rate was independent of $[HCO_2^-]$ for $[HCO_2^-] = 0 - 0.5$ M; substituting acetate as the buffer gave essentially the same results.

(vi) Temperature

The influence of temperature on the dissolution rate was investigated for both formate and acetate buffers in the temperature range 40 - 80°C. Good agreement with the Arrhenius law was obtained, as

---

* Triton X-100 is a proprietary name for a non-ionic surfactant composed of iso-octylphenoxypolyethoxyethanol containing approximately 10 ethoxy units.

† Hyamine 1622 is a proprietary name for di-iso-butylphenoxyethoxy-ethyldimethylbenzylammonium chloride monohydrate.

shown in Fig. 22. The activation energies obtained are shown in Table A7. The figures are very similar, and it is clear that the reaction is independent of the nature of the buffer.

(vii) Oxide Calcining Temperature

A number of experiments was done in which the calcining temperature of the oxide was varied. The range of temperatures over which calcining could be varied was limited to ca.1000 - 1400°C. The lower limit is set by the need for a temperature of at least 800°C in order to form the spinel phase, and the upper limit by the materials of construction of the calcining furnace, and indeed the oxide itself. As will be seen from the results in Table A8, increasing the temperature in this range decreased the rate by no more than a factor of two, a result probably due to the effects of sintering.

(viii) Other Factors

The influence of a number of other factors was also investigated, with the results shown in Table A9. Of particular note are the lack of effect of borate + Li^+, which would of necessity be present in any PWR decontamination as a nuclear poison; the minor effect of radiolysing the picolinic acid prior to dissolution; and the essential independence of the dissolution kinetics on stirring rate. In addition some blank experiments were performed. In no case did any significant amount of dissolution take place.

DISCUSSION

The linear dependence on $[V^{II}]$ clearly establishes that $V^{II}(pic)_3^-$ is involved in the rate-determining step. The dependencies on pH and [pic] we interpret according to the following simplified model based on the Langmuir adsorption isotherm. We suppose the surface of the oxide particles to be composed of identical reactive sites (designated s), which are independent of one another, and that picolinate or protons can be adsorbed at these sites to give s-pic or $s\text{-}H^+$ respectively. Reduction of the sites by $V^{II}(pic)_3^-$ leads to dissolution, the rate of the reaction depending on the nature of the adsorbate. In terms of chemical reactions we can write :-

$$V^{II}(pic)_3 + s \xrightarrow{k_o} V^{III}(pic)_3 + s^- \qquad (9)$$

$$s + H^+ \overset{K_1}{\rightleftharpoons} s - H^+$$

$$V^{II}(pic)_3 + s - H^+ \overset{k_1}{\rightarrow} V^{III}(pic)_3 + s - H \qquad (10)$$

$$s + pic \overset{K_2}{\rightleftharpoons} s - pic$$

$$V^{II}(pic)_3 + s - pic \overset{k_2}{\rightarrow} V^{III}(pic)_3 + (s - pic)^- \qquad (11)$$

The surface sites, s, can be identified with Fe^{3+} ions in the oxide. The appropriate rate expression is :

$$\frac{dM}{dt} = -\frac{1}{x} \cdot \frac{d[Fe]}{dt} = -kA = (k_o f_o + k_1 f_1 + k_2 f_2)\ A \qquad (12)$$

where M = mass of particles, x = fraction of Fe in oxide,

A = surface area of the oxide, k is a constant, f_o is the fraction of the surface uncovered, and f_1 and f_2 are respectively the fractions of the surface covered by protons and picolinate.

Rearranging and integrating Eqn. 12 and expressing f_o, f_1 and f_2 according to the Langmuir adsorption isotherm, gives

$$\frac{k}{r_o \rho} = k_{obs} = \frac{k_o + k_1 K_1 [H^+] + k_2 K_2 [pic]}{1 + K_1 [H^+] + K_2 [pic]}\ [V^{II}]$$

where r_o = mean initial radius of the particles and ρ = density of oxide.

Since increasing proton concentration increases the rate of dissolution and increasing excess picolinate reduces the rate the implication is that $k_1 > k_o > k_2$. Some estimated values for these rate constants, and the equilibrium constants K_1 and K_2 are given in Table A10.

3.3.2 Dissolution of Non-Stoichiometric Nickel Ferrite by $V^{II}(pic)_3$

The previous section described an extensive series of experiments on the dissolution of stoichiometric nickel ferrite by $V^{II}(pic)_3$. In this section attention is focussed on the dissolution of non-stoichiometric nickel ferrite. Three non-stoichiometric oxides have been used in this work, $Ni_{0.4}Fe_{2.6}O_4$,

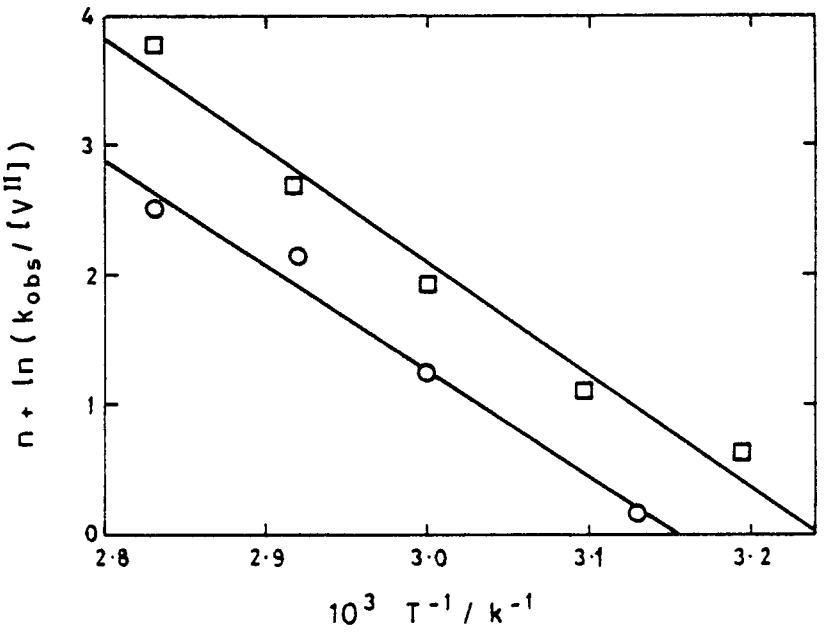

FIG. A22. Arrhenius Plot for the $V(pic)_3^-$ + $NiFe_2O_4$ Reaction. Measurements Made in Solutions Containing ca. 3×10^{-3} M $V(pic)_3^-$ + $2{\cdot}9 \times 10^{-2}$ M Free Picolinate, pH 4·4 and (o) 0·10 M HCO_2^- (n = 2) or (□) 0·10 M Acetate (n = 3)

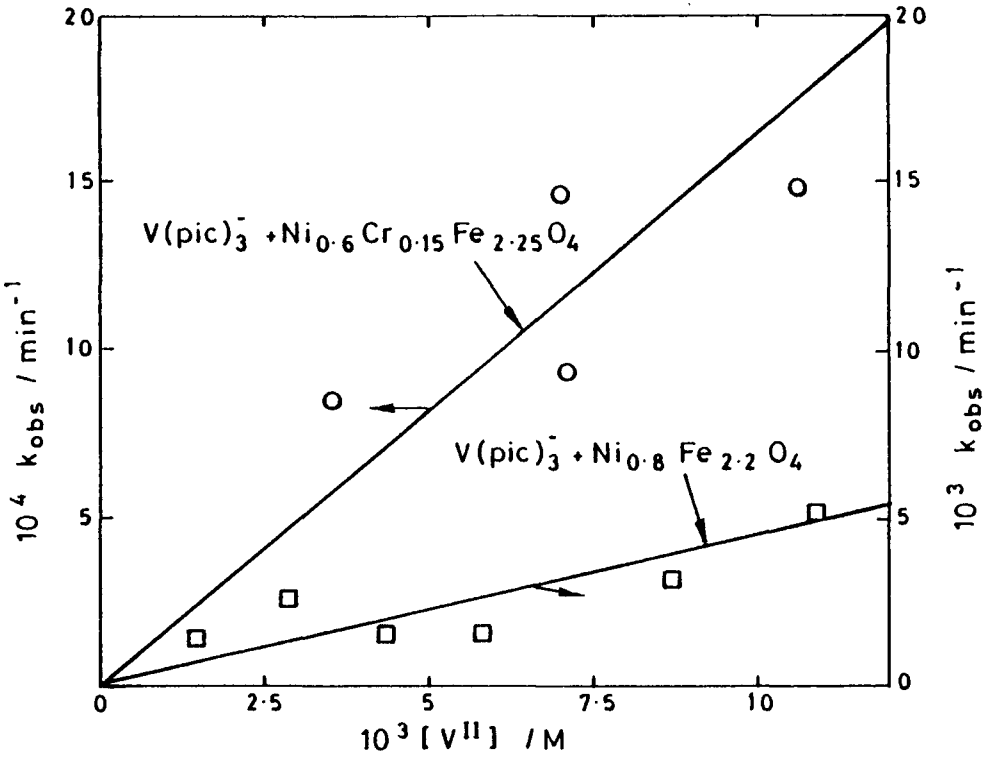

FIG. A23. Dependence of k_{obs} on [V^{II}] in the Dissolution of Non-Stoichiometric Nickel Ferrite by $V(pic)_3^-$. Measurements Made in Solutions Containing ca. 0·02M Free Picolinate + 0·1M HCO_2^- + 20 ppm Triton X-100, pH ca. 4·0, 80°C Lines Fitted by Eye

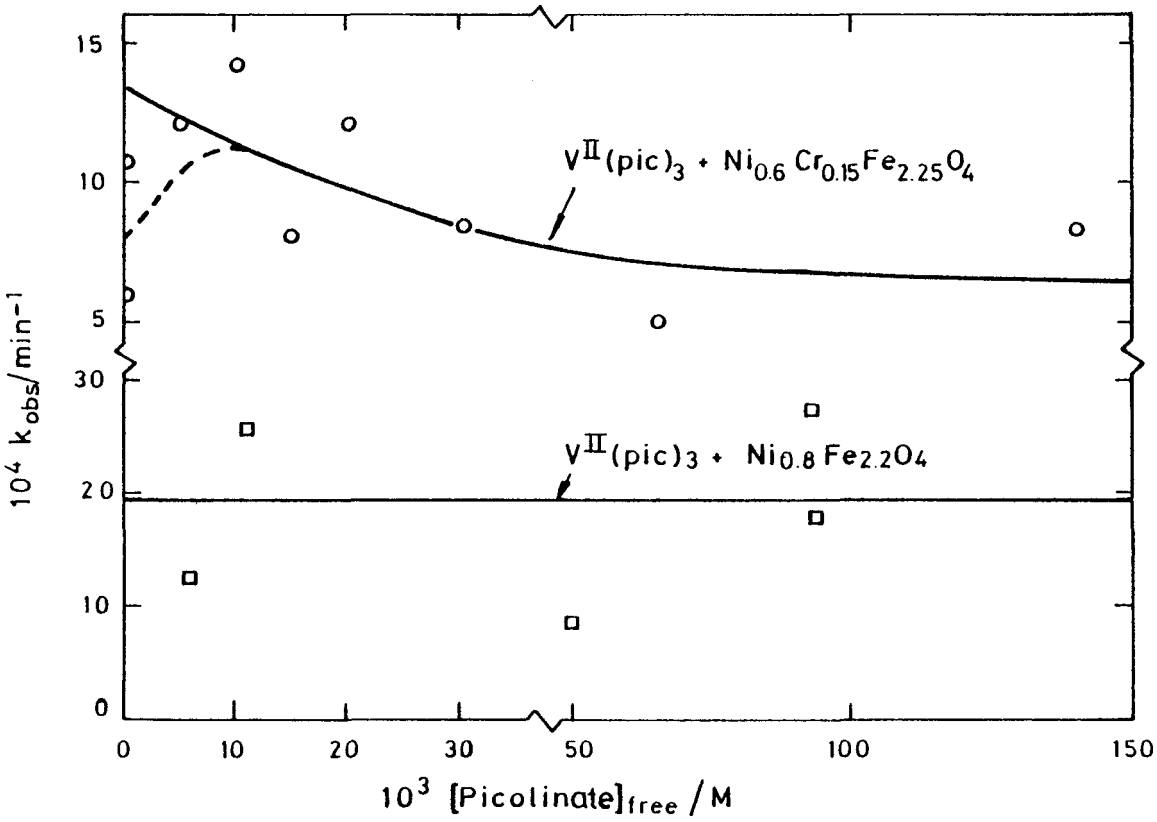

FIG. A 24 Dependence of k_{obs} on Free Picolinate Concentration in the Dissolution of Non-Stoichiometric Nickel Ferrites by $V(pic)_3^-$. Measurements made in Solutions Containing ca 3×10^{-3} M V^{II} + 0.1 M HCO_2^- 20 ppm Triton X-100, pH ca. 4.5, 80° C. Lines Fitted by Eye

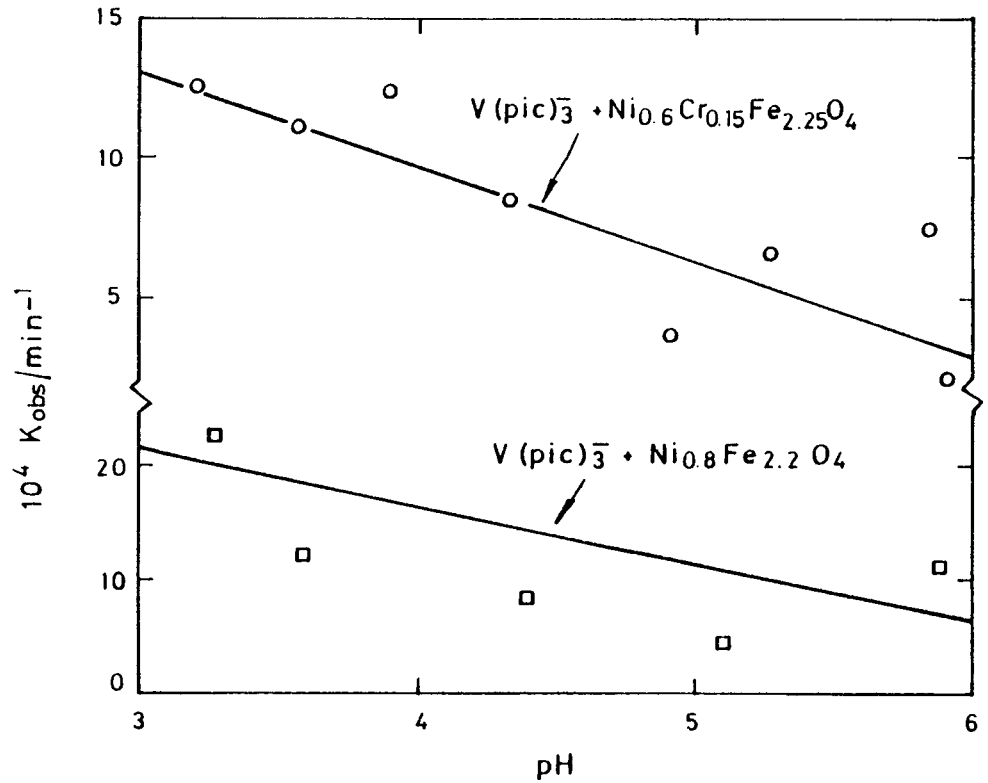

FIG. A 25. Dependence of k_{obs} on pH in the Dissolution of Non-Stoichiometric Nickel Ferrite by V(pic)$_3^-$. Measurements made in Solutions Containing ca 3×10^{-3}M V(pic)$_3^-$ + ca 3×10^{-2}M Free Picolinate + 0.1M HCO_2^- + 20ppm Triton X-100 at 80°C

$Ni_{0.8}Fe_{2.2}O_4$, and one containing a small amount of Cr^{3+}, $Ni_{0.6}Cr_{0.15}Fe_{2.25}O_4$. These oxides were chosen since they cover approximately the range of compositions found in crud samples removed from a number of American PWR's (Sandler 1978).

For each oxide the dependence of the dissolution rate on pH, [free picolinate], temperature and $[V^{II}]$ was investigated as described in the previous section. The results are shown in Figs. A23, A24, A25 and can be summarised as follows :-

i) $[V^{II}]$: For all three oxides the dissolution rate exhibited a first-order dependence on $[V^{II}]$ at $[V^{II}] \leq 10^{-2}$M. Other minor pathways may be present, but as noted with $NiFe_2O_4$ the experimental uncertainties are too great for these to be characterised.

ii) [Picolinate] : With the chromite-containing oxide, a small reduction in dissolution rate with increasing [picolinate] for concentrations in the range 0 - 0.1 M was found.

iii) pH : A small dependence on pH was found for all three oxides, decreasing the pH from 6 to 3 increased the rate by about a factor of two.

iv) Temperature : The effect of temperature was investigated in the range 40 - 80°C. In each case the dissolution rate depended on temperature according to the Arrhenius Law. The activation energies found are shown in Table A11.

The most striking difference between the results for the stoichiometric and non-stoichiometric oxides is the reduced sensitivity to experimental variables shown by the latter. The most likely cause of this is the calcining temperature, rather than the oxide stoichiometry, and probably arises through a reduction in the number of active surface sites. We interpret these results accordingly to the Langmuir adsorption mechanism described in the previous section.

3.4 DISSOLUTION KINETICS WITH OTHER V^{II} COMPLEXES

3.4.1 Dissolution Kinetics

In addition to the dissolution work described above a series of experiments was conducted to investigate the dissolution of $NiFe_2O_4$ by V^{II} complexed with other ligands. Varying the complexing group can have a number of effects, the

most obvious being to change the redox potential of the system as determined by the equilibrium :

$$V^{2+}(L)_n = V^{3+}(L)_n + e^-$$

In addition, or often perhaps as a result of this, the rate at which the LOMI reagent can reduce Fe^{3+} ion in this oxide surface on the one hand, or the solvent water on the other, can vary. Clearly an ideal reagent would have higher reactivity towards Fe^{3+} and be stable with respect to thermal decomposition.

Some 20 ligands were investigated with the results shown in Table A12. Also given are some observations on the thermal stability (expressed as a half-life) of the $V^{II}L_n$ complexes. These are based on visual assessments of changes in the colour of the reagent during the course of the reaction, and are intended only as a rough guide to the relative stability of the reagents. In some cases even this proved impossible either because the reagents were not coloured or because colour changes were only slight.

For comparative purposes some representative kinetic data obtained with $V^{II}(pic)_3$ are included.

Considering those complexes in which some dissolution took place, two broad conclusions can be drawn as follows :-

(i) Complexes of V^{II} which dissolve $NiFe_2O_4$ more rapidly than $V^{II}(pic)_3$ are generally not stable in water. (Histidine seems to be an exception - see also comment below).

(ii) Ligands which give complexes having adequate stability and which dissolve $NiFe_2O_4$ at a rate comparable with the picolinate system are generally much more expensive than picolinic acid.

Note that many of the ligands in the second category have structures similar to picolinic acid. The only ligand which showed any appreciable improvement over picolinic acid was histidine. This produced a complex which dissolves $NiFe_2O_4$ *ca.*3 times more rapidly than that with picolinate, yet was thermally stable at 80°C for several hours. Histidine forms 2:1 complexes with divalent metal ions such as Co^{2+} (Sillén and Martell), and this is presumably what happens with V^{2+}. Histidine has 4 coordinating positions, and so each $V^{II}(his)_2$ complex has two free coordinating positions on the ligand which by comparison with other divalent complexes with histamine and imidazole we

take to be ring nitrogens. It seems possible that this may account for the greater reactivity of the histidine complex over the picolinate complex in terms of the provision of a 'lead-in' group to facilitate electron transfer to the surface. Certainly this aspect deserves further study and suggests a possible way of improving on the complexing agents found to date.

A detailed study of the histidine system has not been made, although the system merits further attention. Something of the radiation chemistry of histidine is known (see for instance, Rao, Simic and Hayon, 1975; Bansal and Sellers, 1975; Swallow, 1978, p. 320), and there is no reason to anticipate complications from this source.

3.4.2 Thermal Stability

In the light of these observations, detailed tests were carried out on the stability of vanadous picolinate. Careful spectrophotometric measurement showed that the complex was fully stable for several hours at 80°C, in the absence of oxidising impurities (e.g. sulphate). Only a few percent decomposes in 24 hours. However, the complex is capable of reducing water at pH < 7, according to its redox potential. This reaction can be catalysed by metal surfaces; metal oxides have little effect, but clean stainless steel does catalyse the decomposition of the reagent. At a surface area: volume ratio of 100 cm^2/litre, which is of a similar order to reactor conditions, the half-life for disappearance of V^{II} can be as little as two hours (at 80°C). This is very variable, and presumably depends on the exact condition of the metal surface. This is not considered to be a major problem in a reactor decontamination, as it occurs only when the surfaces are clean.

3.5 RESULTS AND DISCUSSION OF LARGE-SCALE RUNS

The purpose of building the 5-litre scale apparatus was to obtain some experience with metal specimens in the reagents which had been put forward as a result of the dissolution experiments with powders.

The objectives could be sub-divided into the following categories :

1) to test the process of introducing reagents (with appropriate exclusion of aggressive counter-ions) into a central reservoir;

2) to test oxide solubilisation in the reagent using a variety of metal specimens which contained oxides grown or deposited in high temperature water.

TABLE A7

Activation Energies for the $V(pic)_3^-$ + $NiFe_2O_4$ Reaction

Buffer	E_a/kJ mol^{-1}
formate	67
acetate	72

TABLE A8

Effect of Oxide Calcining Temperature on the Kinetics of the $V(pic)_3^-$ + $NiFe_2O_4$ Reaction[a]

Oxide preparation method	Calcining Conditions	$k_{obs}/[V^{II}]$ M^{-1} min^{-1}
oxalate	6h at 1000°C	1.6
oxalate	12h at 1000°C	1.7
oxalate	24h at 1400°C	0.90
carbonate	6h at 1000°C	0.41
carbonate	6h at 1200°C	0.34
carbonate	6h at 1400°C	0.31
carbonate	72h at 1400°C	0.29

a Measurements made in solutions containing ca. 3×10^{-3} M $V(pic)_3^-$ + 2.9×10^{-2} M free picolinate + 0.10 M HCO_2^- + 20 ppm Triton X-100, pH 4.3, T = 80°C.

TABLE A9

Effect of Stirring Rate and Additives on the $V(pic)_3^-$ + $NiFe_2O_4$ Reaction, and Blank Experiments

Reagents etc.	$k_{obs}/[V^{II}]$ M^{-1} min^{-1}
Effect of stirring rate[a]	
no stirring	1.9
small stirring bar at maximum speed[b]	1.6
large stirring bar at maximum speed	1.6
Effect of other Additives[a]	
no other additives	1.6
0.10 M NaCl	1.7
0.10 M Na_2SO_4	1.8
0.10 M KSCN	1.5
0.10 M boric acid + 1 x 10^{-4} M Li^+	2.0
Picolinic acid irradiated (ca. 20 M rad) in deaerated aqueous solution before dissolution run	1.4
Blank experiments[c]	
0.04 M picolinate + 0.10 M HCO_2^-, pH 4.6	< 1% dissolution in 4½h
1.0 M H_2SO_4	< 1% dissolution in 4½h

a Measurements made in solutions containing also ca. 3 x 10^{-3} M $V(pic)_3^-$ + 2.9 x 10^{-2} M free picolinate + 0.10 M HCO_3^- + 20 ppm Triton X-100, pH 4.3, T = 80°C.

b Standard conditions used for all other dissolution runs.

c Solutions contained also 20 ppm Triton X-100, T = 80°C.

TABLE A10

Rate and Equilibrium Constants for the Individual Processes in the $V(pic)_3^-$ + $NiFe_2O_4$ Reaction

reaction[a]	value[b]
k_o	0.75 M^{-1} min^{-1}
k_1	13 M^{-1} min^{-1}
k_2	0.75 M^{-1} min^{-1}
k_1	2300 M^{-1}
k_2	20 M^{-1}

a See p. A24.

b At 80°C, I = 0.1 M.

TABLE A11

Activation Energies for the Reaction of Non-Stoichiometric Nickel Ferrite with $V(pic)_3^-$ [a]

Reaction	E_a/kJ mol^{-1}
$V(pic)_3^- + Ni_{0.4}Fe_{2.6}O_4$	68 ± 10
$V(pic)_3^- + Ni_{0.6}Cr_{0.15}Fe_{2.25}O_4$	75 ± 11
$V(pic)_3^- + Ni_{0.8}Fe_{2.2}O_4$	72 ± 11

a) Measurements made in solution containing ca. 3×10^{-3} M $V(pic)_3^-$ + 2.9×10^{-2} M free picolinate + 0.10 M HCO_2^- + 20 ppm Triton X-100, pH 4.4, with oxide calcined at 1400°C.

TABLE A12

Dissolution of $NiFe_2O_4$ by V^{II} Complexes[a]

Ligand	[L]/M	pH	$10^3 k_{obs}/min^{-1}$	Thermal Stability of $V^{II}L_n$ Complex[b]	Comments
Picolinic Acid	0.03	4.4	6.0	Stable	
Picolinic acid	0.1	4.2	4.9	Stable	Precipitate Formed
Nicotinic acid	0.1	4.2	4.8	Stable	
Iso-nicotinic acid[c]	0.1	4.1	∿ 0	$\tau_{\frac{1}{2}}$ < 1 min.	
2-pyridylacetic acid hydrochloride	0.1	3.4	6.7	Stable	
Pyridine-2,6-dicarboxylic acid	0.025	4.0	ca. 20	$\tau_{\frac{1}{2}}$ ∿ 10 min.	
Pyridine-2,2-dicarboxylic acid	0.1	4.1	∿ 0	$\tau_{\frac{1}{2}}$ ∿ 2 min.	
3-hydroxy picolinic acid	0.025	4.7	∿ 0	$\tau_{\frac{1}{2}}$ ∿ 2 hrs.	
3-hydroxy pyridine	0.025	5.3	5.2	Stable	
Pyrazine-2-carboxylic acid	0.1	3.2	∿ 0	$\tau_{\frac{1}{2}} \leq$ 2 min.	
1,4-piperazine bis(ethanesulphonic acid) [PIPES]	0.1	4.9	∿ 0.1	Probably Stable or Long-lived	Precipitate Formed
N-methyl pyrrole-2-carboxylic acid	0.1	4.6	1.4	$\tau_{\frac{1}{2}}$ ∿ 0.5 hr.	
Furan-2,5-dicarboxylic acid	0.1	3.1	0.9	Stable	Precipitate Formed
Tetrahydrofuran-2,3,4,5-tetracarboxylic acid[d]	0.1	2.4	0.9	Stable	
Potassium hydrogen phthalate[e]	0.1	4.3	∿ 0	$\tau_{\frac{1}{2}}$ < 1 min.	
Ethyleneidamine diacetic acid [EDDA]	0.03	5.5	ca. 16	$\tau_{\frac{1}{2}}$ ∿ 10 min.	

a) Unless otherwise stated other conditions were: 3×10^{-3} M V^{II} + 0.1 M HCO_2^- + 20 ppm Triton X-100, T = 80°C.

b) Thermal stability assessed from colour changes - the half-lives are very approximate and intended only as a guide.

c) T = 50°C

d) Mixture of isomers : T = 43°C

e) T = 34°C

TABLE A12 (cont'd)

Dissolution of $NiFe_2O_4$ by $V^{II}L_n$

L	pH	k/m^{-1}	Thermal Stability
1-Piperidine propionic acid 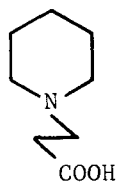	4.7	4.3×10^{-4}	$t_{\frac{1}{2}} \sim$ ca. $\frac{1}{2}$ hr.;ppt formed
4-Amino salicylic acid 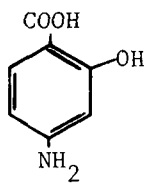	7.5	< 5% diss in 4hr.	$t_{\frac{1}{2}}$ ca.hr.
Pipecolinic acid 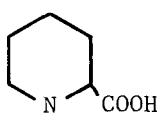	4.8	4.8×10^{-4}	?
Picolinic acid N-oxide 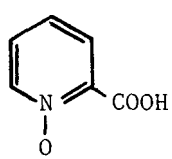	3.6	< 5% diss in 4hr.	White ppt formed
Histidine 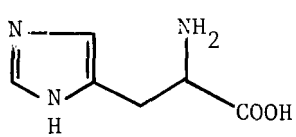	6.7 6.2 5.7	6.1×10^{-3} 8.5×10^{-3} 1.6×10^{-2}	$t_{\frac{1}{2}} > 1$ hr.

Continued/..

TABLE A12 (cont'd)

Dissolution of $NiFe_2O_4$ by $V^{II}L_n$

L	pH	k/m^{-1}	Thermal Stability
Morpholine 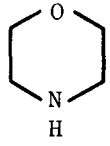	9.2	< 5% diss in 4 hr.	$t_{\frac{1}{2}}$ ∿ few minutes greyish ppt formed

All solutions containing 0.1 M total ligand + 3.4×10^{-3} M V^{II}; T = 80°C + 0.1 M HCO_2^- + 20 ppm Triton X-100

$NiFe_2O_4$: calcined 6 h at 1000°C

3) to obtain preliminary information concerning corrosion behaviour in the reagent, by weight loss measurement and metallographic examination;

4) to test ion-exchange purification procedures appropriate to the waste-management of resultant decontamination liquors.

A summary of the runs conducted in the 5-litre apparatus is given in Table A13. An analysis of the results contained in Table A14 is given below.:

The first run was conducted to commission the apparatus and to test the anion-exchange behaviour of sulphate to acetate in the reagent preparation. The anion-exchange column functioned as expected and no obvious colour change occurred on the passage of the vanadium sulphate/sulphuric acid solution through the column. Previous smaller scale ion-exchange tests had shown that the solution emerging from the column was sulphate free. There was no evidence of massive loss of vanadium by precipitation on the column.

Complex formation occurred on introduction of the vanadium acetate solution to the bipyridyl/water/haematite mixture. The mixture was held at 80°C for 20h. At the end of the run it was noted that a small quantity of precipitate had formed in the vessel and it was surmised that this was probably present in the smaller scale experiments, but was insufficient to be observable. The apparent deviation from cubic kinetics in the V/bipy small-scale runs could well have been a result of this precipitation occurring on the suspended oxide, thereby progressively retarding dissolution.

The most likely explanation of the precipitation is that it is vanadium(III) hydroxide formed as a result of the low stability of the V(III) bipy complex. This is supported by the literature on vanadium bipy complexes. The vanadium (II), once oxidised by the iron oxide, is relinquished from the tris-bipy complex and deposits as vanadium(III) hydroxide.

Ion exchange of the resulting liquor was conducted by passing it through a cation-exchange column. Analysis of the effluent showed it to be free of iron (< 1% of influent) and the bipyridyl content was tested by the following procedure. The effluent was buffered with acetic acid/sodium acetate and excess ferrous chloride was added. No colour was observed. On addition of bipy a brilliant red colour developed from the iron/bipy complex. Though the test is crude it indicates that the bipy concentration was not significant in

the column effluent. Thus it would seem that the cations are held on the ion exchange column as the bipy complexes and excess bipy is held as the protonated cationic form ($H\text{-bipy}^+$).

Runs 2-10 were conducted with the 9-chrome steel sample (see Appendix 2.4). The purpose of these runs was to gain experience with the reagents and metallographic techniques before proceeding to actual reactor specimens.

In run 2 citrate was added to the mixture in order to prevent the deposition of V(III) hydroxide. The citrate V(II) complex is relatively weak, and thus it was expected that in the presence of a mixture of bipyridyl/citrate the V(II) would form the bipyridyl complex preferentially. Indeed the colour formed indicated this to be the case. At the end of the run there was no precipitate indicating that the citrate was holding the V(III) in solution as planned. The specimen was found to be partially cleaned - the black magnetite overlayer was completely removed and the underlying chrome-rich layer was exposed but not completely dissolved.

In runs 3 and 4 the possibility of omitting bipy was tested. In this case the V(II) citrate complex is not stable, as mentioned above, but decomposes by a pathway as yet unknown to give V(III) citrate. Similar dissolution behaviour was observed as in run 2.

In runs 5, 6 and 7 the dissolution behaviour of the 9-chrome sample in citrate alone was investigated in order to gauge the effect of the reductant metal ion. The fact that good dissolution was observed in the absence of reductant suggested that the base metal was itself acting as a reducing agent by the corrosion reaction

$$Fe \rightarrow Fe^{2+} + 2e^-$$

In run 6 all cut metal edges of the specimen were blanked to prevent the exposed metal area acting as the reducing agent, and in run 7 a whole tube section was used without exposed cut surfaces, but very little difference was observed. It is possible that the corrosion reaction occurs in the bottom of pits on exposed metal. The metal specimen must enhance the rate of dissolution in some way, since the rates observed would be inconsistent with the measurements made on magnetite itself.

In run 8 the vanadous picolinate reagent was tested prior to its use on an active sample. Similar results were obtained to those in the other runs. Ion exchange was carried out, and both iron and vanadium were found to be absent in the ion exchange eluate.

The first active sample used was the SGHWR specimen which was of stainless steel 321 exposed in-reactor to oxygenated water. The sample activity was measured with a counter at fixed geometry and the decontamination conducted (the specimen did not have blanked edges). A DF of 7.5 was obtained in the 12-hour run. Metallographic examination before and after the exercise showed that the residual oxide was associated with deep (2-3 μ) pits in the 'as received' sample, Figure A26a. Analysis of measured DF and solution activity indicated that the oxide was still being removed at the end of the exercise (Figure A27). Metallography showed residual oxide in the bottom of surface pits (Figure A26b).

The sample was resubmitted to the reagent for a further 24 h period (run 10, Figure A28). Further activity removal took place yielding a total DF of ∿ 35. This figure was confirmed by comparison of an 'as received' and cleaned coupon by GeLi gamma spectrometry, which also confirmed that the gamma activity was entirely ^{60}Co.

Ion exchange of the solution yielded an activity-free eluate (> 99% removal). Elution of the resin with hydrochloric acid yielded the following results :-

	Bed Vol's	Picolinate	Activity	Vanadium
0.5 N HCl fraction	4	0.2	Trace	Trace
2.0 N HCl fraction	4	0	1	1
6.0 N HCl fraction	4	0	Trace	Trace

(Normalised to total calculated in each column).

It is surmised that the missing 80% of picolinate was eluted with the column eluate at the end of the decontamination run (c.f. bipy which is held by the column).

Weight loss measurements on run 10 indicated that the total corrosion during the 24-hour run was not greater than 0.5 μ.

Run 11 was conducted using the mild steel sample. Activity removal was more gradual in this case, possibly because of the high pH of the run (6.0 → 6.7), see Figure A29). During the run the pH was lowered by addition of acetic acid and the activity removal rate accelerated. The run was terminated prematurely by loss of nitrogen supply, but an overall DF of 5 had nevertheless been achieved.

Two further runs were carried out using samples of SGHWR pipework. In Run 17 the specimen was decontaminated in vanadous picolinate, at 4×10^{-3} M concentration, and the plot of activity remaining against time is shown in Fig. A30. A DF of 30 was achieved after 700 mins. Also shown in Fig. A30 is a decontamination plot for a similar S21 rise specimen being cleaned in a synthetic 'TURCO 4521' mixture used at 6% w/w concentration in the same apparatus. This gave a DF of 5.5 after 500 min. and a final value of 12 after 1350 min. and was therefore both slower and rather less effective than the low concentration LOMI reagent.

3.6 ADSORPTION OF PICOLINATE ON Fe_2O_3

The kinetic results of the system $NiFe_2O_4/V^{II}$ picolinate showed a slight rate dependence on the concentration of free picolinate. Since this is probably due to adsorption of the ligand at the oxide surface, a separate study was made of this phenomenon. The oxide used for this study was Fe_2O_3, calcined at 350°C; this had by far the greatest specific surface area of the oxides under consideration, making measurement of the extent of adsorption easy. We should expect the other oxides to give qualitatively similar results, allowing for the differences in surface area.

3.6.1 Experimental

Weighed samples of the oxide (typically 0.5g) were placed in suitable conical flasks, and the ligand, buffer and water added to the correct volume (10 ml). The flasks were sealed with bungs, shaken thoroughly and left to equilibrate for at least 24 hours, either at room temperature or in a thermostatted water-bath. The solid was then removed by filtration through a 0.22 μm filter, and the concentration of picolinic acid remaining in the solution was determined spectrophotometrically. In order to overcome the pH dependence of the spectrum, this measurement was carried out after dilution in 0.1 M HCl in all cases.

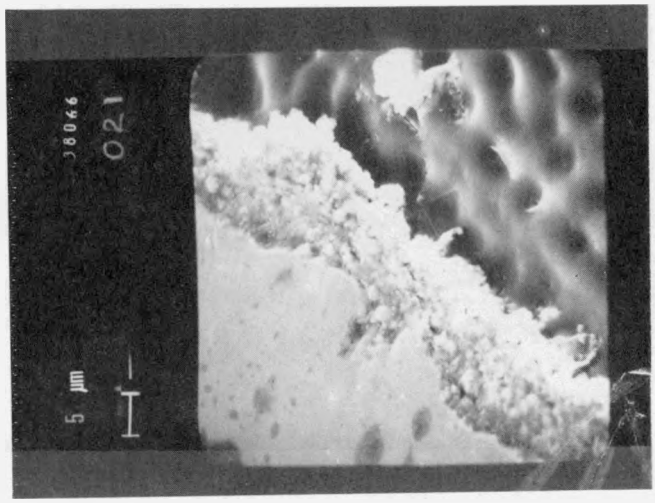

Fig. A26a. Electron Micrograph of SGHWR tubing prior to cleaning

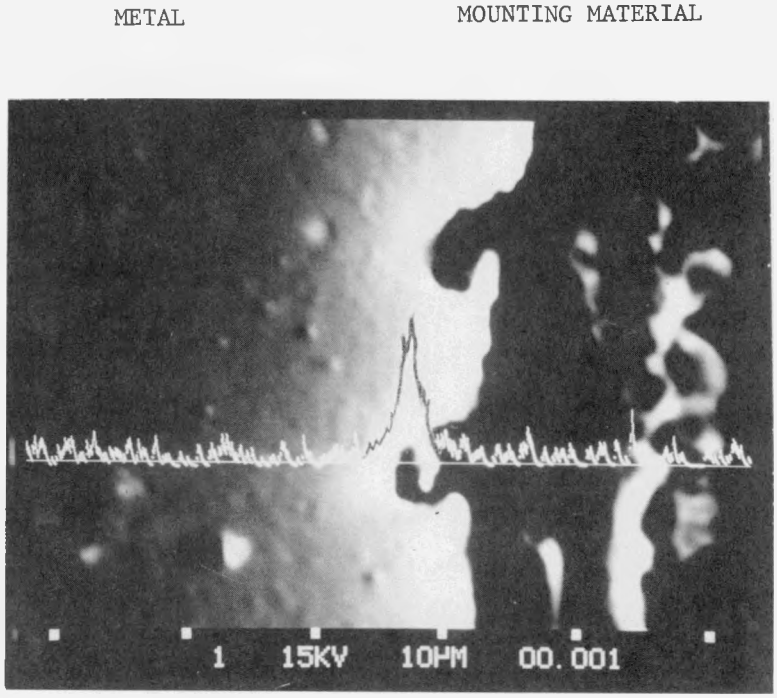

Fig. A26b. Electron Micrograph of cleaned WSGHWR tubing with EDAX Oxygen Scan (Run 9)

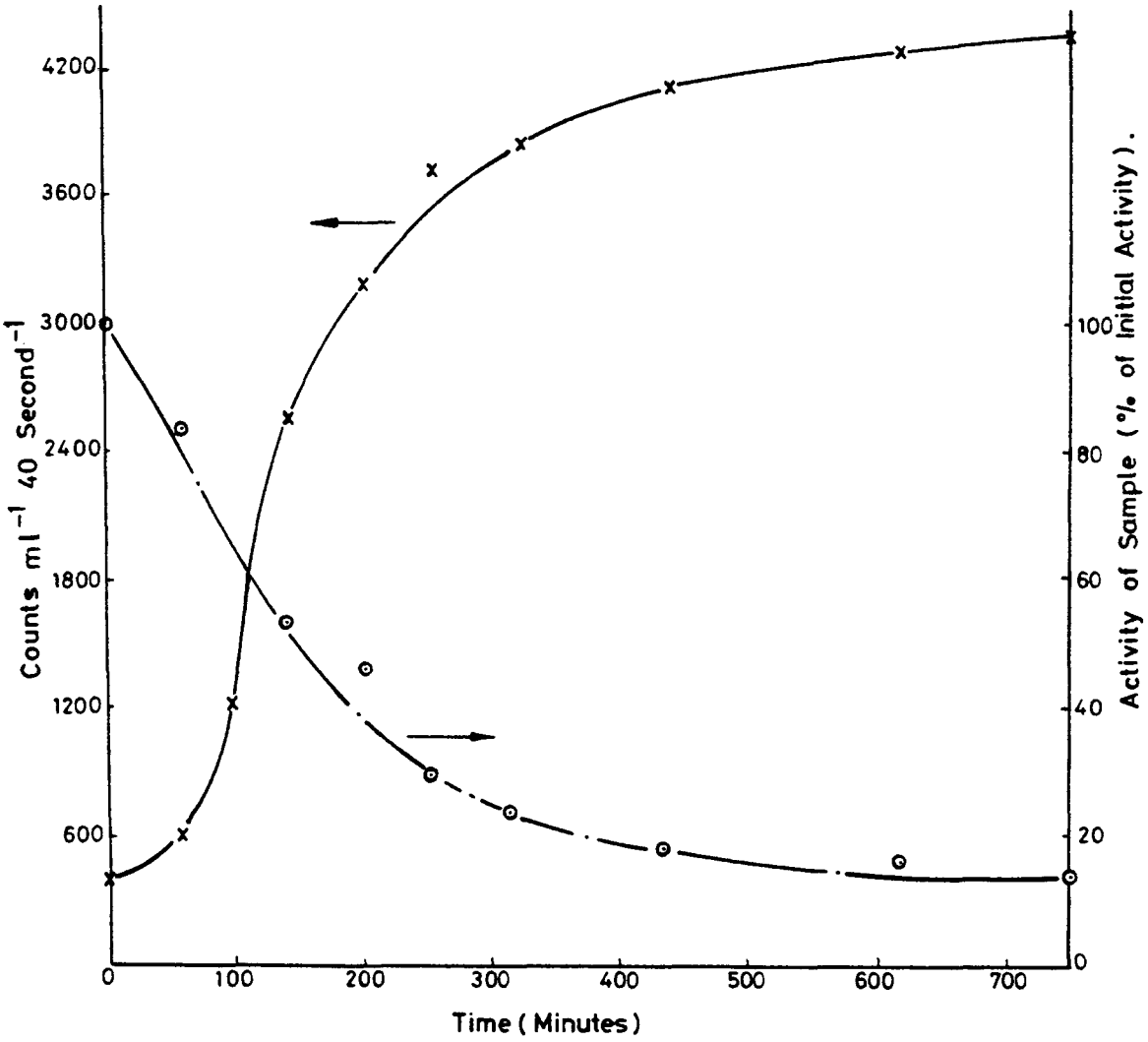

FIG A27 Decontamination of WSGHWR Riser Pipework Sample in Vanadium II Picolinate at 80°C. Run 9; Specimen & Solution Activity .v. Time

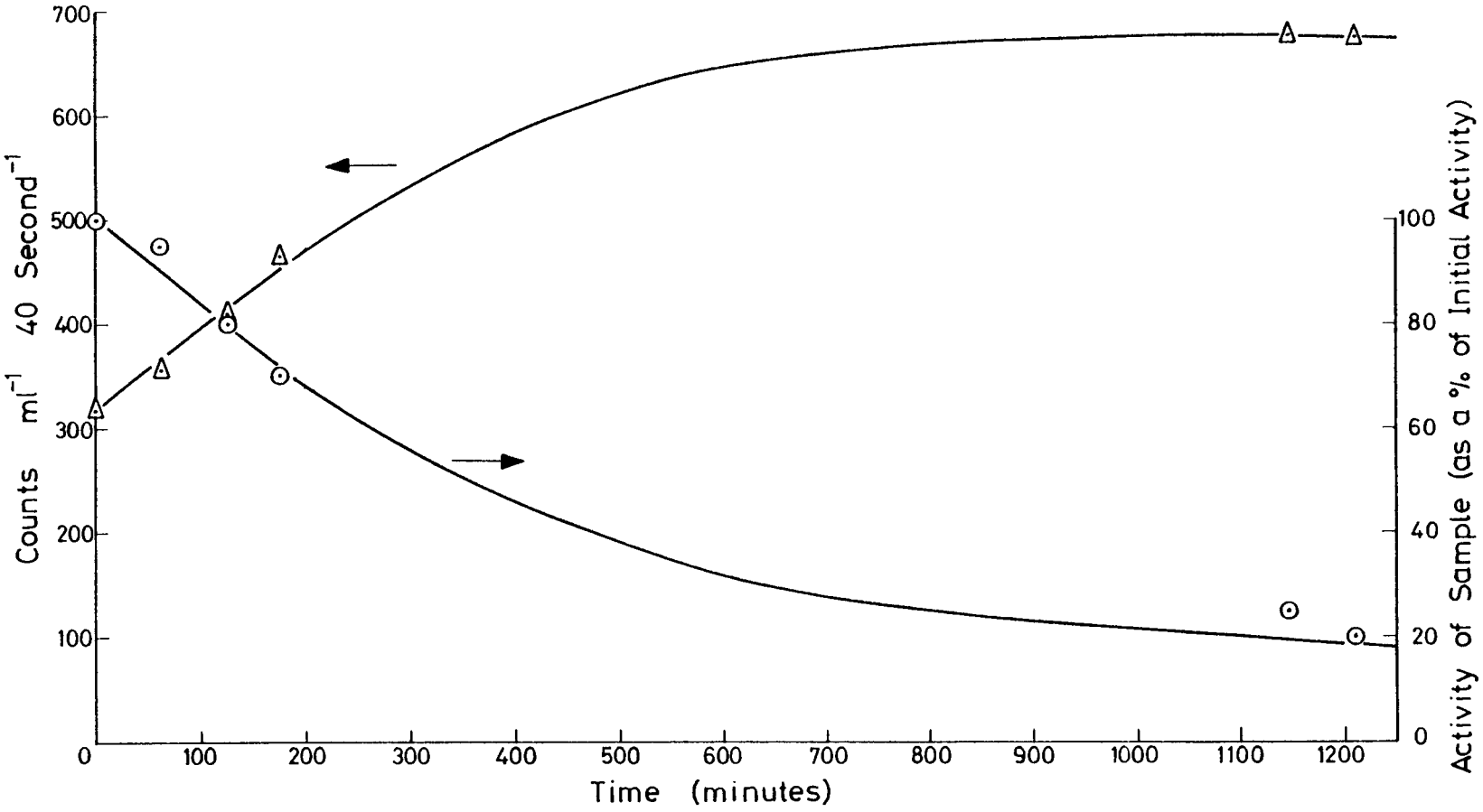

FIG. A28. Further Decontamination of WSGHWR Riser Pipework Sample in Vanadium II Picolinate at 80 °C. Run 10; Sample and Solution Activity v Time

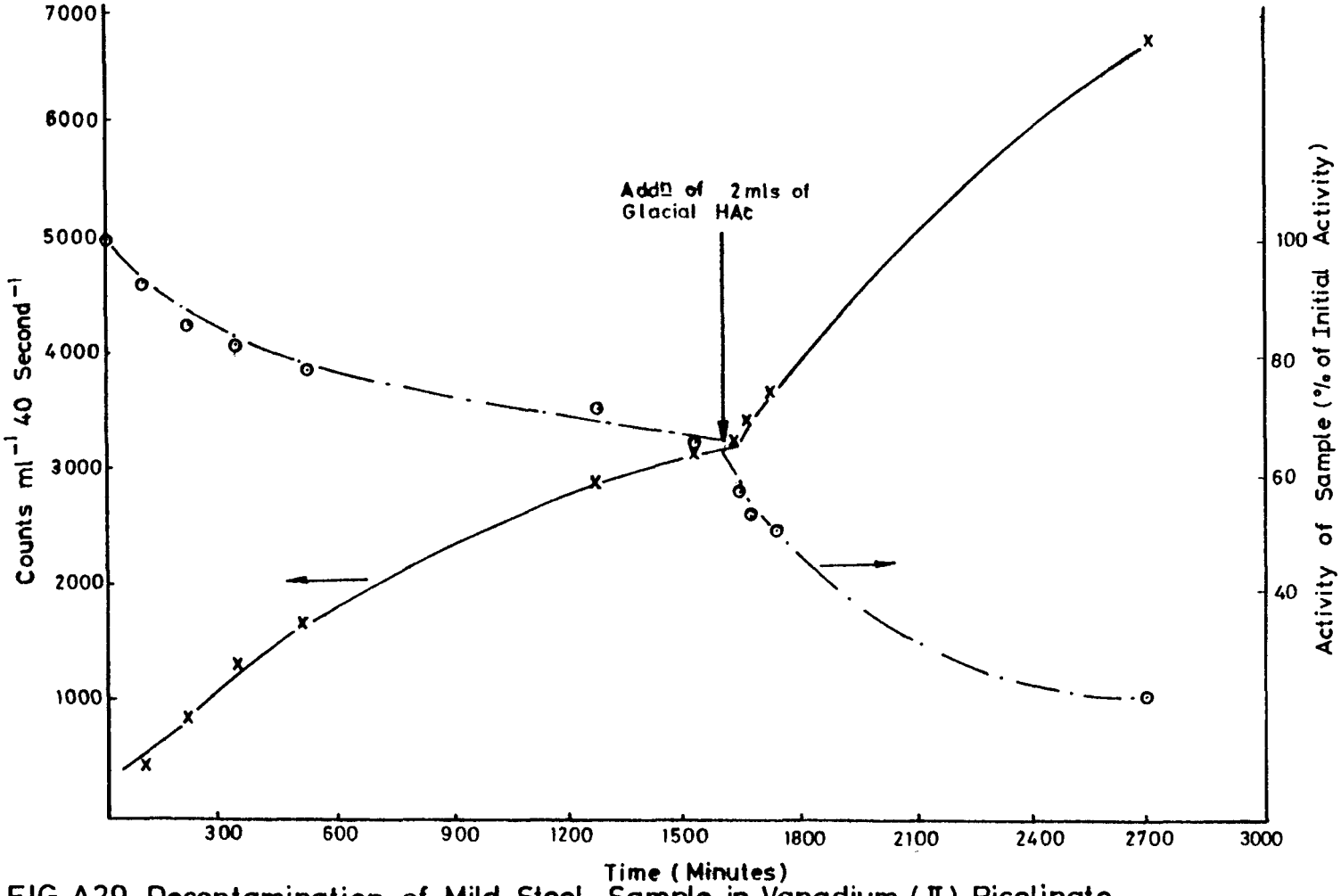

FIG A29. Decontamination of Mild Steel Sample in Vanadium (II) Picolinate. Run 11; Specimen & Solution Activity . v . Time

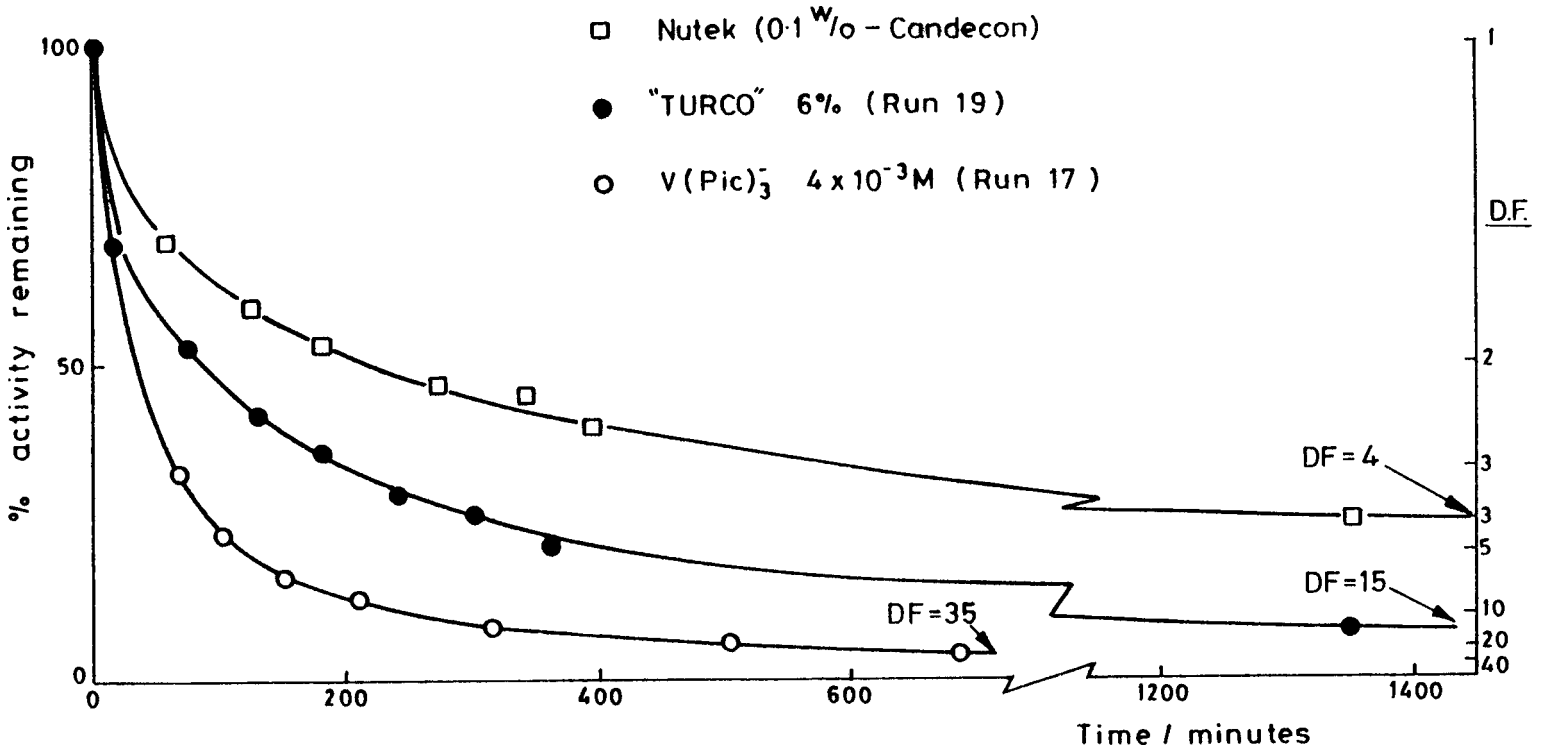

FIG. A30. SGHWR S21 Riser Tube Decontaminations

TABLE A13

Summary of 5-Litre Apparatus Runs

Run No.	Sample	Metal/Conc. (M)	Ligand/Conc. (M)	Temp.	pH
1	250 mg Fe_2O_3	V^{II} 2×10^{-3}	Bipy 1×10^{-2}	∿ 80	5.6
2	A	V^{II} 2×10^{-3}	{Bipy 7.5×10^{-3}} {Citrate 7.5×10^{-3}}	∿ 80	5
3	A	V^{III} 2×10^{-3}	Citrate 1.5×10^{-2}	∿ 80	4.5
4	A	V^{III} 2×10^{-3}	Citrate 1.5×10^{-2}	∿ 80	5.6
5	A	Nil	Citrate 1.5×10^{-2}	∿ 80	6.2
6	A (bonded edges)	Nil	Citrate 1.5×10^{-2}	∿ 80	6.2
7	A (whole tube section)	Nil	Citrate 1.5×10^{-2}	∿ 80	6
8	A	V^{II} 2×10^{-3}	Pic. 1×10^{-2}	∿ 80	5.6
9	B	V^{II} 2×10^{-3}	Pic. 1×10^{-2}	∿ 80	?
10	B (Same sample as 9)	V^{II} 2×10^{-3}	Pic. 1.5×10^{-2}	∿ 80	4.8
11	C	V^{II} 4×10^{-3}	Pic. 1.5×10^{-2}	∿ 80	6.0
17	B	V^{II} 4×10^{-3}	Pic. 1.5×10^{-2}	∿ 80	5.1
19	B	Nil	"TURCO 4521" 6%	∿ 80	4.3

Samples : A) 9-chrome ferritic steel oxidised at 350°C in steam/water under alkaline deoxygenated conditions.

B) AISI 321 stainless steel sample oxidised in Winfrith SGHWR reactor (BWR-type, neutral oxygenated water).

C) Mild steel sample oxidised under alkaline deoxygenated conditions in a reactor loop.

TABLE A14

Iron/Chromium Analyses of Large Scale Runs 1 - 8

Run 1 - Reagent V^{II}/bipy

Time (mins)	Iron in Solution (ppm)
0	∿ 0
120	11
200	14.5
1200	27

Run 2 - Reagent V^{II}/bipy/citrate

Sample Weight 25.80 g Solution Volume = 4 litres

Time (mins)	Iron in Solution (ppm)	Chromium (ppm)
15	2.1	
120	11.0	
240	17.8	0.14
330	21.5	

Run 3 - Reagent V^{III}/citrate

Sample Weight 22.28 g Solution Volume = 3 litres

Time (mins)	Iron in Solution (ppm)	Chromium (ppm)
10	9.75	
60	15.75	
100	21.00	
240	28.75	
1400	45.75	0.75

Run 4 - Reagent citrate

Sample Weight 24.14 g Solution Volume = 3 litres

Time (mins)	Iron in Solution (ppm)	Chromium (ppm)
0	1.7	
120	12	
200	16.3	
350	23.0	0.27

Run 5 - Reagent citrate

Sample Weight 7.95 g Solution Volume = 3 litres

Time (mins)	Iron in Solution (ppm)	Chromium (ppm)
150	3.67	
200	6.2	
1200	16.4	0.2

TABLE A14 (cont'd)

Iron/Chromium Analyses of Large Scale Runs 1 - 8

Run 6 - Reagent citrate

Sample Weight 12.67 g Solution Volume = 3 litres

Time (mins)	Iron in Solution (ppm)
120	4
400	10.5

Run 7 - Reagent citrate

Sample Weight ? Solution Volume = 3 litres

Time (mins)	Iron in Solution (ppm)	Chromium (ppm)
30	0	
80	1.5	
400	12.0	
1100	27.5	0.2

Run 8 - Reagent V^{II}/pic

Time (mins)	Iron in Solution (ppm)	Chromium (ppm)
35	2.4	
290	12.7	
320	14.0	
1100	32.5	0.22

3.6.2 Results

Plots of (amount absorbed) against (free ligand) at various pH values are given in Fig. A31 ($23^{o}C$) and Fig. A32 ($50^{o}C$). The data fit well to Langmuir adsorption isotherms, giving linear plots of c/m against c. (c = free ligand concentration, m = amount adsorbed). The full equation is

$$\frac{c}{m} = \frac{c}{m_s} + \frac{1}{bm_s}$$

where b is the binding constant and m_s the saturation coverage. We observe that the absorption rises to a maximum around pH 4.8, and falls away at higher pH. This is due to changes in b, the binding constant, which peaks at pH 4.8; the saturation coverage falls with pH over the whole range covered. Values of b and m_s were determined from least-squares straight line plots, and are given in Table A15. The dependence of b on temperature is small, with a factor of about two decrease from 23^{o} to 50^{o}. This implies a value of some 5 kcals mol^{-1} for the enthalpy of binding, $\Delta H^{\ominus}$.

3.6.3 Discussion

A clear pattern emerges from these results. The major interaction between the ligand and the surface is based on the attractions between Fe^{3+} ions and picolinate anions. The binding force is partly electrostatic and partly the chemical bond formation between the metal and the donor atoms of the ligand (N and O). The charge on the oxide surface varies with pH, being more positive at low pH, whereas the ligand is fully protonated at low pH, having a pK of 5.4. Thus the binding rises to a maximum in the pH range where significant deprotonation of the picolinic acid occurs, and falls away again as the charge on the oxide falls at higher pH. On the other hand the values of m_s are highest at low pH; this may be due to the repulsion between bound ligands being affected by surface protonation, or there may be a physical change in the oxide, exposing more metal ions in the surface.

The enthalpy of binding, $\Delta H^{\ominus}$, is low because electrostatic interactions are largely entropy-driven; with homogeneous solution reagents, typically, small positive values of $\Delta H^{\ominus}$ are greatly outweighed by large positive $\Delta S^{\ominus}$ values in processes such as ion-pair formation. The replacement of two or more bound water molecules by one picolinate also leads to a favourable entropy change.

TABLE A15

Adsorption of PicH on Fe_2O_3

T °C	pH	$\frac{m_s}{\mu \text{ moles/g}}$	$\frac{b}{10^2 \text{ M}^{-1}}$
23	3.8	88 ± 4	6.5 ± .6
	4.8	76 ± 3	20.5 ± .3
	5.4	79 ± 1	9.5 ± .5
	6.1	41 ± 2	3.3 ± .3
	8.8	$b \times m_s \approx 1.5 \times 10^3$	μ moles/g/M
50	3.8_5	107 ± 8	5.4 ± .8
	4.8	90 ± 4	10.5 ± 1
	6.1_5	48 ± 11	1.4 ± .5

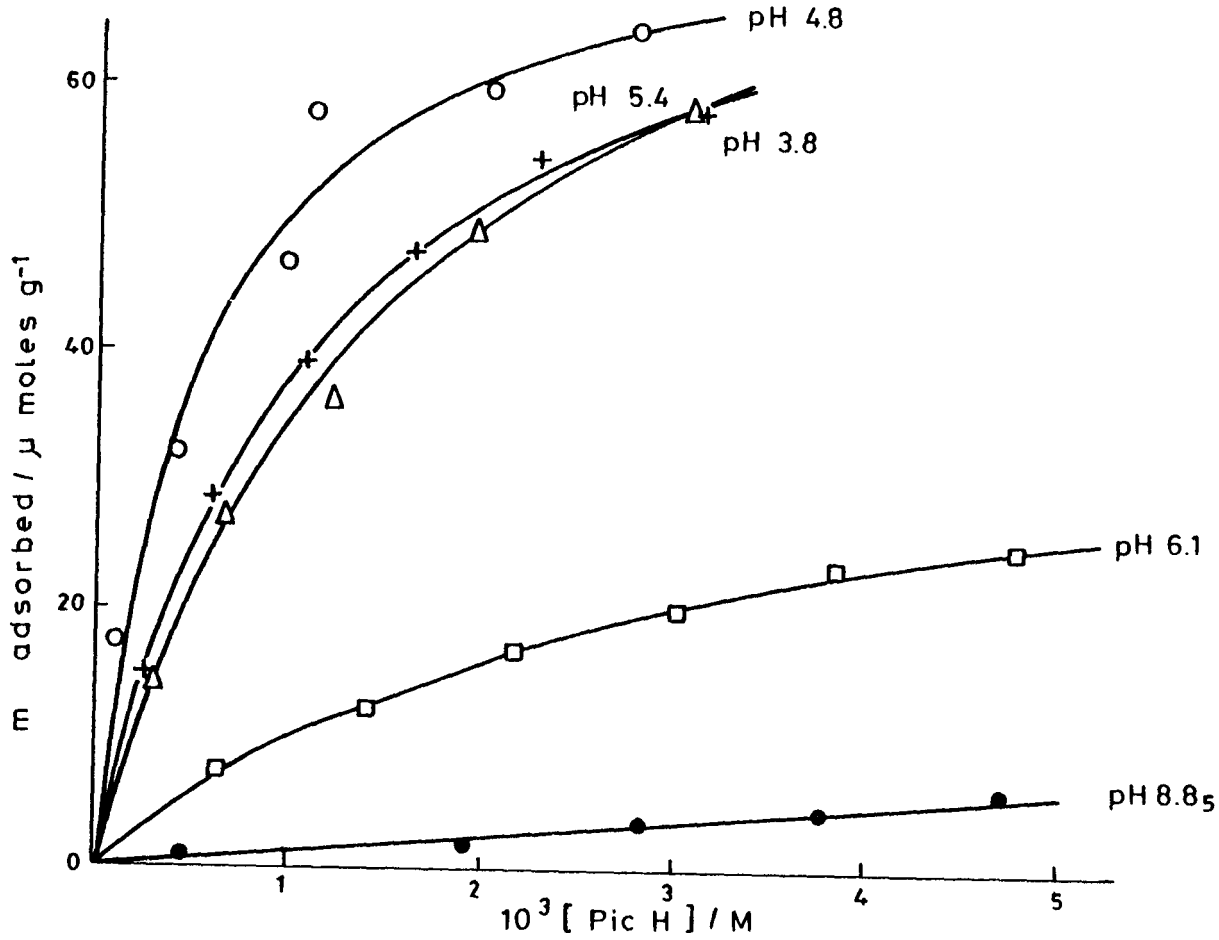

FIG. A 31. Adsorption of Picolinic Acid on Fe_2O_3 (23°C)

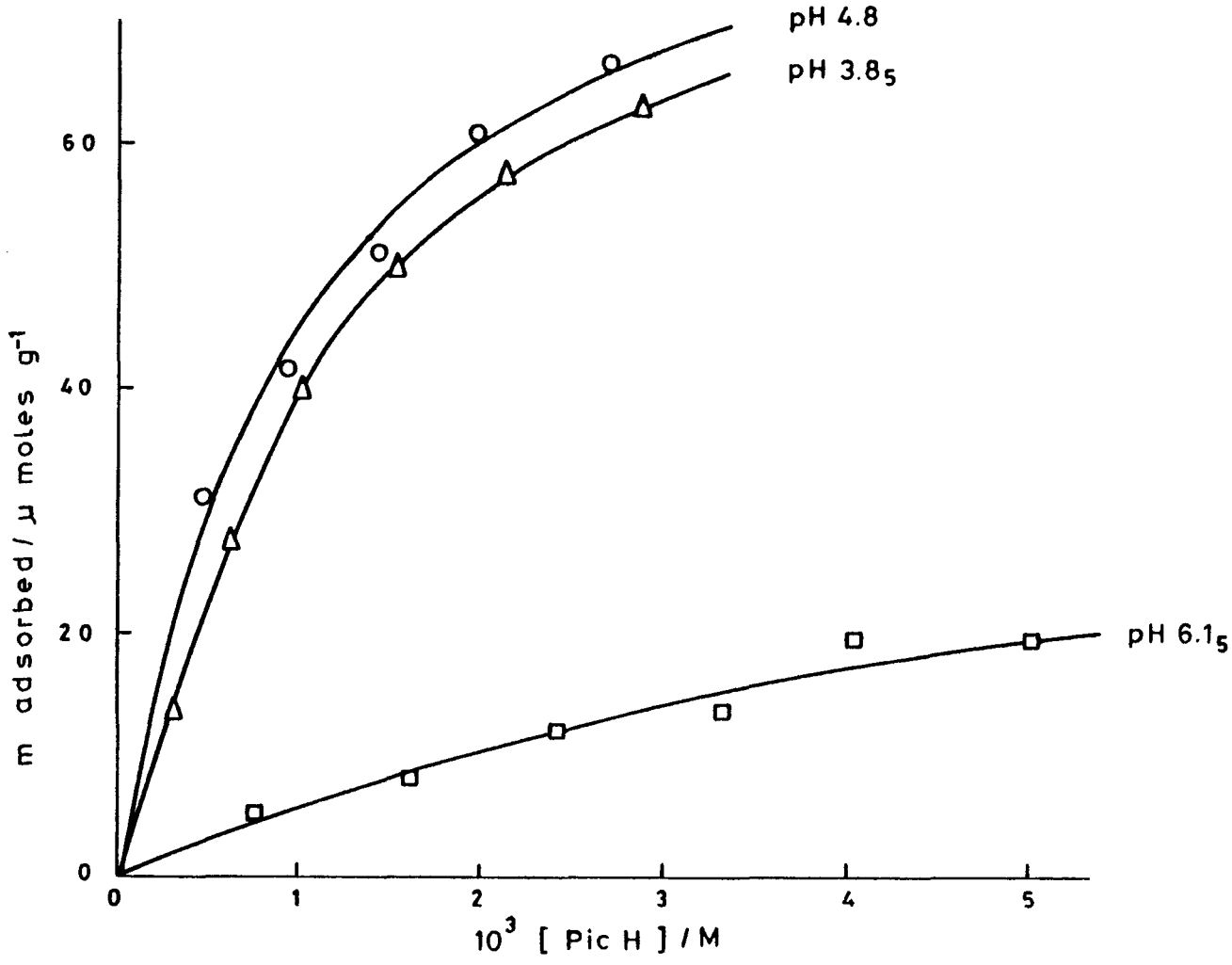

FIG. A32. Adsorption of Picolinic Acid on Fe_2O_3 (50°C)

If we use the surface area figure of 37 $m^2\ g^{-1}$ obtained by the BET method, these values of m_s lead to a typical area for a picolinate ligand at saturation of 69 $Å^2$. This can be compared with the data of Matijevic (1979), who found that EDTA occupied 33 $Å^2$ on FeOOH, which is interpreted as one EDTA molecule per Fe^{3+} ion at the surface. On this basis the figure for picolinic acid implies that one ligand molecules binds to two metal ions. This is not unusual, since SO_4^{2-}, PO_4^{2-} and oxalate are also believed to bridge two ions.

3.7 DISSOLUTION KINETICS - SUMMARY AND CONCLUSIONS

It is clear from the results of our kinetic experiments that dissolution of oxides containing iron(III) can be effected by one-electron reducing agents. Even at concentrations in the millimolar range, we find that a variety of such reducing agents dissolve many of the oxides likely to be found in reactor chemistry. These concentrations, which are typically 0.1% or less, compare very favourably with the concentrations required for conventional, chelating reagents. Even at the level of several percent, such conventional reagents are several orders of magnitude slower at dissolving the oxides.

We have been able to distinguish two basic types of mechanisms, which allow alternative strategies for development of a reagent system. An inner-sphere strategy would require a reducing agent (e.g. Cr^{2+}), and a bridging ligand. There are two major disadvantages to this approach when applied to reactor circuits: very low pH (≤ 3) is necessary to keep the metal ions in solution, and the bridging ligand may also be very corrosive to circuit materials. This combination is clearly undesirable. As a result, our efforts have concentrated on development of an outer-sphere reagent system. In order to keep the reagent and product ions in solution at higher pH levels, this requires the presence of a strongly binding ligand. Thus we have experimented with different chelating agents and reducing metal ions. There is potentially a very great number of such combinations capable of performing the required dissolution reactions.

Of those tried so far, three systems have been the most successful at oxide dissolution. $Cr(bipy)_3^{2+}$ dissolves the oxides very rapidly, and appears thermally stable in the pH range 5 - 7 which is highly practicable. $V(bipy)_3^{2+}$ is also very effective, is stable at temperatures up to 100°C (at least), but requires the presence of another ligand such as citrate to prevent precipitation of V(III) hydroxide. $V(pic)_3^-$ is even more reactive towards the oxides, but is not rapidly oxidised by water in the way V^{II}(EDTA) is, and

requires no other ligand. Many other ligands have been tested with V^{2+}, but none show significant advantages over picolinate. Therefore the combination of V^{2+} and this ligand has been the reagent system studied further.

We have developed a method of introducing these V(II) reagents into larger scale systems, with removal of undesired anions that might be corrosive and replacement by acetate. In these large-scale runs we have successfully cleaned samples of oxidised steels, though without removing the chromium-rich inner oxide layer, and have removed essentially 100% of all dissolved metals from the resulting solution by ion exchange.

Having demonstrated that these reagents dissolve oxides rapidly and efficiently we still had to determine their suitability for reactor use. The stability of such systems in radiation, and the extent to which they corrode the materials of a reactor circuit, are considered in the next two chapters.

APPENDIX A4

4.0 RADIOLYTIC STABILITY OF DECONTAMINATING REAGENTS

This section describes experiments to determine the effect of radiation on the decontaminating reagents being employed in the present study. The main compounds of interest are the complexing agents 2,2'-bipyridyl, picolinic acid, citric acid, EDTA and NTA and their complexes with vanadium, chromium, iron, cobalt and nickel. In the context of decontamination the complexing agents and complexes are respectively required to hold metal ions in solution and to act as reducing agents and it is the influence of radiation on these two properties which is important. These two properties are discussed for each complexing agent in turn, but first there follows a description of the experimental measurements.

4.1 EXPERIMENTAL

4.1.1 Irradiation Procedure

Irradiations were carried out in a 2000 Ci AECL Gamma Cell 200 ^{60}Co γ-ray source. The dose rate as determined by the Fricke dosimeter was ca 0.8 MRad h^{-1}, taking $G(Fe^{3+}) = 15.5$. Solutions (4 - 10 ml) were irradiated in 10 ml glass syringes or stoppered containers. All experiments were performed at room temperature (ca 25°C), although some increase in temperature occurred during long irradiations (hours) due to the decay heat from the ^{60}Co.

4.1.2 Measurement of Changes in Complexing Ability

Radiation-induced changes in complexing ability were determined by the addition of known amounts of Cu^{2+} to irradiated solutions of complexing agent, and the determination of how much remained uncomplexed using a copper specific ion electrode. Complexing ability (α) was calculated according to :

$$\alpha = \frac{x[Cu^{2+}]_T - (x+y)\,[Cu^{2+}]_f}{y[L]} \qquad (13)$$

where x is the number of ml of standard $CuSO_4$ used in the analysis, y is the number of ml of irradiated solution used in the analysis, $[Cu^{2+}]_T$ is the concentration of the standard $CuSO_4$ solution, $[Cu^{2+}]_f$ is the concentration of uncomplexed Cu^{2+} as determined by the specific ion electrode, and [L] is the

concentration of the complexing agent before irradiation. This equation is equivalent to analysing the complexing behaviour of the species formed in the radiolysis in terms of the concentration of starting material that would complex the same proportion of the $CuSO_4$ added. Possible sources of interference, details of the analytical procedure, etc. have been described elsewhere (Sellers, 1979b).

4.1.3 Measurement of the Effect of Radiation on Reducing Agents

The effect of radiation on low valency state metal complexes, etc. was determined by monitoring the changes in absorption spectrum of the complexes under γ- or pulse radiolysis.

4.2 RADIATION CHEMISTRY OF AQUEOUS SOLUTIONS

The passage of high-energy radiation through matter brings about ionisation and excitation. The situation shortly after passing through water is described by Eqn.(14) where the numbers are the radiation chemical yields or G-values in units of molecules per 100eV of energy deposited. Three of these species, H, OH and e_{aq}^-, are highly reactive, unstable intermediates, and it is the reaction of these that bring about degradation of solutes dissolved in the

$$4.9\ H_2O \rightarrow 2.7\ e_{aq}^- + 2.7\ OH + 3.4\ H^+ + 0.7\ OH^- + 0.45\ H_2 + 0.75\ H_2O_2 + 0.6\ H \qquad (14)$$

water. To find out which of the intermediates is responsible it is convenient to add scavengers which selectively remove or interconvert the radiolytic transients. A simple and effective way of doing this used in this study is to vary the gas with which the solution is purged. In deaerated solutions (obtained by bubbling with argon) at neutral pH's the reactive intermediates are 0.6 H + 2.7 e_{aq}^- + 2.7 OH. At low pH the hydrated electrons are converted into H atoms, according to reaction (15), so that the yields of intermediates become 3.3H + 2.7 OH. In N_2O saturated solutions the hydrated electrons are

$$e_{aq}^- + H^+ \rightarrow H \qquad (15)$$

converted into an additional yield of hydroxyl radicals by reaction (16), to give as reactive intermediates 5.4 OH + 0.6 H.

$$e_{aq}^- + N_2O \xrightarrow{H_2O} N_2 + OH + OH^- \qquad (16)$$

In O_2 saturated solutions H and e_{aq}^- are rapidly scavenged according to reactions (17) - (19).

$$H + O_2 \rightarrow HO_2 \quad (17)$$

$$e_{aq}^- + O_2 \rightarrow O_2^- \quad (18)$$

$$HO_2 \rightleftharpoons H^+ + O_2^- \quad pK_a = 4.9 \text{ (Behar et al. 1970)} \quad (19)$$

Reactive intermediates are thus 3.3 O_2^- (or HO_2 at low pH) + 2.7 OH.

4.3 2,2'-BIPYRIDYL AND 1,10-PHENANTHROLINE

4.3.1 Effect of Radiation on Complexing Ability

Results :

A rapid reduction in complexing ability was determined for both these compounds in solutions saturated with Ar, N_2O and O_2, as shown in Figs. A33 and A34. Aerated solutions of bipyridyl appear to be the least sensitive but even here the complexing ability was very small after a dose of only ca 2 Mrad. Concomitant with these changes in complexing ability the solutions changed colour. Deaerated and N_2O saturated solutions become cloudy, and developed a yellowish colour, oxygenated solutions remained clear and colourless.

Discussion :

Hoffman (pers. comm.) has investigated the reduction of bipyridyl and phenanthroline by e_{aq}^- and H produced radiolytically, and finds that the insoluble material formed is a trimer of dihydrobipyridine isomers. Such a product can only arise by polymerisation (albeit with short chain lengths), and this explains why the complexing ability falls so rapidly with dose. Apparently OH radicals can also induce polymerisation, and somewhat surprisingly, O_2 does not inhibit the process.

4.3.2 Effect of Radiation on Compexes with V^{II}, Cr^{II} and Other Metal Ions

Bipyridyl Compexes with Co^{II}, Cu^{II}, Ni^{II} and Zn^{II}

The absorption spectra of the tris-bipyridyl complexes with these metal ions are characterised by a rising edge at $\lambda < 320$ nm. On γ-radiation of N_2O saturated 1×10^{-3} M solutions of these complexes there was a gradual increase in absorption in the 320 - 500nm region, as shown in Fig. A35 for the Ni^{II} complex, and the solutions become yellowish. The rate of formation of the

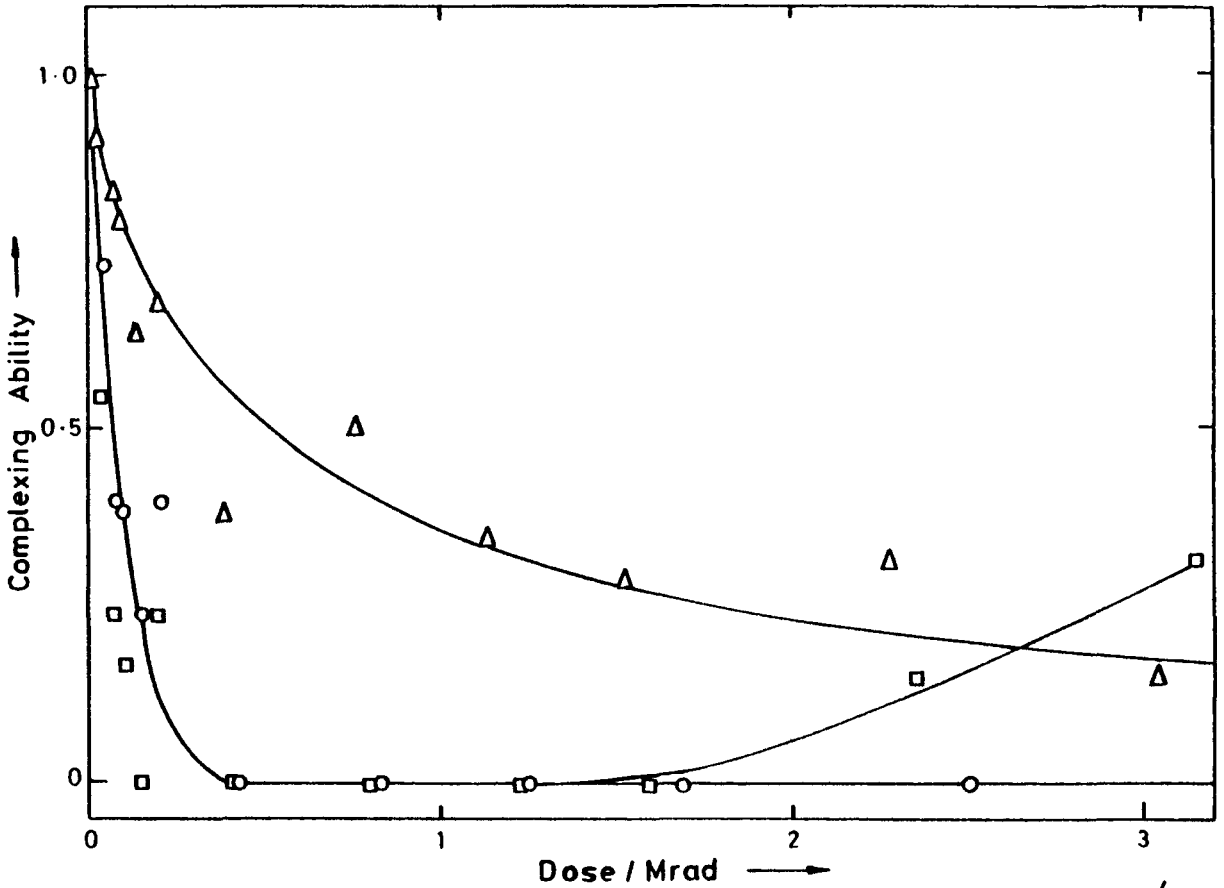

FIG A33. Effect of Radiation on the Complexing Ability of 2×10^{-4}M 2,2'-Bipyridyl Solutions Saturated with N_2O (o), Ar (Δ) or O_2 (□)

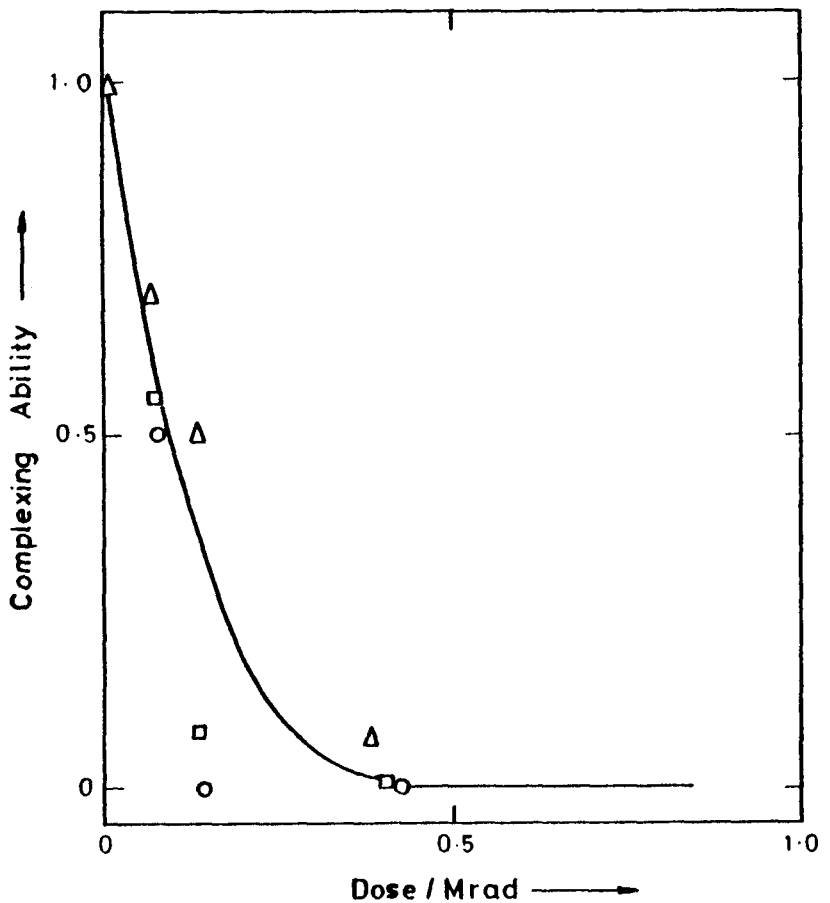

FIG. A34. Effect of Radiation on the Complexing Ability of 2×10^{-4} M 1,10 Phenanthroline Solutions Saturated with N_2O (o), Ar(Δ) or O_2(□)

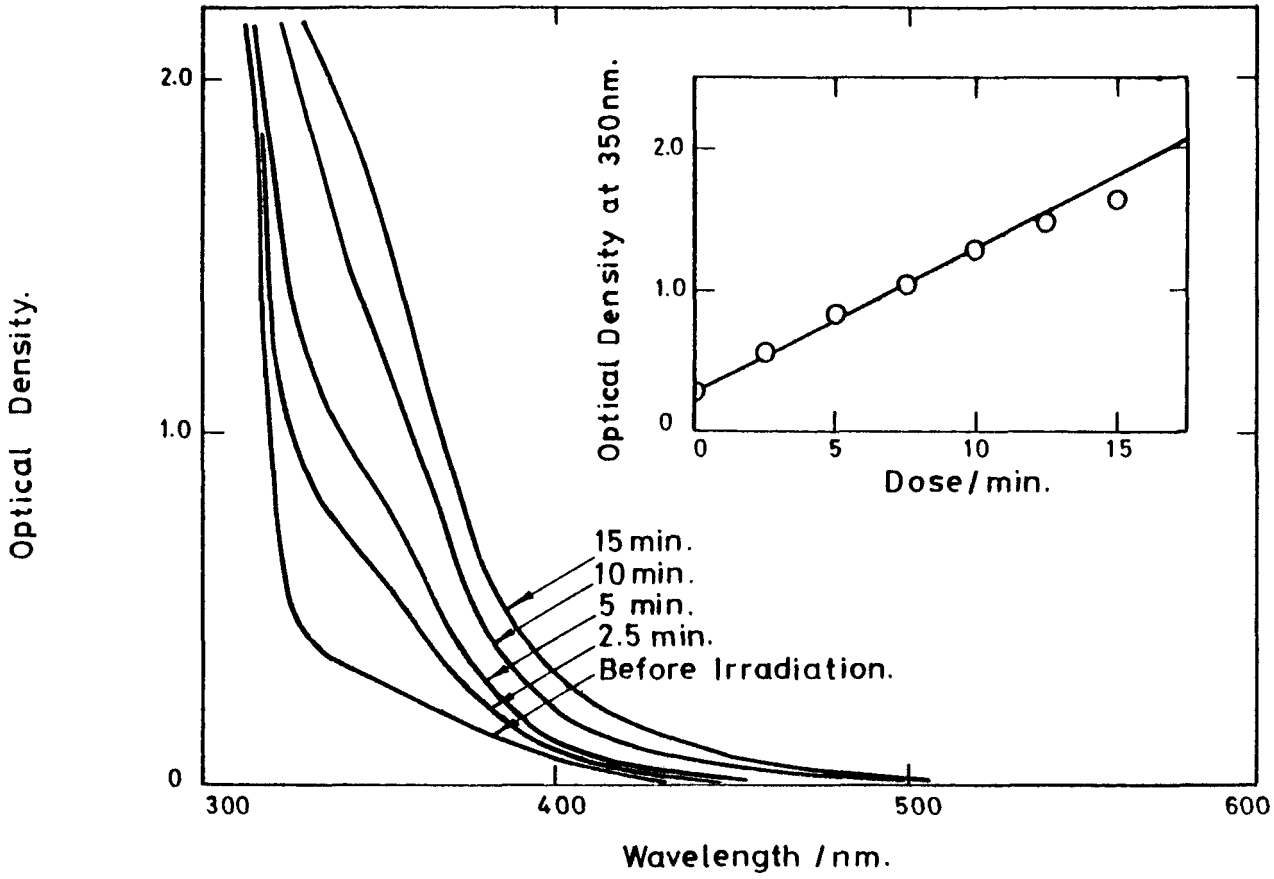

FIG. A35. Radiation Induced Absorption in N_2O Saturated Solutions Containing 1×10^{-3} M Ni (bipy) $_3^{2+}$, pH 7.0 Inset: Change in Absorption at 350nm with Dose. Dose Rate : 0.79 Mrad h^{-1}

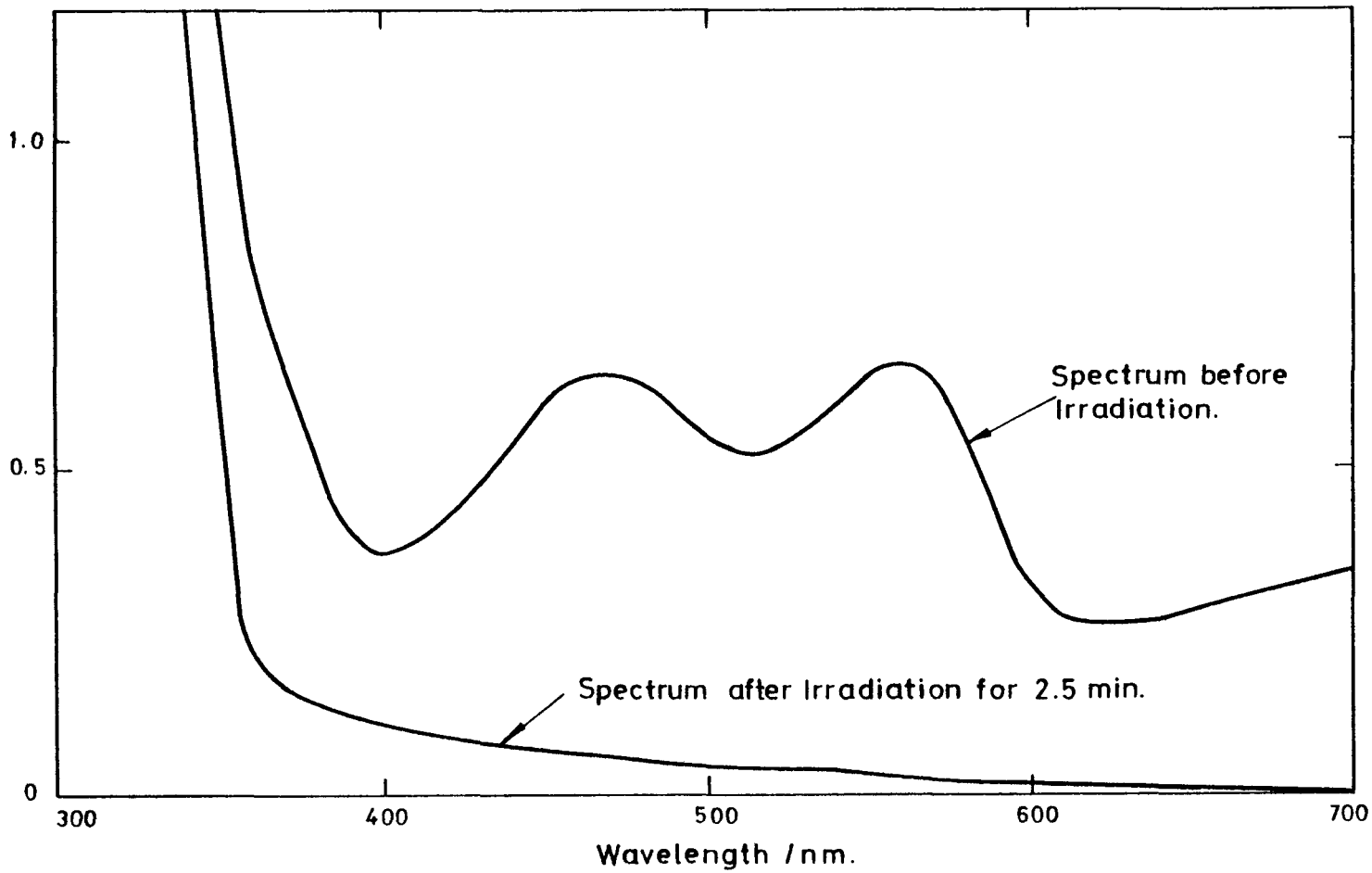

FIG. A36. Spectral Changes in the Radiolytic Decomposition of $Cr(bipy)_3^{2+}$, pH ca 2. Dose rate: 0·79 Mrad h^{-1}

absorption was linear at small doses, but increased less rapidly at higher doses, indicating that the products of radiolysis are able to complete with the starting material for OH radicals. Values of $G\varepsilon$* determined from the initial portions of the yield-dose plots are summarised in Table A16. No precipitation was observed. The products were not sensitive to oxygen, but the intensity of their absorption increased somewhat on adjusting the pH to 12. This indicates that they have acid-base properties.

There is no evidence from these experiments for any change in valency of the central metal ion, or polymerisation of the ligand (although this possibility cannot entirely be ruled out). The most likely mechanism for the formation of the products is OH addition to the ligand followed by disproportionation or possibly combination. The OH-substituted products that would result would be expected to show acid-base properties.

$\underline{Cr(bipy)_3^{2+}}$:

Attempts to prepare this complex by addition of solutions of Cr^{2+} to bipyridyl in the molar ratio 1:3 were unsuccessful due to the formation of a black precipitate. This is probably $Cr(bipy)_3^+$ produced by disproportionation of the divalent complex (Cotton and Wilkinson, 1966). To prevent this it was found necessary to work in solutions containing an excess of free bipyridyl. Unfortunately this complicates the radiation chemical studies, since free bipyridyl is very reactive with the products of water radiolysis, and scavenges them before they can react with the Cr^{II} complex. Even so, on irradiation in deaerated solutions (pH <u>ca</u> 2; $[Cr^{II}(bipy)_3]_0 \sim (0.5 - 12) \times 10^{-4}$ M), the intense optical absorption (λ_{max} = 467 and 562.5 nm with ε = 3950 and 4340 M^{-1} cm^{-1} respectively: Candlin, Halpern and Trimm, 1964) was destroyed as shown in Fig. A36. The rate of destruction was constant to quite high percent destruction of the starting material. Plots of optical density v. dose did become non-linear at high conversion, however, indicating that the products to interfere to a small extent (Fig. A37). Values of the destruction yield $G[-Cr(bipy)_3^{2+}]$, calculated from the linear portions of these plots, are given in Table A17. The nature of the products is not known with certainty, but the loss of the chromophore indicates that the Cr^{II} centre changes its valency.

---

* $G\varepsilon$ is the product of the radiation chemical yield (G) and the difference in extinction coefficients (ε) of the products and starting material.

Reduction is unlikely, particularly as no precipitate is obtained on irradiation, and so presumably it is oxidised to Cr^{III}.

The value of $G[-\ Cr(bipy)_3^{2+}]$ decreased as the [free bipyridyl]/$[Cr(bipy)_3^{2+}]$ ratio increased (Table A17), suggesting a competition between free bipyridyl and $Cr(bipy)_3^{2+}$ for some intermediate. In fact a plot of $1/\ G[-\ Cr(bipy)_3^{2+}]$ v. $[bipy]/[Cr(bipy)_3^{2+}]$ corresponds closely to a straight line with slope 6.6×10^{-3} and intercept 0.13. The species responsible are probably H and OH. The reactions occurring are shown in eqn. (20) - (23).

$$H + bipy \rightarrow products \tag{20}$$

$$H + Cr(bipy)_3^{2+} \rightarrow Cr(bipy)_2\ (bipy\ H)^{2+} \xrightarrow{H^+} Cr(bipy)_2\ (bipy\ H_2)^{3+} \tag{21}$$

$$OH + bipy \rightarrow Products \tag{22}$$

$$OH + Cr(bipy)_3^{2+} \rightarrow Cr(bipy)_2(bipy\ OH)^{2+} \begin{cases} \xrightarrow{H^+} Cr(bipy)_2\ (bipy\ OH_2)^{3+} \\ \rightarrow Cr(bipy)_3^{3+} + OH^- \end{cases} \tag{23}$$

The small amount of destruction of $Cr(bipy)_3^{2+}$ not inhibited by the free bipyridyl corresponds to oxidation by radiation-induced hydrogen peroxide [reaction 24].

$$Cr(bipy)_3^{2+} + H_2O_2 \rightarrow Cr(bipy)_3^{3+} + OH + OH^- \tag{24}$$

The destruction yield of $Cr(bipy)_3^{2+}$ will then be given by :

$$G[-Cr(bipy)_3^{2+}] = G_H \left\{ \frac{k_{16}[Cr(bipy)_3^{2+}]}{k_{16}[Cr(bipy)_3^{2+}] + k_{15}[bipy]} \right\}$$

$$+ (G_{OH} + G_{H_2O_2}) \left\{ \frac{k_{18}[Cr(bipy)_3^{2+}]}{k_{18}[Cr(bipy)_3^{2+}] + k_{17}[bipy]} \right\} + G_{H_2O_2} \tag{25}$$

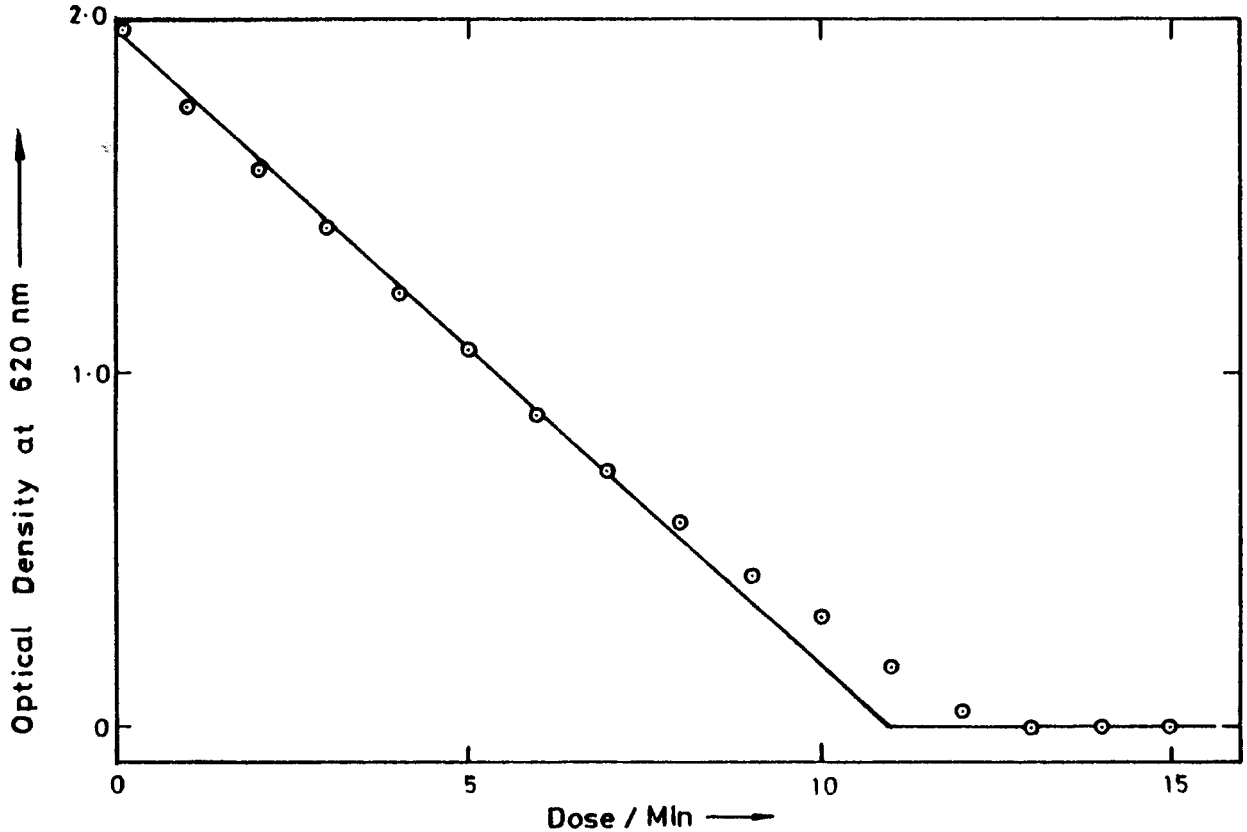

FIG. A37. Yield - Dose Plot for the Radiation - Induced Decomposition of $Cr(bipy)_3^{2+}$, pHca 2. Dose Rate 0·79 Mrad h^{-1}

TABLE A16

Spectral Changes in the Radiolysis of tris (2,2'-bipyridyl) Metal (II) Complexes Induced by OH Radicals

metal[a]	Gε	λ/nm
Co^{II}	1980	380
Cu^{II}	3340	380
Ni^{II}	7790	350
Zn^{II}	5500	340

a All solutions containing 1×10^{-3} M complex and were saturated with N_2O pH ca. 7.

TABLE A17

Destruction Yields in the Radiolysis of $Cr(bipy)_3^{2+}$ [a]

$[Cr(bipy)_3^{2+}]$/M	$[Cr(bipy)_3^{3+}]$/M	$[bipy]_{free}$/M	$[H^+]$/M	$G(-Cr^{II})$ (measured)	$G(-Cr^{II})$ (calc.)
1.16×10^{-3}	0	3.02×10^{-3}	0.011	8.2	6.4
7.51×10^{-4}	0	4.35×10^{-3}	0.011	5.8	5.5
1.38×10^{-4}	0	5.59×10^{-3}	0.010	2.5	2.4
8.99×10^{-5}	0	6.23×10^{-3}	0.011	1.8	1.8
5.62×10^{-5}	0	6.18×10^{-3}	0.011	1.1	1.5
2.51×10^{-4}	5.50×10^{-5}	5.59×10^{-3}	0.011	4.0	3.1
9.33×10^{-5}	1.97×10^{-4}	7.54×10^{-4}	0.0028	2.7	2.8
7.83×10^{-5}	5.97×10^{-5}	5.59×10^{-3}	0.010	0.6	1.7

Assuming $k_{16}/k_{15} = \frac{k_{18}}{k_{17}}$* gives eqn. (26).

$$G[-\ Cr(bipy)_3^{2+}] = (G_H + G_{OH} + G_{H_2O_2}) \left\{ \frac{k_{18}[Cr(bipy)_3^{2+}]}{k_{18}[Cr(bipy)_3^{2+}]+k_{17}[bipy]} \right\} + G_{H_2O_2} \quad (26)$$

Substituting literature values of $G_H = 3.3$, $G_{OH} = 2.7$ and $G_{H_2O_2} = 0.75$, and taking $k_{18}/k_{17} = 13$ gives the calculated values of $G[-\ Cr(bipy)_3^{2+}]$ shown in Table A17. The agreement with the experimental measurements is reasonable considering the approximation involved.

Some experiments were also performed in which a small fraction of the $Cr(bipy)_3^{2+}$ was deliberately converted to $Cr(bipy)_3^{3+}$ by aerial oxidation. The Cr^{III} complex did not significantly protect $Cr(bipy)_3^{2+}$ from radiolysis (Table A17) and seems to be intermediate between $Cr(bipy)_3^{2+}$ and free bipyridyl in its reactivity with H and OH. There is now a three-way competition for H and OH and eqn. (26) is replaced by (27), again making the assumption that the relative reactivity of H and OH with each of the three species is the same. Choosing $k_{18}/k_{17} = 13$ as before and $k_{18}/k_{23} = 1.3$ gives the calculated G-values shown in Table A17. Again the agreement with the experimental measurements is reasonably good.

$$G[-\ Cr(bipy)^{2+}] = (G_H + G_{OH} + G_{H_2O_2}) \left\{ \frac{k_{18}[Cr(bipy)_3^{2+}]}{k_{18}[Cr(bipy)_3^{2+}] + k_{17}[bipy] + k_{23}[Cr(bipy)_3^{3+}]} \right\} + G_{H_2O_2} \quad (27)$$

$$OH + Cr(bipy)_3^{3+} \rightarrow \text{products } (\neq Cr^{II}) \quad (28)$$

---

* This is justified to a first approximation by the linear dependence of $1/G[-\ Cr(bipy)_3^{2+}]$ on $[bipy]/[Cr(bipy)_3^{2+}]$.

TABLE A18

Spectral Changes in the Radiolysis of V^{II}-bipyridyl Complexes

$[V^{II}]_{Total}$/M	$[bipy]_{Total}$/M	$\frac{[bipy]}{[V^{II}]}$	$[H^+]$/M	$G\varepsilon_\lambda$	
				410 nm	640 nm
1.08×10^{-3}	1.5×10^{-3}	1.4	0.0025	3530	3970
5.4×10^{-4}	1.5×10^{-3}	2.8	0.0025	8890	8800
5.4×10^{-4}	7.5×10^{-3}	14	0.0125	15400	17600
5.4×10^{-4}	2.25×10^{-2}	42	0.0375	10100	13500

$V(bipy)_3^{2+}$:

As in the Cr^{II} work described above, difficulty was experienced in preparing $V(bipy)_3^{2+}$ by addition of V^{2+} to bipyridyl in a molar ratio of 1:3. The spectrum of such solutions showed the characteristic peaks of $V(bipy)_3^{2+}$ at 402 and 649 nm (Bennett and Taube, 1968). However the ratio of their intensities was ca. 1:1. Addition of excess bipyridyl changes this to ca. 1:1.7, in agreement with literature observations. The problem seems to arise because of the lability of the third bipyridyl ligand. Unfortunately the extinction coefficient of the 1:2 complex is unknown, so the radiation chemical yields (G-values) could not be measured directly. Instead the product $G\varepsilon$ was determined. Irradiation of the complex in deaerated solutions containing various amounts of excess bipyridyl led to destruction of the V^{II} chromophore, the V^{II} presumably being oxidised to V^{III}. Yield-dose plots were approximately linear up to ca.80% conversion. Values of $G\varepsilon$ determined from these plots at two different wavelengths are shown in Table A18. The initial increase in $G\varepsilon$ is probably due to changes in ε, the decrease at [bipyridyl]/$[V^{II}]$ > ca.15 to a reduction in G. The reactions occurring appear to be similar to those described above for the Cr^{II} complex.

Complexes with phenanthroline have not been investigated, but it is likely that they behave in a similar fashion.

4.4 PICOLINIC ACID. (pic)

4.4.1 Effect of Radiation on Complexing Ability

It was found that the Cu^{2+} specific ion electrode was sensitive to both the 1:1 and 1:3 complexes of Cu^{II} with this ligand, and so the effect of radiation on its complexing ability could not be investigated by this method.

An alternative test involving the effect of complexing agents on the precipitation of $Cu(OH)_2$ at pH 12 was used. In the absence of a complexing agent adjustment of the pH of a neutral solution of Cu^{2+} to 12 causes a blue gelatinous precipitate to be formed. If a solution of 5×10^{-3} M picolinic acid is added before adjustment of the pH no precipitate is obtained. Irradiated picolinic acid solution (N_2O saturated solution, dose 0.5 MRad) has the same effect, indicating that the picolinic acid has not under these circumstances lost its complexing ability.

Irradiation of picolinic acid solution at doses up to ca.0.5 Mrad induced no

TABLE A19

Spectral Changes in the Radiolysis of Picolinic Acid and its Complexes with Cu^{II} and Ni^{II}

Complex [a]	λ/nm	$G\varepsilon_\lambda$
pic	300	3390
$Ni(pic)_3^-$	310	2270
$Cu(pic)_3^-$	310	1450

a) All solutions contained 1×10^{-3} M complex/free ligand and were saturated with N_2O. pH ∿ 7.

change in colour, and in no case was any precipitate detected.

It appears from these limited observations that picolinic acid is more stable towards radiation than either bipyridyl or phenanthroline, probably because it does not polymerise. Further experiments to characterise the products of radiolysis more completely are planned.

4.4.2 Effect of Radiation on Metal Complexes

Radiation-induced changes in the absorption spectrum of N_2O saturated solutions of 1 x 10^{-3}M pic, and its 3:1 complexes with Ni^{II} and Cu^{II}, were studied. In each case there was a slight increase in absorption in the 270 - 400nm range. Yield-dose plots were linear for doses up to ca.0.04 Mrad for the free ligand and ca.0.1 Mrad for the complexes. From these the $G\varepsilon$ values given in Table A19 were found.

The results are similar to those of the corresponding bipyridyl complexes described above. There appears to be no change in the valency of the central metal ion, so the spectral changes must result from changes in the ligands. OH addition followed by disproportionation, or possibly combination, appears most likely, although polymerisation cannot entirely be ruled out.

$V^{II}(pic)_3$:

The effect of radiation on $V^{II}(pic)_3$ was studied in solutions containing 6.7 x 10^{-4}M $V^{II}(pic)_3$ + 0.005 M phosphate buffer (pH 8.0). Under these conditions the solutions have an absorption spectrum with a broad peak centred on 660 nm (ε = 3800 $M^{-1}cm^{-1}$) and a shoulder at ca.480 nm and a deep blue-black colour. Irradiation caused a bleaching of this absorption and yielded utlimately an orange-yellow coloured solution. This slowly (hours) disappeared on standing in air. Admission of air before irradiation instantaneously produced an orange-yellow colour, and this also slowly disappeared on standing in air. The absorption spectrum showed isosbestic points at 310 and 372 nm, optical density decreasing below and above these figures respectively (see Fig. A38). The spectrum of the product is similar to that reported for $V^{III}(pic)_3$, and the isosbestic points for the $V^{II}(pic)_3/V^{III}(pic)_3$ change (Mercier and Paris, 1964). Accordingly the product is identified as a V^{III} species.

The change in optical density with dose was linear up to ca.50% conversion, and with only minor deviations up to ca.80%. From the linear portion as measured

at 560 nm the G-values shown in Table A20 were obtained, taking $\epsilon_{560} = 3080$ $M^{-1}cm^{-1}$.

Addition of excess picolinic acid caused no appreciable change in the absorption spectrum, indicating that the third picolinate ligand is more tightly held than with the corresponding bipyridyl complex. Values of $G(-V^{II})$ were lower than without excess picolinic acid.

The high yields in N_2O saturated solution (Table A20) indicate that OH, H and H_2O_2 all bring about oxidation of the V^{II} to V^{III} according to :

$$V^{II} + H + H^+ \rightarrow V^{III} + H_2 \quad (29)$$

$$V^{II} + OH + H^+ \rightarrow V^{III} + H_2O \quad (30)$$

$$V^{II} + H_2O_2 \rightarrow V^{III} + OH + OH^- \quad (31)$$

These equations indicate stoichiometric relationships; the mechanisms of the reaction are not firmly established, but by comparison with the behaviour of other complexes (for general review see Buxton and Sellers, 1977), they probably involve addition to the ligand followed by intra-molecular electron transfer from metal to ligand [reactions (29) and (30)], and outer sphere electron transfer (31). The destruction yield predicted by eqn. (29) - (31) is given by (32). Using literature values for the G-values [cf eqn. (14)] gives

$$G(-V^{II}) = G_H + G_{OH} + G_{e^-_{aq}} + 2G_{H_2O_2} \quad (32)$$

$G(-V^{II}) = 7.5$, close to the experimental value of 7.1.

In deaerated solutions the yields were much smaller, and this is taken to indicate that the hydrated electrons are involved in some back reaction to reform the starting material. There are two ways in which this might occur : either the hydrated electron reduces V^{III} species (33) produced by H, OH and H_2O_2 [reactions (29) - (31)], or it reduces V^{II} to V^{I} (34), which reduces V^{III} produced in (29) - (31).

$$V^{III} + e^-_{aq} \rightarrow V^{II} \quad (33)$$

$$V^{II} + e^-_{aq} \rightarrow V^{I} \quad (34)$$

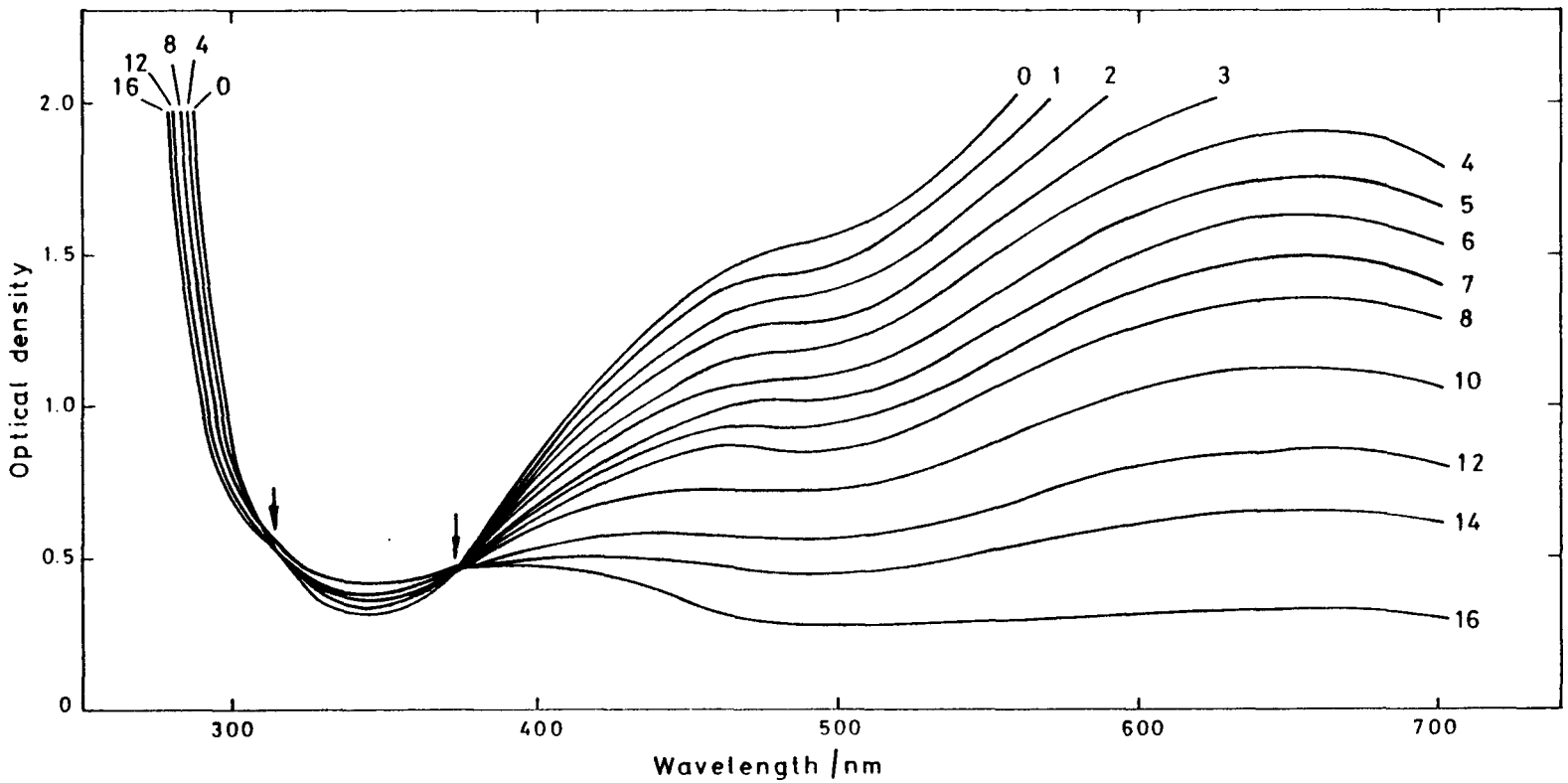

FIG.A38. Radiation Induced Changes in the Absorption of N_2O Saturated Tris-picolinato V^{II} Solutions at pH 8.0. Doses shown in Minutes of Irradiation at a Dose Rate of 13 krad Min^{-1}

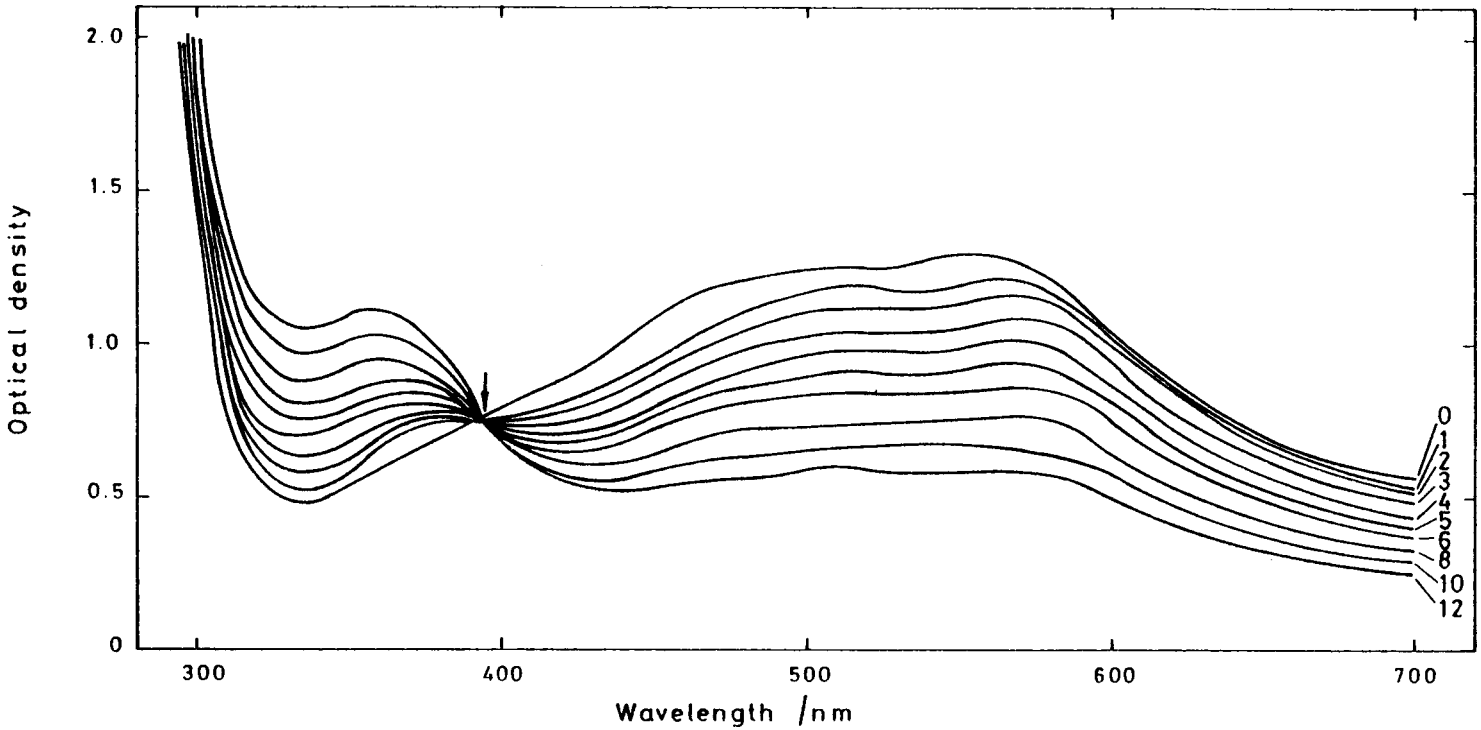

FIG. A39. Radiation Induced Changes in the Absorption of Deacrated Tris-picolinato V^{II} Solutions at pH 2.0. Doses shown in Minutes of Irradiation at a Dose Rate of 13 krad Min^{-1}

$$V^{I} + V^{III} \rightarrow V^{II} \quad (35)$$

In either case the stoichiometry will be given by :

$$G(-V^{II}) = G_{H} + G_{OH} + 2G_{H_2O_2} - G_{e^-_{aq}} \quad (36)$$

which with literature values for the G-values gives $G(-V^{II}) = 2.1$ in good agreement with the experimental value.

At pH 2 (no phosphate buffer present), the absorption spectrum was different from that at pH 8.0. It now showed peaks at 560nm (ε = 710 $M^{-1}cm^{-1}$), and the solution had a magenta-blue colour. Irradiation again destroyed the absorption in the visible region (see Fig. A39), the spectrum showing an isosbestic point at 393 nm. A plot of optical density (at 560nm) v. dose was linear (to ca.40% conversion) from which a destruction yield of 7.2 was calculated. The mechanism appears to be the same as that at pH 8.0 in N_2O saturated solutions. The effect of adding excess picolinic acid has not been investigated at pH 2.0.

The change in absorption spectrum between pH 2.0 and 8.0 probably indicates that the V^{II}-picolinate complex hydrolyses. The presence of phosphate buffer in the pH 8 solutions may also have some effect. Studies to investigate this behaviour more thoroughly are planned.

4.4.3 Effect of Formate Ion on the Radiolysis of $V^{II}(pic)_3$ and $V^{III}(pic)_3$

In an attempt to increase the stability of $V^{II}(pic)_3$ towards radiation some experiments were performed to investigate the effect of formate ion. Formate is a rapid scavenger of both H and OH radicals (k_{37} = 3 x 10^8 $M^{-1}s^{-1}$ k_{38} = 3.3 x 10^9 $M^{-1}s^{-1}$ converting them into the powerful reducing species, CO_2^-. Formate is much less reactive towards the hydrated electron

$$H + HCO_2^- \rightarrow H_2 + CO_2^- \quad (37)$$

$$OH + HCO_2^- \rightarrow H_2O + CO_2^- \quad (38)$$

($k \sim 10^4$ M^{-1} s^{-1}), a reaction which results in the formation of a hydrolysed form of the formyl radical, $HC(OH)_2$. Potentially, therefore, formate can provide protection to $V^{II}(pic)_3$ (i) by scavenging H and OH (but not e^-_{aq}) (ii) by reducing any $V^{III}(pic)_3$ formed through reaction with CO_2^-. To investigate

TABLE A20

Destruction Yields in the Radiolysis of $V^{II}(pic)_3$ [a]

[Picolinic Acid]$_f$/M	Saturating Gas	pH	G
0	Ar	2.0	7.2
0	Ar	8.0	1.9
0	Ar	8.0	1.9 [b]
5.0×10^{-3}	Ar	8.0	1.0
0	N_2O	8.0	7.1
5.0×10^{-3}	N_2O	8.0	3.5

a) Solutions contained also 6.7×10^{-4}M $V^{II}(pic)_3$ initial concentration) and 0.005M phosphate buffer.

b) [Phosphate buffer] = 0.0013M.

whether the latter actually occurs in practice solutions containing $V^{III}(pic)_3^+$ formate were irradiated. $V^{III}(pic)_3$ was prepared by mixing $V^{II}(pic)_3 + VO^{2+}$. In the first experiment excess VO^{2+} was added to give a solution containing (deaerated) : 9.4×10^{-4} M $V^{III}(pic)_3$ + 6.9×10^{-4} M VO^{2+} + 7.2×10^{-3} M free pic. + 0.10M HCO_2^- at pH ≈ 4.9. Irradiation of this brought about an increase in absorption throughout the visible region. In part this was due to the formation of further $V^{III}(pic)_3$, presumably through reduction of VO^{2+} by CO_2^-/ e_{aq}^-. A second component, thought to be $V^{II}(pic)_3$ (see below) was apparent also at λ 450 - 650nm.

In the second experiment, the $V^{III}(pic)_3$ was produced by mixing equimolar amounts of $V^{II}(pic)_3$ and VO^{2+}, so that there was, essentially no free VO^{2+} present. The spectral changes induced by irradiation are shown in Fig. A40. The $V^{III}(pic)_3$ band at 365nm showed a decrease whilst at λ = 450 - 700nm the absorption increased to give, after only a few minutes irradiation, the characteristic absorption of $V^{II}(pic)_3$. Visually the solution changes from orange to blue-black. On standing overnight, this colour was bleached (due to aerial oxidation), but was readily regenerated by reirradiation. From the change to OD with dose at 460nm, the yield of $V^{II}(pic)_3$ was estimated to be ≈6. These results clearly establish that CO_2^- reduces $V^{III}(pic)_3$ to $V^{II}(pic)_3$.

In another series of experiments solutions containing 8×10^{-4}M $V^{II}(pic)_3$ + 6.0×10^{-3} M free picolinic acid (i.e. concentrations similar to those proposed for use in a reactor clean) and various formate concentrations were irradiated to assess the relative amount of formate required to regenerate V^{II}. $V^{III}(pic)_3$ was not deliberately added to these solutions, but was present as an impurity in the V^{II} at a concentration of ca. 5% of the $V^{II}(pic)_3$. The results are shown in Fig. A41. Under the conditions used it will be seen that there was destruction of V^{II} at $(HCO_2^-) \leq 10^{-3}$M and regeneration at concentration > 4×10^{-3} M. By interpolation from Fig. A41: it is found that the rates of radiolytic oxidation and reduction are equal at 1.5×10^{-3} M. With higher initial amounts of $V^{III}(pic)_3$ present this value would be smaller - that is, more CO_2^-'s would be scavenged by the $V^{III}(pic)_3$ and the line in Fig. A41 would be displaced to the left.

4.5 EDTA AND NTA AND ETHYLENEDIAMINE

4.5.1 Effect of Radiation on Complexing Ability

EDTA and NTA Results :

The behaviour of EDTA and NTA was qualitatively the same in deaerated

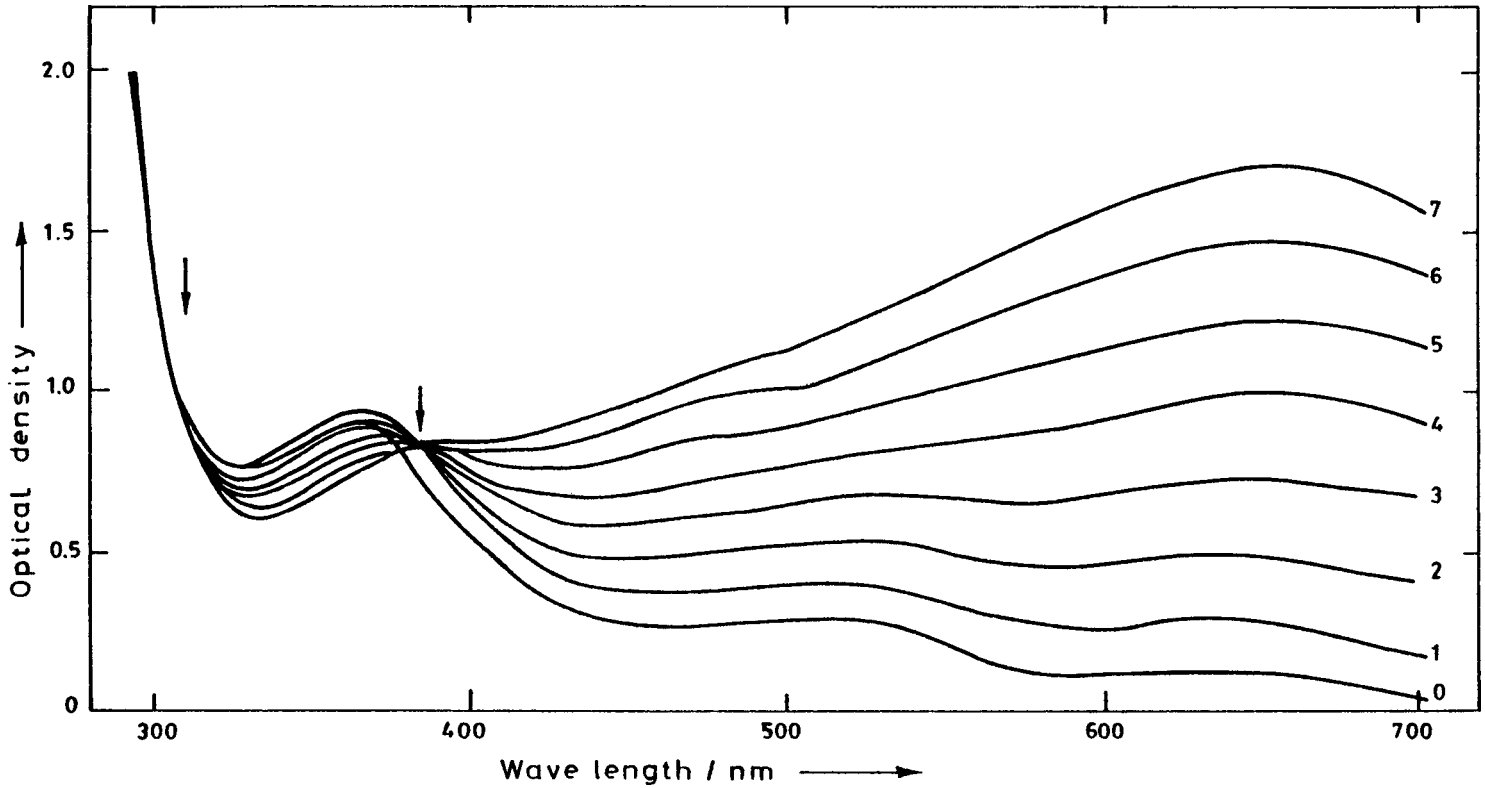

FIG. A40. Radiation Induced Changes in the Absorption of Deaerated Solutions Containing 8.4×10^{-4} M $V^{III}(pic)_3 + 7.5 \times 10^{-3}$ M pic + 0.10 M HCO_2^- at pH 5.3. Doses shown in Minutes of Irradiation at a Dose Rate of 13 krad. min^{-1}

and N_2O saturated solutions. In N_2O saturated solutions there was a rapid decrease in complexing ability, a subsequent increase (EDTA) or plateau region (NTA) and finally a gradual decrease again, whilst in deaerated solutions there was a small increase (Figs. A42, A43). In oxygenated solutions however, the two compounds were surprisingly different. With EDTA there was hardly any change in complexing ability, whilst for NTA the complexing ability varied much as in N_2O saturated solutions.

Discussion : The mechanism of the radiolysis of amino-carboxylates and a detailed interpretation of the above results have been given elsewhere (Sellers, 1979, a,b). The important features are as follows :

i) Attack by H and OH is primarily at the 'acetate' methylene groups and yields glyoxylic acid and the starting compound with one less acetate group. As the dose received increases the products too are degraded by loss of acetate groups.

ii) Hydrated electrons react rather slowly with amino-carboxylates, so that after only a small percentage of decomposition, they react preferentially with the degradation products (e.g. glyoxylic acid) and molecular hydrogen peroxide. The effect of saturating with N_2O (which converts hydrated electrons into OH radicals) shows clearly the important role of hydrated electrons in increasing the lifetime under radiolysis.

The overall effect is twofold. Firstly the complexing ability does not decrease significantly until quite high doses since the products have complexing properties almost as good as the starting material. Secondly the byproducts such as glyoxylic acid interfere either to reform compounds similar to the starting material, or other species with complexing properties. These features are clearly highly desirable in a reagent for use in a radiation field.

Ethylenediamine

Results : These solutions were studied at total doses of 17 Mrad. An initial decrease in complexing ability was found with each of the saturating gases used, deaerated solutions being the least sensitive (Fig. A44). In oxygenated and deaerated solutions some subsequent restoration of complexing ability was apparent, but it remained at a low level in N_2O saturated solutions.

Discussion : The rapid initial loss of complexing ability in these solutions

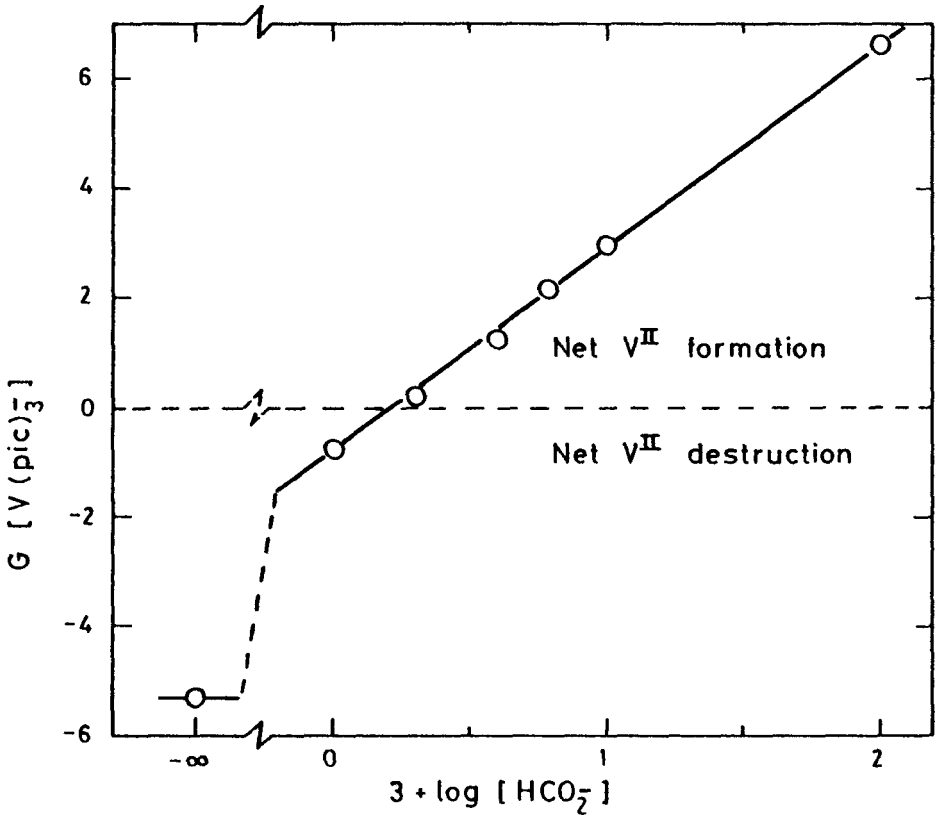

FIG. A41. Effect of Formate Concentration on the Radiolysis of $V(pic)_3^-$ Solutions. Measurements Made in Solutions Containing 8×10^{-4} M $V(pic)_3^-$ + 4×10^{-5} M $V(pic)_3$ + 6×10^{-3} M Free Picolinate

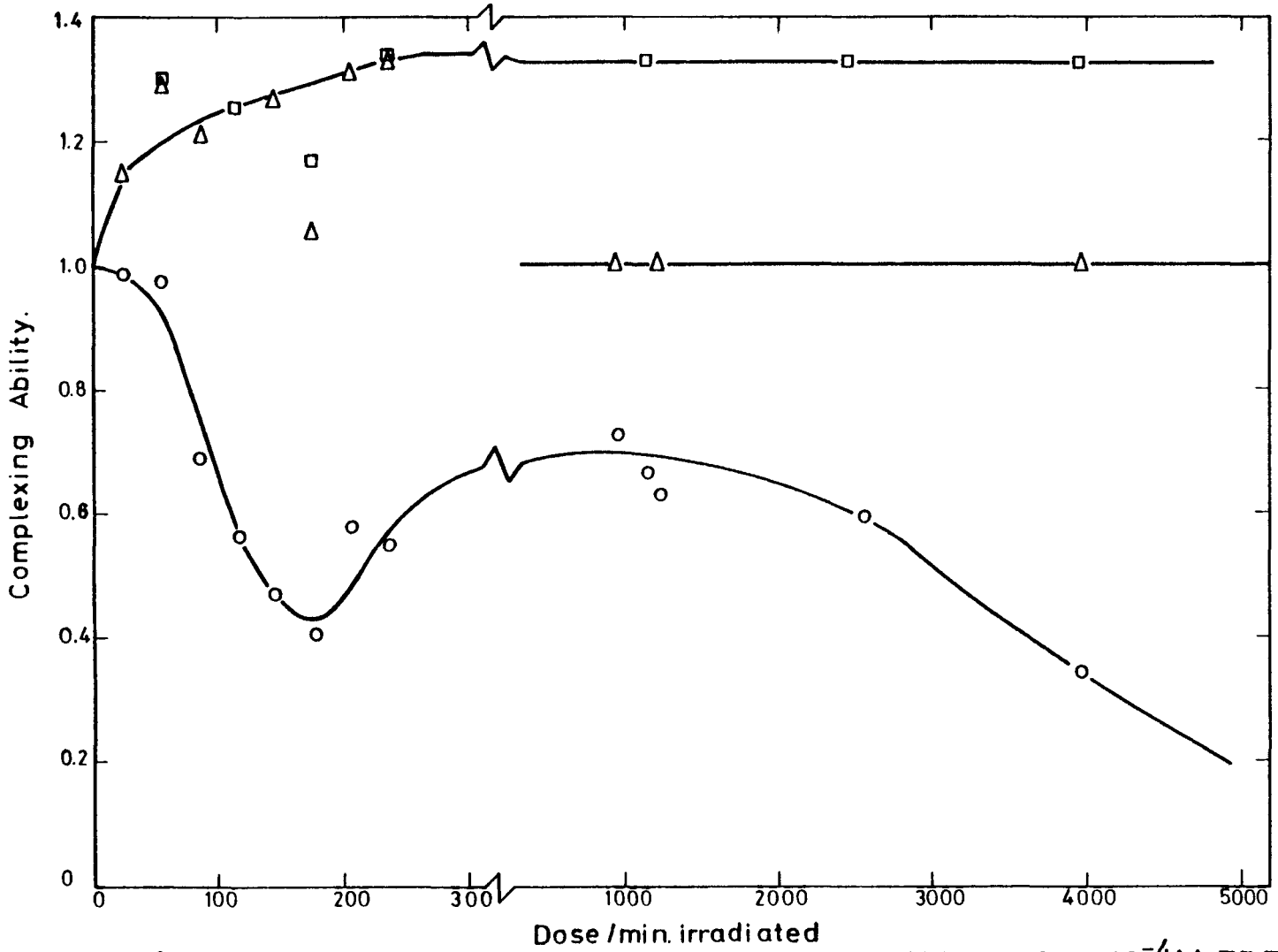

FIG. A42. Effect of Radiation on the Complexing Ability of 2×10^{-4} M EDTA Solutions Saturated with N_2O (o), Ar (Δ) or O_2 (□)

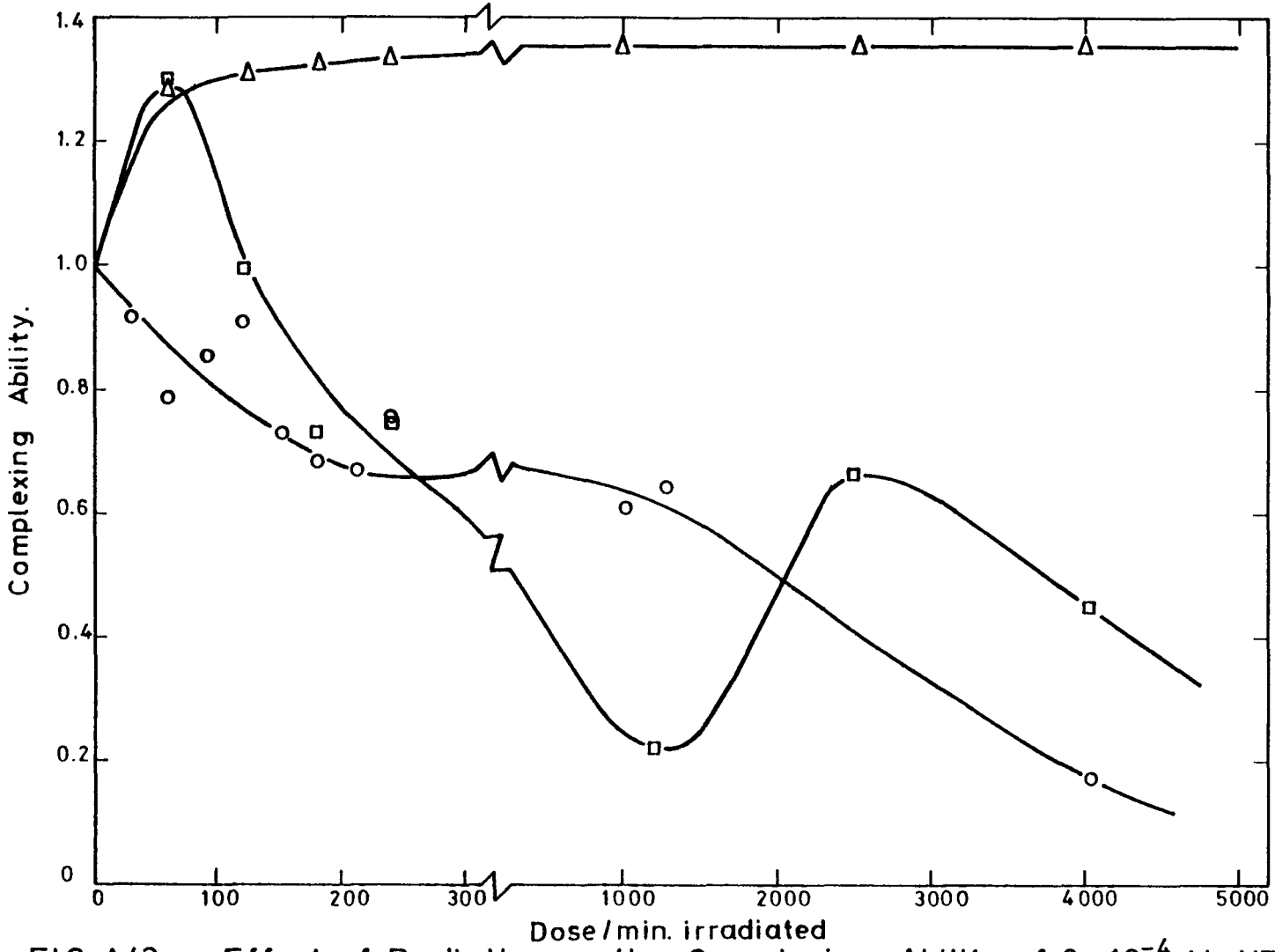

FIG. A43. Effect of Radiation on the Complexing Ability of 2×10^{-4} M NTA Soiutions Saturated with N_2O (o), Ar (Δ) or O_2 (□)

is due to the elimination of ammonia (Anbar et al., 1963) from the starting material. The mechanism by which this happens is not entirely clear, but is probably similar to that reported for elimination of water from the ethylene glycol radical (Bansal et al., 1973). The other products are probably a mixture of aldehydes, ketones and amines with poor complexing properties. The slower loss of complexing ability in deaerated solutions probably arises through e^-_{aq} repair of damage induced by OH [reactions (37) and (38)]. The

$$OH + H_2N.CH_2.CH_2.NH_2 \longrightarrow H_2O + H_2N.CH.CH_2.NH_2 \quad (37)$$

$$e^-_{aq}. + H_2N.CH.CH_2.NH_2 \xrightarrow{H_2} H_2N.CH_2CH_2.NH_2 \quad (38)$$

subsequent increase in complexing ability in oxygenated solution is probably due to the formation of amino-carboxylate compounds, from peroxy radical intermediates.

4.5.2 Effect of Radiation on some Metal Complexes of EDTA

An extensive literature on the radiation chemistry of metal complexes with EDTA and other amino-carboxylates such as nitrilotriacetate (NTA), iminodiacetate and glycine exists (for general review see Buxton and Sellers, 1977). A series of papers by Bhattacharyya and co-workers deal with the γ-radiolysis of these complexes (Bhattacharyya and Kundo, 1971, 1972b, 1973, 1976; Bhattacharyya and Srisankar, 1977, 1978). From an analysis of the products they conclude that attack of OH (and H) occurs at the ligand, and results in its degradation by loss of glyoxylic acid or formaldehyde, although in more recent work (Bhattacharyya and Srisankar, 1978) they find that the Cu^{II} NTA complex undergoes, at least in part, an outer-sphere electron transfer to give Cu^{III} NTA. However it is not entirely certain that their analytical procedures are valid for the complex mixtures which may result on irradiation, and their conclusions need to be treated with caution.

Hydrated electrons are relatively unreactive towards these complexes, and after only a few percent decomposition react predominantly with the degradation products or other radiolysis products such as hydrogen peroxide. (Anbar et al., 1973; Ross, 1975).

Pulse radiolysis studies, notably by Meyerstein and co-workers (Meyerstein, 1971; Lati and Meyerstein, 1972, 1975, 1978; Lati, Koresh and Meyerstein, 1975), suggest that OH radicals react by outer-sphere electron transfer with a

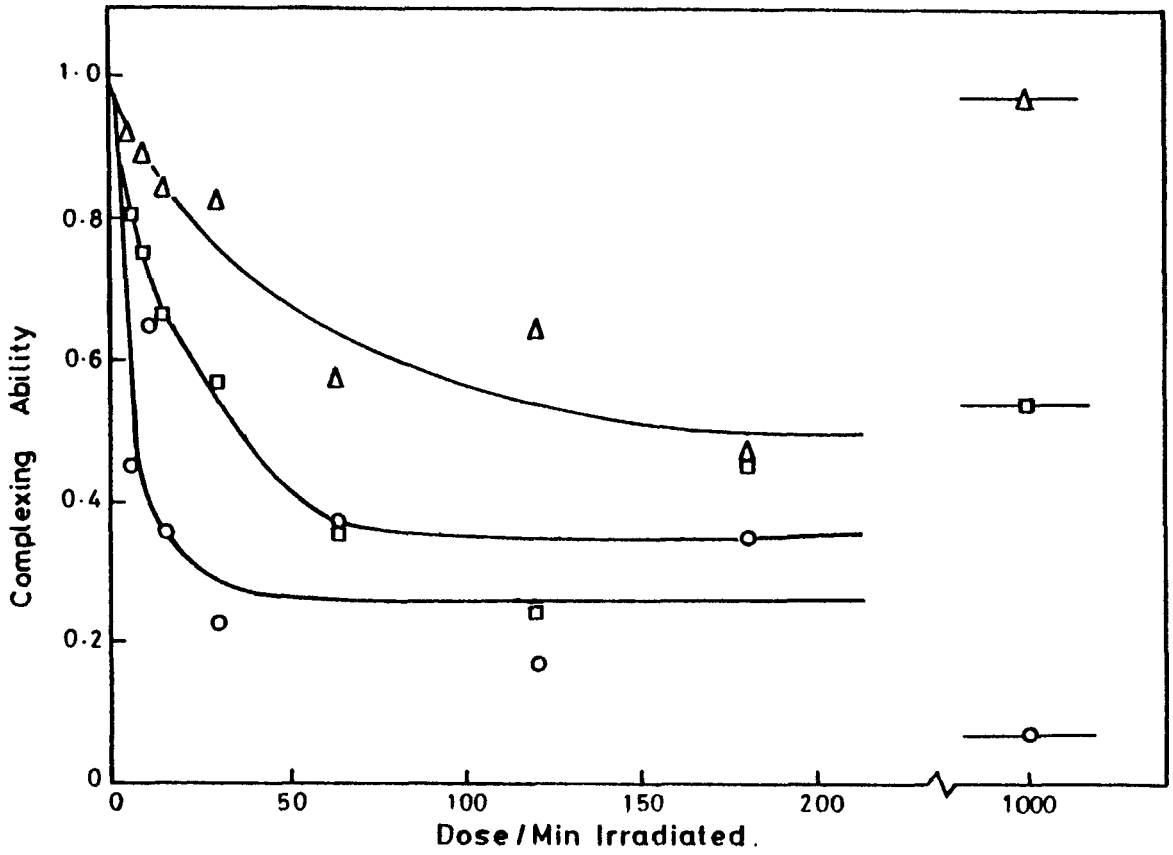

FIG. A44. Effect of Radiation on the Complexing Ability of 2×10^{-4} M Ethylenediamine Solutions Saturated with N_2O(○), Ar (Δ) or O_2(□)

number of complexes including Cu^{II}, Fe^{II}, Ni^{II} and Co^{II} (in part), whilst evidence for H atom abstraction was given with Mn^{II}, Zn^{II} and Co^{II} (in part). A study of the reaction of OH with these metal-EDTA complexes using pulse radiolysis has also been made as part of this work. To distinguish between the various reaction pathways the reactivity of the product of OH attack with O_2, 1,4-benzoquinone (a powerful oxidising agent), and its decay in the absence of solutes was studied. The principal findings are summarised in Table A21.

Of particular interest for reactor decontamination is the behaviour of Fe^{II}EDTA. Radiation induces oxidation of this compound to Fe^{III}EDTA. Interestingly the reverse reaction also occurs, albeit at the expense of oxidation of the ligand, following attack by H and OH. Hydrated electrons are also very reactive. In this system therefore the product of radiolysis affords considerable protection to the primary Fe^{II} complex.

4.6 IMPLICATIONS FOR REACTOR DECONTAMINATION

4.6.1 General Remarks

Even several hours after shutdown the residual radiation field in the core of a nuclear reactor may have a dose rate of ca. 1 Mrad h^{-1}. Thus radiolytic degradation potentially limits the usefulness of decontaminating reagents. Radiation chemists measure the destruction of a compound (R) in terms of G-value where G is the number of molecules of R destroyed for every 100 eV energy deposited in solution. If the concentration of the reagent is [R], the dose rate D (in units of eV $l^{-1}h^{-1}$*), then the time, t, (in h) taken to destroy the reagent will be :

$$t = \frac{N\,[R]\,10^2}{GD} \qquad (39)$$

where N is Avogadro's number (= 6.023×10^{23} molecules mol^{-1}). If [R] $\sim 10^{-2}$M, and it is required that the reagent last 20h, then G must be ≤ 0.5. Since the yields of the transient species OH and e^-_{aq} are both ca.2.7 it would appear that for the reagent to be effective it must not be reactive with e^-_{aq} and OH.

In practice things are not quite as bad as these figures suggest for the following reasons :

---

* 1 Mrad h^{-1} = 6.24×10^{22} eV l^{-1} h^{-1}

TABLE A21

Consequences of OH Attack on some Metal - EDTA Complexes[a]

Metal	Product of OH Attack	Subsequent Reactions of Product	Overall Change
None	Radical	Disproportionation	Degradation
Co^{II}	Coordinated radical	Disproportionation	Ligand degradation
Co^{III}	Coordinated radical	Intra-molecular electron transfer	Ligand degradation and reduction of metal centre
Cu^{II}	Coordinated radical	Intra-molecular electron transfer	Ligand degradation and reduction of metal centre
Fe^{II}	Fe^{III} complex[b]	None	Oxidation of metal centre
Fe^{III}	Coordinated radical	Intra-molecular electron transfer	Ligand degradation and reduction of metal centre
Mg^{II}	Coordinated radical	Disproportionation	Ligand degradation
Mn^{II}	Coordinated radical	Disproportionation	Ligand degradation
Ni^{II}	Ni^{III} complex	None (v. slow oxidation of ligand by Ni^{III} centre)	Oxidation of metal centre (Ultimately ligand degradation)
Zn^{II}	Coordinated radical	Disproportionation	Ligand degradation

a) Based on unpublished data of R.M. Sellers, M.Z. Hoffman and M.G. Simic.

b) Reaction occurs by H atom abstraction to give a co-ordinated free radical followed by a very rapid ($\tau_{\frac{1}{2}} < 5$ μs) intra-molecular electron transfer from metal ion to radical ligand.

i) The reagent's radiolytic decomposition products may interfere and lead to protection of the starting material. For instance it is unusual (although by no means unknown) to find that the concentration of a reagent being decomposed by radiation decreases linearly up to 100% destruction. Often the decrease is more nearly exponential. For this effect to be of maximum benefit it is clearly advantageous to have products which have a higher reactivity with H, OH and e^-_{aq} than the starting materials. If this occurred, for instance, with the low oxidation-state metal ion reducing agents it might be possible to regenerate the reagent by e^-_{aq} reduction of its oxidised form.

ii) It is important to remember that it is the reagent's function (i.e. its ability to complex, or reduce) that needs to be considered, rather than its structural integrity. The degradation product of a complexing agent may also have complexing properties, so that although decomposition is taking place there is no loss of function. The results described above for EDTA illustrate this point quite clearly.

This consideration has perhaps less bearing on radiolytic stability of reducing agents, although V^{III} species generated by one-electron oxidation of V^{II}-containing starting materials may also exhibit reducing properties.

iii) The metal ions taken into solution during the decontamination may dramatically affect the course of the radiolysis. Principal among the metal ions are Fe^{2+} and Fe^{3+}. Since many complexes of these metal ions are reactive with OH/e^-_{aq}, there is the possibility of protecting the reagent. This arises because they may in effect operate as a 'catalyst' combining e^-_{aq} and OH to give OH^-, as shown in reactions (40) - (42).

$$Fe^{II} + OH/H \rightarrow Fe^{III} + OH^-/H_2 \quad (40)$$

$$Fe^{III} + e^-_{aq} \rightarrow Fe^{II} \quad (41)$$

$$Fe^{III} + H/OH \rightarrow Fe^{II} + H_2/H_2O + H^+ \quad (42)$$

Whether such reactions occur in practice is determined by the relative rates of the various reactions, which vary according to the ligand, and the ratio $[Fe^{II}]$ to $[Fe^{III}]$.

iv) The complexing and reducing agents should not be considered in isolation. It seems likely that all LOMI-type reducing agents will be oxidised by OH, and many also by H and e^-_{aq}. In order to ensure an adequate lifetime for the reagents it will clearly be advantageous for the excess free complexing agent present to afford some protection. This will be favoured by its having higher reactivity with H, OH and e^-_{aq} than the reducing agent.

The problem of the 'molecular' H_2O_2* remains. Many LOMI type reagents are likely to be oxidised by this. The only other species that could complete are the radiolytic e^-_{aq} (which reacts very rapidly, but will most probably be scavenged by other species present), and Fe^{II} complexes formed from dissolved metal oxide.

4.6.2 Implication for Reagents Considered in this Report

Complexing Agents : It is clear from the experiments described above that ethylenediamine, bipyridyl and phenanthroline would not be suitable as complexing reagents in a high radiation zone, because of their rapid loss of complexing ability on irradiation. EDTA and NTA on the other hand would appear to be suitable with respect to their radiolytic stability. The less extensive data for picolinic acid indicate that this compound would also have adequate stability.

Reducing Agents : The complexes of Cr^{II} and V^{II} with bipyridyl are unlikely to be suitable as reducing agents in a high radiation zone, because of the instability of the ligand towards radiation, whereas $V^{II}(pic)_3$ would appear to be much more suitable. The presence of formate is clearly of considerable importance. In its absence a rough estimate of the reagent's lifetime can be obtained from Eqn.(39). Taking D = 1 Mrad h^{-1}, [R] = 10^{-2}M and assuming a three fold excess of free ligand, for which the appropriate G-value is ca.1, gives a lifetime of ca.10h. This should perhaps be treated as a lower limit. In the presence of adequate formate there is not only no radiolytic oxidation of the $V^{II}(pic)_3$, but a continual regeneration of the reagent through radiolysis. This is clearly a very important feature for any reagent for use in a radiation field. The key reaction in this regeneration is the reduction of the V^{III} complex by CO_2^-. No systematic survey of CO_2^- reduction rates with V^{III} complexes (or the oxidised form of other LOMI reagents) has been

* The term 'molecular' refers to the fact that it is produced in the primary radiolytic event, summarised in Eqn. (9).

undertaken but it is likely that such reactions do in fact occur. In situ regeneration by the residual radiation field is likely then to be a feature of all, or almost all, LOMI type reagents.

One other possible advantage of using formate is that it may be possible to destroy any remaining after a decontamination by radiolysis. The particular merit of this method is that the degradation product, CO_2, is gaseous.

These remarks refer to the effect of radiation fields with dose rates of ca.1 Mrad h^{-1}. At lower dose rates (say < 10^4 rad h^{-1}) as found out of core none of the reagents described here would be seriously affected by radiation, and they would therefore be suitable for decontaminating components associated with low radiation.

APPENDIX A5

5.0 THE APPLICATION OF LOW OXIDATION-STATE METAL ION (LOMI) REDUCTANTS TO REACTOR DECONTAMINATION

The task of the chemist in designing a decontamination system is to provide a reagent which can be introduced into the coolant of a reactor, will provide the necessary displacement of radioactivity from the pipework and can subsequently be removed from the system. The reagent must not cause degradation of reactor materials and should be suitable from the point of view of availability of chemicals, convenience of operation, cost and radioactive waste requirements.

Most decontamination experience to date has involved the use of organic chelating acids and only limited use has been made of metal ion reductants (Baybarz, 1961). In fact in the patent describing the use of chromium(II) the conditions used were such that no efficient electron-transfer pathway was open to the chromium reductant and the exercise was probably successful only as a result of the massive concentration of chromium used. To repeat such an exercise on full-scale power producing reactor would involve the use of hundreds of tonnes of chromium metal and would therefore be not very attractive.

By contrast the development of high efficiency reduction pathways as described in this work allows the concentrations to be reduced and pH to be increased in the decontaminant solution while still maintaining rapid dissolution of corrosion product deposits. The use of ion exchange techniques means that the dilute reagents (and radioactive contamination) can be removed in small scale plant leading to small volumes of radioactive waste.

Table A22 shows the approximate quantities of metals and chemicals that would be required for a PWR plant having a coolant volume of 300 tonnes.

5.1 MATERIALS CORROSION IN LOMI REAGENTS

Before any new reagent system can be applied to a reactor, it must be established that no serious attack will occur in the circuit. Since the corrosion of metals in an aqueous environment is generally an oxidative process, the strong reducing agents used here would be expected to protect most metals, or corrode them only slowly. A series of tests was carried out

to investigate the compatibility of the vanadous picolinate reagent with most common reactor materials. Picolinic acid alone was also tested in the absence of the LOMI component. A few comparative tests were carried out with a high concentration citrate/oxalate reagent, with added corrosion inhibitor.

5.1.1 Electrochemical Measurements

The technique ot potentiokinetic anodic polarization (PAP) was used to investigate the effects of picolinic acid solutions on the corrosion of four common reactor materials. A diagram of the experimental apparatus is given in Fig. A45. The results of these experiments appear as plots of E against log I; tests were carried out in deoxygenated buffer solution both in the presence and in the absence of picolinic acid, and the two curves compared. Fig. A46 shows the results for Zircaloy 2, and clearly indicates that the ligand has no significant effect on the metal. Similar results were obtained for AISI 316 and 430 stainless steels and Inconel 600. For comparison purposes a similar experiment was carried out using a 6% solution of a citrox reagent similar in composition to TURCO 4521, with a sample of AISI 430 steel. (Steels of this type are known to be attacked by high-concentration oxalate reagents.) This is shown in Fig. A47: the corrosive effect of the reagent is clearly visible.

5.1.2 Coupon Corrosion

Most of the materials testing was carried out on coupons of various metals. Specimens of surface area of the order of 10 cm^2 were exposed to the reagent, either in a jacketted reaction vessel or in a recirculating loop; conditions such as pH were varied and a number of additives tested. Of all the materials tested only the ferritic stainless iron, AISI 410, showed any significant corrosion in $V(Pic)_3^-$, and so most experiments were carried out with this alloy.

The results of these tests are shown in Tables A23 and A24. The extent of corrosion was determined in all cases by weight loss; the release of iron into solution was also monitored in a few experiments, and some specimens were examined by optical and electron microscopy. A comparative test was also carried out on an AISI 410 coupon with the simulated TURCO 4521 mixture, including 2-mercaptobenzthiazole corrosion inhibitor. Figs. A48 and A49 shows the results of these experiments, and also a similar comparative study on specimens containing an AISI 321/AISI 410 weld transition. These weld specimens were also examined on the scanning electron microscope: no anomalous corrosion was observed in the LOMI reagent, but the citrox reagent caused

TABLE A22

Approximate Quantities of Materials Required for Low Oxidation-State Metal Ion Decontamination. (300 te Primary Circuit)

		CONCENTRATION (M)	QUANTITY
1)	Metal Ion (Cr V)	2×10^{-3} 6×10^{-3}	30 kg 90 kg
2)	Complexing Agent (bipy or picolinic acid)	3×10^{-2}	1.1 te*
3)	Ion Exchange Resin. Cation Anion		 2.5 m^3 2.5 m^3
4)	Electricity (For metal ion reduction)		80 kWh.

Compare with 9.0 te* chemicals required for 3% acid citrate clean.

* (1te = 1000 kg)

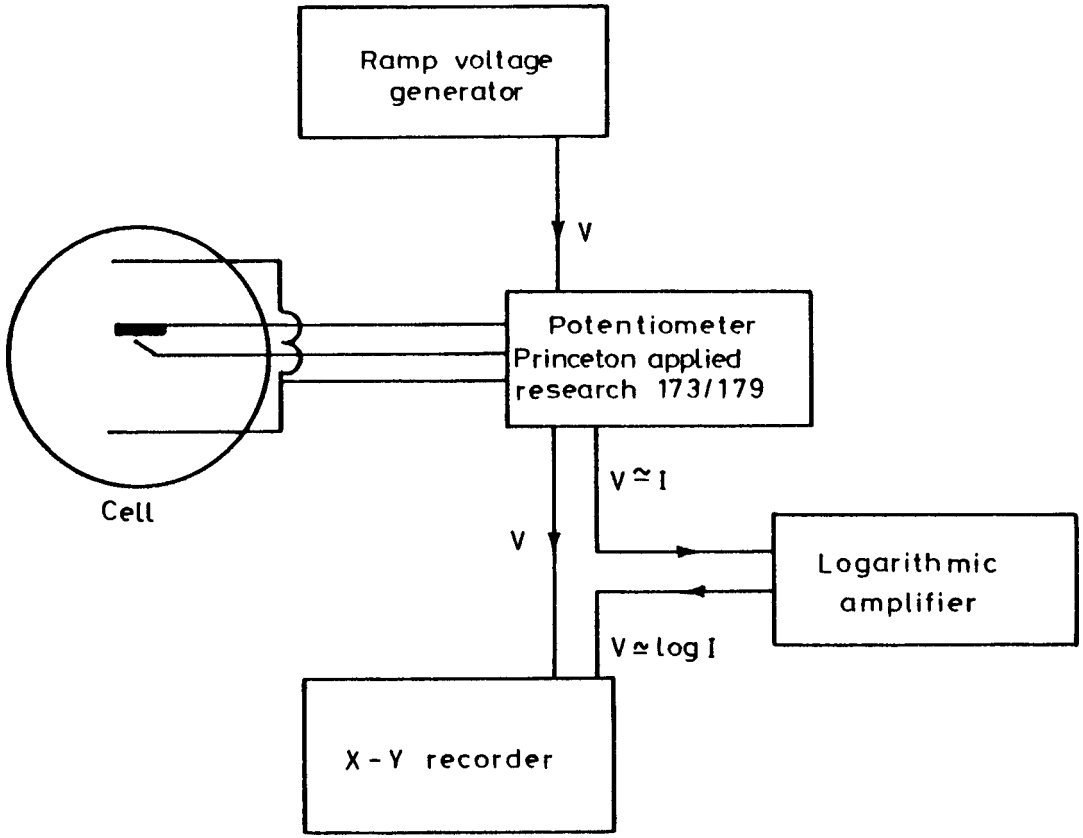

FIG. A45. Block Diagram of Equipment used for Potentiodynamic Corrosion Tests

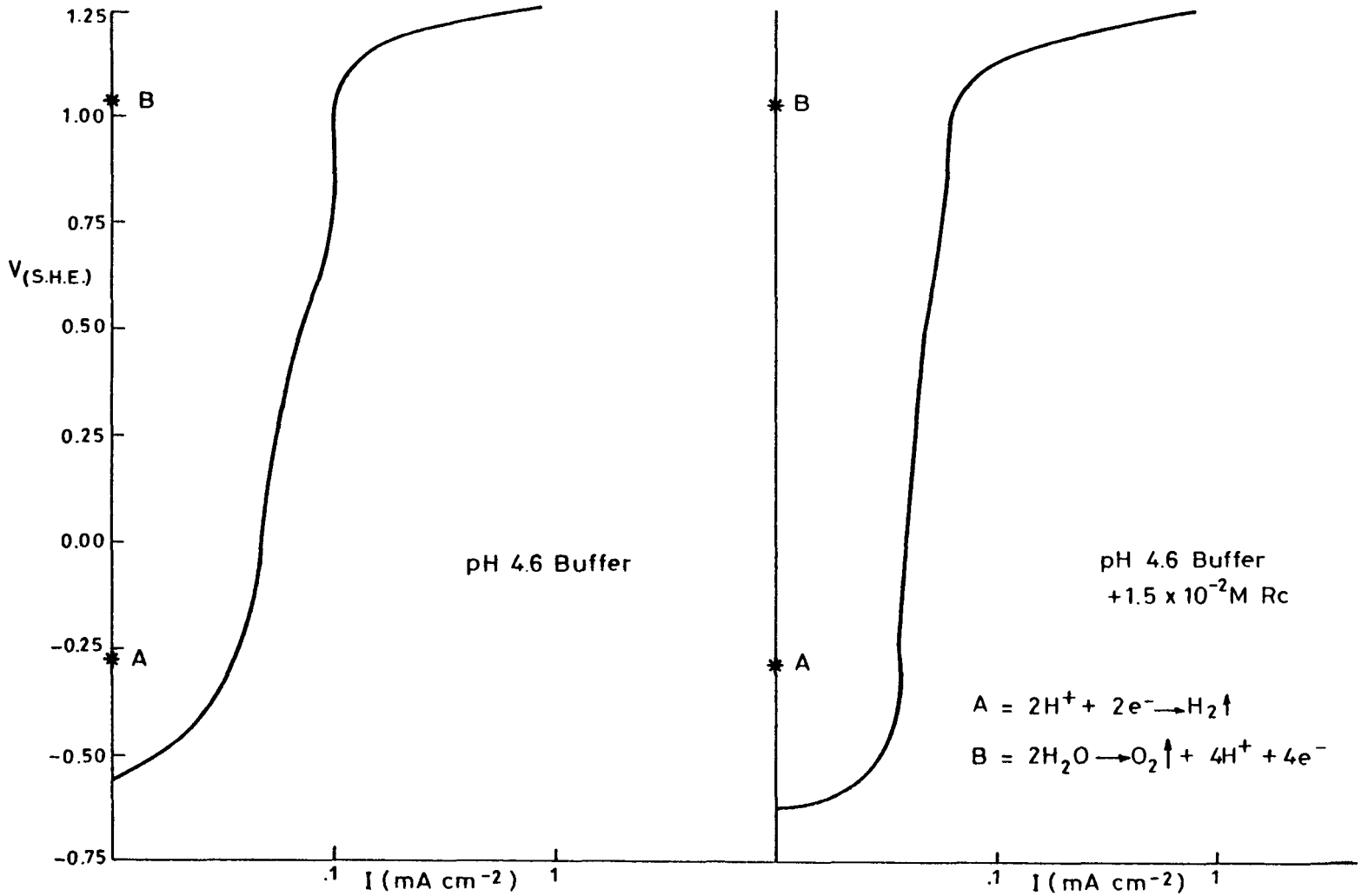

FIG. A46, Anodic Polarization Plots for Zircaloy-2

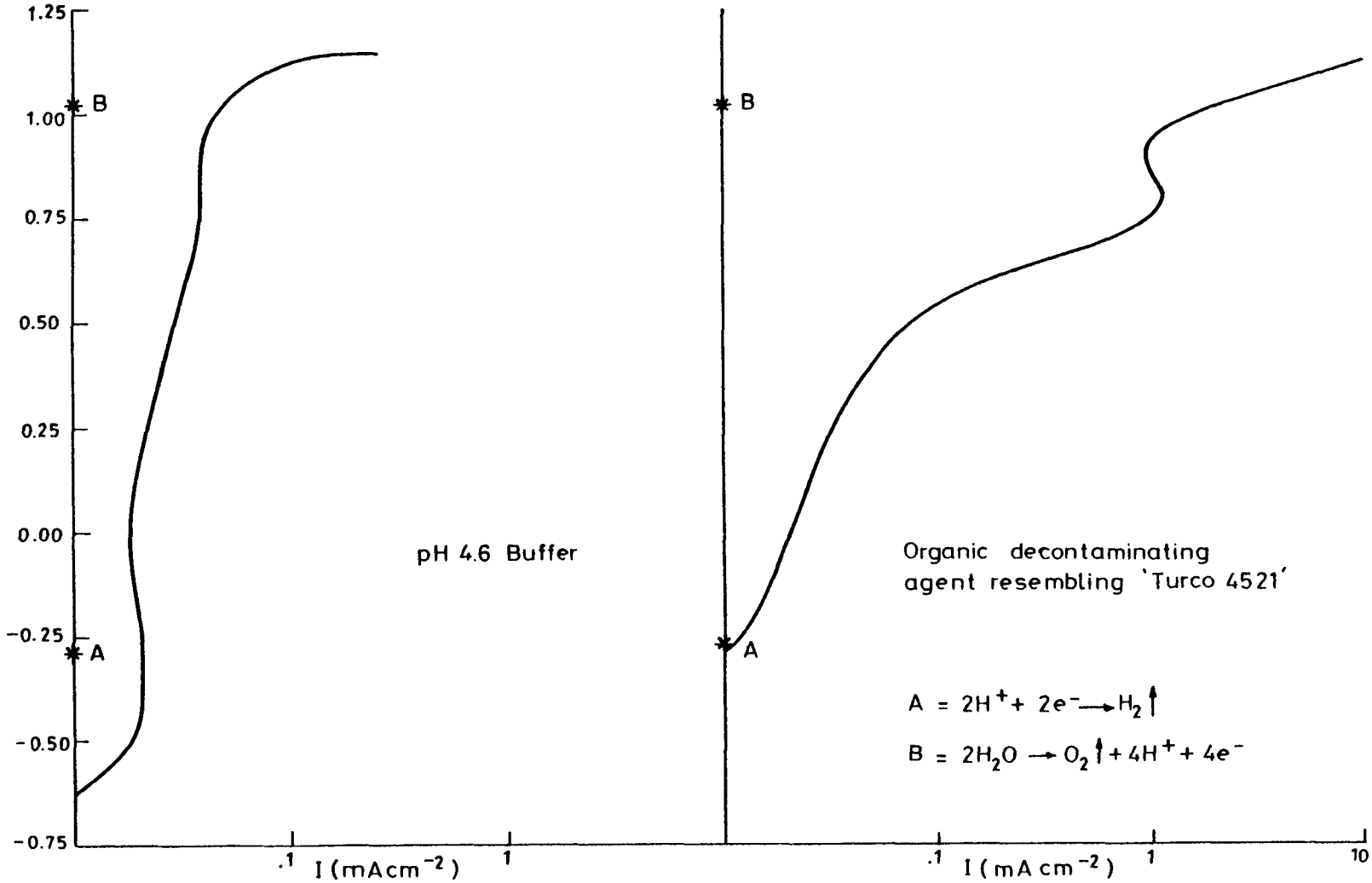

FIG. A47. Anodic Polarization of AISI 430 Steel

pitting in the 410 component near the transition. AISI 410 surfaces are also covered in a layer of crud after citrox treatment, so the dissolved iron and weight loss give a conservative estimate of the extent of corrosion. Other weld specimens were also unaffected by the LOMI reagent.

In the recirculating loop experiments two corrosometer probes were also used to monitor the attack on AISI 410 and EN2 carbon steel. The corrosion of the ferritic steel was more or less uniform, and was not significantly affected by the oxidation state of the reagent. The carbon steel, however, was not corroded at all, as long as there was vanadium(II) present to maintain a low redox potential. All the measured corrosion occurred when the V^{II} had been oxidised to V^{III}, either by reaction with Fe^{III} oxides, or by the catalytic action of the stainless steel surfaces.

It is clear from these results that no significant attack occurs on any of the materials tested. On the timescale of a reactor clean even the most sensitive of alloys would lose only a few microns in corrosion, much less than in the more aggressive citrox type of reagent. The use of surfactants seems to reduce the rate of attack slightly, but the benefit is not significant. A strong γ-radiation flux, at the sort of level likely to be found in a PWR core one week after shut-down, also seems to reduce the corrosion rate slightly.

One mode of attack not determined by these tests is the possible hydriding of Zircaloy fuel cladding. It was thought that the low electrochemical potential of the LOMI reagent might result in hydrides being formed in the alloy in high radiation fields. An experiment was carried out on a coupon of Zircaloy-2 in the BNL γ-irradiation facility; the conditions were similar to run 4 in Table A23. No change was observed in the specimen on metallographic examination for hydrides, compared to the as-received condition.

5.2 AVAILABILITY OF CHEMICALS

5.2.1 Chelating Ligands

The ligands studied in this work have been chosen on the basis that the materials are or could be easily made available on the 1-tonne scale required for decontamination.

As detailed discussion of possible production methods of ligands is not appropriate to this report, since this would be a matter for a suitable

TABLE A23

Materials Corrosion in LOMI Reagent (JRV Tests)

Run	Metal	Area cm^2	pH	Special Conditions	Time h	wt.loss mg	Penetration μ	Rate μ/h
1	AISI 410	12	4.5	Acetate buffer 0.1 M	3	3.0	0.3	0.1
2	AISI 410	12	4.0	-	3.5	17.0	1.7	0.5
3	AISI 410	12	5.8	-	5	10.3	1.0	0.2
4	AISI 410	12	5.2	γ-radiation field ∿ 0.5 M rad/hr; 70°C	5.5	3.1	0.3	0.05
5	AISI 410	11	4.7	Tetra-n-butyl ammonium hydroxide 20 ppm	5.5	6.8	0.7	0.1
6	AISI 410	11	4.9	Hyamine 1622 (cationic surfactant) 20 ppm	6.2	0.7	0.07	0.01
7	Inconel 600	9	4.8	-	5	0	0	0
8	Inconel 600	9	4.9	Triton X-100 (non-ionic surfactant) 0.1%	5.5	0	0	0
9	AISI 410	10	4.8	-	6	2.7	0.3	0.05
10	AISI 304	10	4.8	-	5.5	0.2	0.02	0.004
11	AISI 304	10	4.9	2 MBT (corrosion inhibitor) 10^{-3} M	6	0	0	0
12	AISI 321	10	4.9	-	5	0	0	0
13	AISI 321	10	4.7	2 MBT 10^{-3} M	5.5	0	0	0
14	Zircaloy-2	12	4.7	-	5.5	0.1	0.01	0.002
15	AISI 321/410	7.6	4.8	Weld specimen	6	0.1	0.01	0.002
16	AISI 321/EN2	4.6	4.4	Weld specimen, $[V^{II}] \sim 10^{-2}$ M	5	0.1	0.02	0.004
17	AISI 321/316	7.6	4.1	Weld specimen, $[V^{II}] = 8 \times 10^{-3}$ M	5	0.4	0.05	0.01

Generation Conditions : 80 C : $[V^{II}] = 4 \times 10^{-3}$ M : Total [Pic] = 2×10^{-2} M : [Formate] = 0.1 M

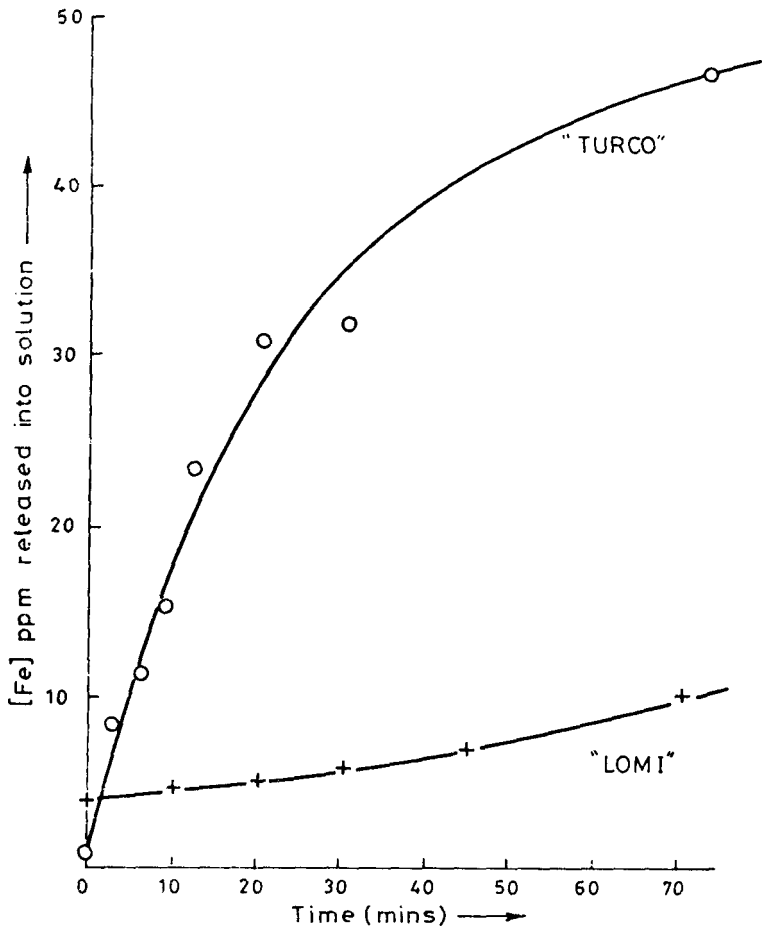

FIG. A48. Comparison of Fe Dissolved from AISI 410 in "Turco 4521" and $V^{II}(Pic)_3^-$ at 80°C

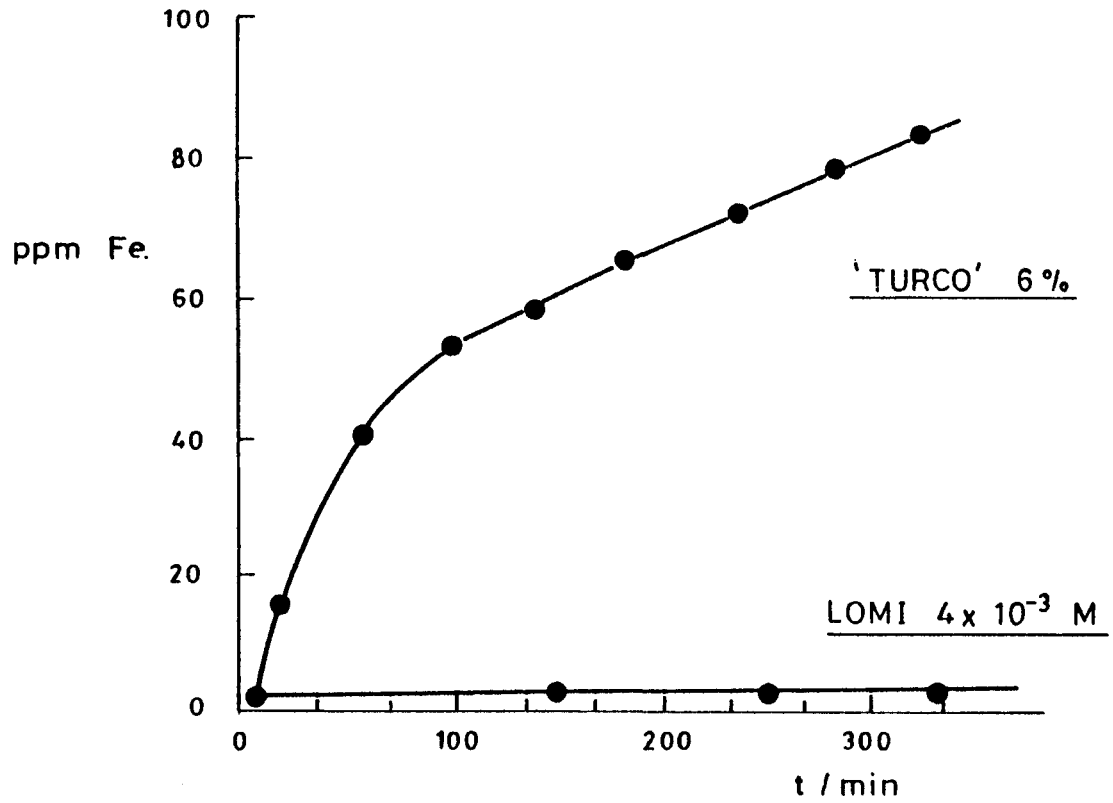

FIG. A49. Comparison of Fe Dissolved from AISI 321/AISI 410 Weld Transition Specimens in "TURCO 4521" and $V(Pic)_3^-$ at 80°C

TABLE A24

Materials Corrosion in LOMI Reagent (Loop Tests)

Metal	Area cm/2	wt.loss/mg	Penetration/μm	Rate μm/hr
AISI 410	10	13.9	1.5	0.47
	10	13.5	1.5	0.47
	10	19.0	2.1	0.66
EN 2 Carbon S	10	18.3	2.0	0.62 *
	10	9.3	1.0	0.31 *
	10	20.7	2.7	0.72 *
AISI 321	10	0	0	0
	10	0	0	0
	10	0	0	0
AISI 304	10	0	0	0
Inconel 600	8	0	0	0
Incoloy 800	10	0	0	0
Zircaloy-2	11	0	0	0

Conditions : $[V^{II}] = 2 \times 10^{-3}$ M (initially)

$[Pic]$ 1.7×10^{-2} M

pH 5.0 - 5.3

Temperature : $80^{o}C$

Run Time : 3.2 hours

* Corrosion of EN2 occurs only when the V^{II} is exhausted.
Corrosion rate quoted is the average for the whole experiment.

chemical manufacturer, the broadest outline only is given here. For example, 2,2'bipyridyl is structurally similar to a product 'Diquat', widely available as a selective herbicide, though the bipyridyl does not possess the latter's toxic properties. The bipyridyl can be manufactured from pyridine (consumed in the U.S. at 20,000 tonnes/year) by dimerisation in the presence of ferric chloride.

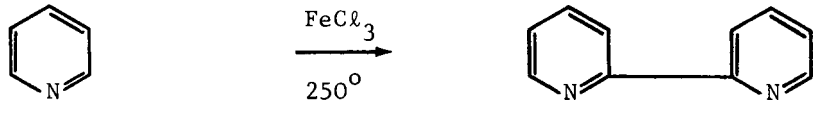

Picolinic acid, can be easily manufactured from 2-picoline, a by-product of coal-tar distillation.

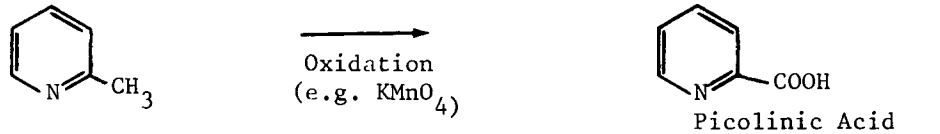

Picolinic Acid
(2 carboxy-pyridine)

Neither of these two reagents should prove difficult to obtain on the modest scale required for decontamination.

5.2.2 Formation of the Low Oxidation-State Metals

The air sensitivity of the low oxidation-state metals (V^{2+} and Cr^{2+}) means that they cannot be stored 'on the shelf' in the usual way, but must be produced and kept under oxygen-free conditions until required. The low oxidation-state metal ion solutions themselves will keep for several weeks, but decompose slowly by the reduction of water. Solutions that have "gone off" in such a way may be regenerated by electrochemical reduction provided the counter ion is not an oxidising agent, e.g. ClO_4^-.

For decontamination of a PWR the low oxidation-state metals are required in quantities of a few tens of kilograms per decontamination.

Suitable sources of vanadium are the sulphate salt, $VOSO_4$, or vanadium pentoxide, V_2O_5. Chromium is available cheaply as chromium metal, or alternatively a number of salts of chromium(III) could be used.

The original method described for production of chromous ions for reactor decontamination, involved the use of zinc metal as reductant (Baybartz 1961). This method involves the dissolution of one zinc ion for each two chromium(II) ions formed.

$$Zn + 2Cr^{+++} \rightarrow Zn^{2+} + 2Cr^{++}$$

The surface of the zinc is normally amalgamated with mercury to prevent the hydrogen production reaction

$$Zn + 2H^{+} \rightarrow Zn^{2+} + H_2$$

Whereas this method is quite satisfactory for the production of both chromous and vanadous ions, the alternative electrochemical method is preferable because no extraneous ions are dissolved in the reduction process.

$$Cr^{3+} + e^{-} \xrightarrow[\text{(cathode)}]{} Cr^{2+}$$

$$VO^{++} + 2e^{-} + 2H^{+} \xrightarrow[\text{(cathode)}]{} V^{2+} + H_2O$$

Studies were undertaken of the electrochemical production of vanadous formate, since this is the most favoured LOMI reagent at the present time. The purpose of these studies was to establish that it would be technically feasible to produce appropriate quantities of the reagent at a reasonable cost.

5.2.3 Small-scale Vanadous Formate Preparation Studies

Three separate routes to vanadous formate were examined, namely electrochemical reduction of vanadyl sulphate followed by ion exchange, direct electrochemical reduction of V_2O_5 in formic acid and a mixed method in which hydrazine was used to reduce V_2O_5 to V(IV) formate and the remaining reduction was performed electrochemically.

For vanadyl sulphate electrolysis, a two compartment cell was constructed with a sinter divider (Brauer 1965). A platinum mesh anode and a lead cathode were used, the latter being pretreated by anodic oxidation in sulphuric acid. The catholyte was 500 ml 2M sulphuric acid containing 2M vanadyl sulphate. During and after the electrolysis the catholyte was kept air free. The electrolysis preceeded at approximately 75% current efficiency and was complete in 48 hours.

A 2.5 litre column of anion resin (AMBERLITE IRA400) was pretreated with sulphuric acid (2N, 5L) to remove the chloride ions present initially, and then alternately with NaOH (2M, 5L) and a 1:1 mixture of formic acid and sodium formate (1M in each, 5L), twice each, to leave the resin fully in the formate form. Finally several litres of de-aereated water were passed down the column and all further operations carried out under argon.

The vanadium sulphate solution was passed down the column, and into a degassed receiving flask. Enough degassed water was loaded onto the column to wash through virtually all the V^{2+}. Some two litres of solution were thus obtained, containing in theory only V^{2+}, $HCOO^-$, HCOOH and traces of V^{3+}.

Analysis of the solution by chemical and spectroscopic methods showed that the total vanadium concentration was 0.26M, of which the V^{II} content was $\geq$ 93%. Losses of vanadium in the overall process were 36% and the final solution contained 7×10^{-3}M sulphate ion.

As an alternative to the vanadyl sulphate electrolysis/ion exchange, an attempt was made to reduce vanadium pentoxide in suspension in formic acid by electrochemical means.

9.1 g V_2O_5, 32 ml of 90% HCOOH and ca.200 ml of water were loaded into the cathode compartment of the cell similar to that used previously. 4M HCOOH was used as the anolyte. The lead cathode was pretreated as before, and had a surface area of about 50 cm^2. The suspension of V_2O_5 was stirred magnetically and flushed with argon. Electrolysis was carried out at 25V, which gave an initial current of 0.14 amps, rising over two days to 0.19 amps. The vanadium solution went through several stages giving a suspension of blue-green material in a blue solution (VO^{2+}), followed by a very dark solution (V^{III}), and finally the red-violet V^{II} colour. As in the other electrolyses, some H_2 evolution occurred towards the end of the process, but the overall current efficiency is quite high. The product was tranferred after 72 hours electrolysis.

Analysis of the solution showed that the total vanadium concentration was 0.35 M, of which at least 90% was V^{2+}. The lead cathode was found to be very much affected by the electrolysis at high voltage, being heavily corroded in some places, with large volumes of grown-on spongy lead metal in others. Despite this, analysis by atomic abdsorption spectroscopy showed only 4ppm of lead in the V^{II} solution. The total formate was found to be 2.8 M. In some

experiments the loss of some vanadium as an insoluble brown precipitate, probably a hydroxide or mixed hydroxide/formate of V^{III}, was observed.

The total volume of solution produced was not measured accurately, but was approximately equal to the intended 250 ml. Thus the losses involved in this process are only about 10%; these are due to diffusion during the electrolysis and to unavoidable wastage on air-free transfer of solutions.

The electrolysis can be made more convenient by preparing the vanadium(IV) formate from V_2O_5 in formic acid by chemical reduction. Hydrazine has been found to be a suitable reductant, and the reaction occurs as follows :

$$V_2O_5 + \tfrac{1}{2}N_2H_4 + 4H^+ \rightarrow 2VO^{2+} + \tfrac{1}{2}N_2 + 3H_2O$$

When stoichiometric amounts of V_2O_5 and hydrazine hydrate were added to formic acid solution the reaction proceeded smoothly to completion. The hydrazine was added in small portions to prevent the nitrogen gas effervescence being too vigorous and gentle heating was provided at the end to assist the reaction. The final product, in the form of a blue solution or suspension of blue solid, was submitted to an electrolysis procedure as previously described with similar results.

5.2.4 Development of Larger Scale Vanadous Formate Preparation

The simplicity and guaranteed freedom from anion impurities afforded by the direct electrolysis made this the best method for further study.

Certain developments were needed before a practical design could be established for large scale preparation of vanadous formate. The platinum anodes used in small scale work were costly, the sintered glass cell divider was insufficiently robust for large scale use, and the poor integrity of the lead cathode would prove inconvenient. Difficulties had also been encountered in the preparation from precipitation of solid as described above. Finally, it was necessary to establish that the preparation was satisfactory if the anolyte volume was only a small fraction of the catholyte.

As an alternative to platinum, graphite was used as an anode material. Performance of the graphite was satisfactory but there was a tendency for the electrode to disintegrate by spallation from areas of high current density. The resulting powdered debris was found to block the pores of the divider

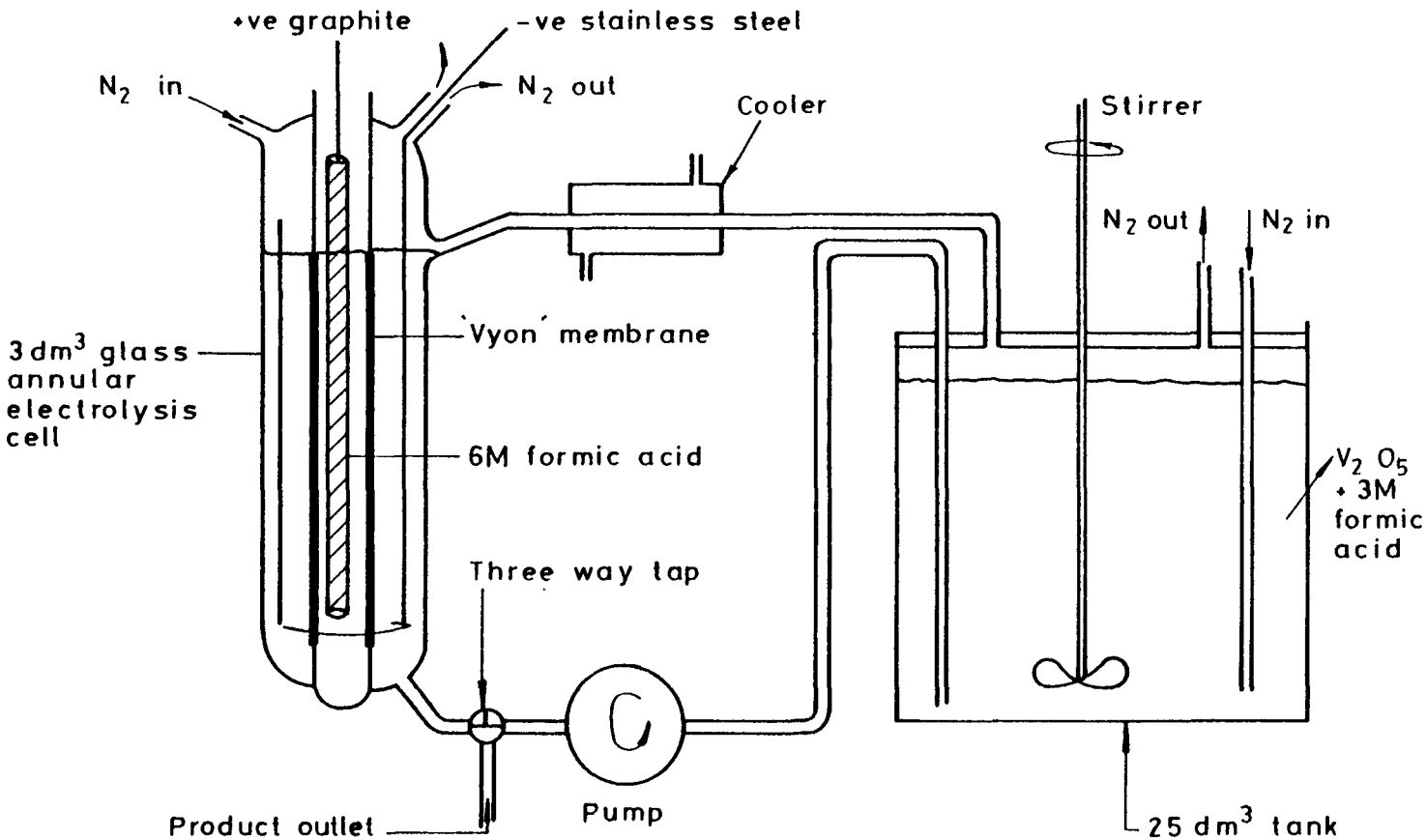

FIG. A50. 25 dm^3 Circulating Electrolysis Cell for Preparation of V^{II} Formate

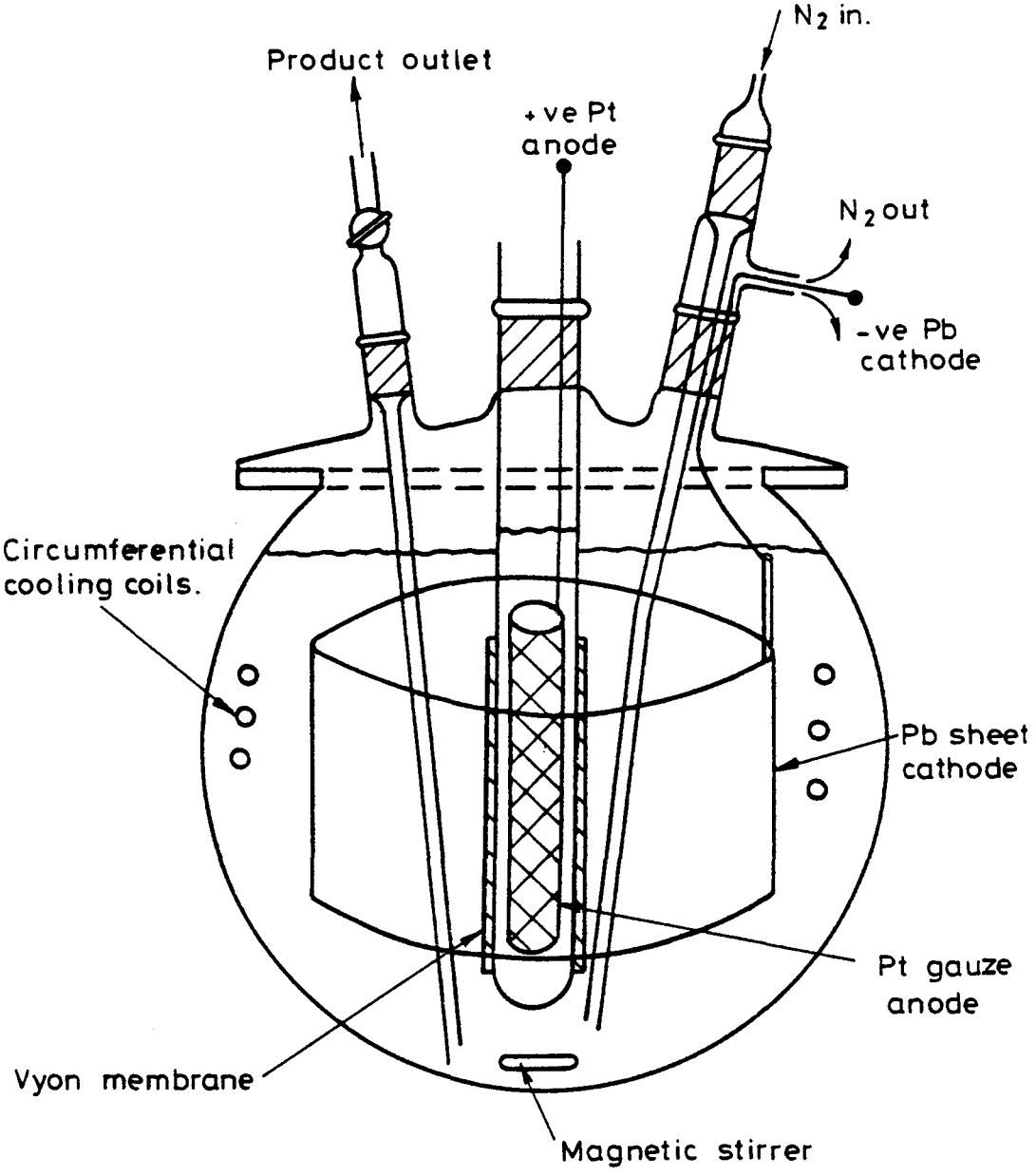

FIG. A51. 5 Litre Scale "Pool Type" Electrolysis Cell

material and could contaminate the catholyte product. Nevertheless graphite anodes have been used successfully in a number of preparations.

Alternative divider materials have been examined for use in the cell and two in particular "Vyon", (Porvair Ltd., U.K.) a porous polythene sheet material, and "Vyledin", (Bondina Ltd., U.K.) a polyester non-woven fabric, have been found to be suitable. The divider must perform the tasks of preventing oxygen diffusion and bulk mixing of the anolyte and catholyte whilst remaining a suitable conductor of ionic current between the two halves of the cell.

The use of a stainless steel cathode was examined. Although this material has a lower hydrogen overvoltage than lead, it was inferred that the weakly acidic nature of the catholyte would allow reduction of vandium to proceed without excessive hydrogen evolution at the cathode. This was in fact the case, and current efficiencies were only slightly lower than when using a lead cathode. The stainless cathode was easy for fabricate and support and did not corrode during the electrolysis, but solid precipitation seemed to be more prevalent when this type of cathode was used.

In other experiments it was concluded that the preparation was not sensitive to cathode:anode volume ratio.

As a result of these tests, two pilot-scale electrolysis cells were built to produce vanadous formate in quantities of several tens of litres of 0.3 - 0.4 M V(II) solution. The outline design of these cells, one a "loop" type and one a "pool" type are shown in Figures A50 and A51.

A total of 55 litres of solution were produced in this equipment having ∿0.3M Vanadium(II) and 0.03 Vanadium(III) present in formic acid solution.

5.2.5 Storage of Vanadous Formate Solution

Experiments were undertaken to examine the storage characteristics of vanadous formate solution. When the reagent was stored in a glass vessel no detectable oxidation occurred over a period of 2 - 3 months, provided that air was kept rigorously excluded. In the presence of polythene powder no degradation occurred, but in the presence of stainless steel a significant fraction of the reagent became oxidised to V(III) within a period of ca.24h.

The reason for this behaviour is probably the steel surface catalysis of the

reduction of water by vanadium(II). V^{2+}_{aq} is thermodynamically capable of reducing H^+ to H_2 in acid solution but this reaction is very slow in the absence of catalysis.

High density polythene or plastic containers can be used for storage or transport of vanadous formate reagent provided that they are thick enough to prevent diffusion of oxygen through the walls.

It is necessary, of course, to have the facilities for air-free transfer of the contents of the container, and a pressure relief device is also advisable if long storage periods are contemplated. 25-litre batches of vanadous formate reagent have been stored for 2 months and transported to AEE Winfrith using commercially available plastic containers.

5.3 NUCLEAR PROPERTIES OF THE METALS

Chromium and vanadium are constituents of reactor steels and their presence in the form of corrosion products in-reactor is therefore accepted already. Residual chromium and vanadium from the decontamination reagent may become activated in subsequent operation to form the isotopes chromium-51 and manganese-54, though the quantities of the metals added in the decontamination are comparable with the corrosion product deposits and therefore are unlikely to be significant after flushing the system.

More likely to be of concern are the impurities in the metals used, particularly cobalt. Fortunately, the two metals have stable anionic high oxidation states and therefore are easily freed of cobalt. Another potential source of contamination is corrosion of the electrochemical apparatus used to generate the low-oxidation state metals. Provided sufficient care is taken, it should be possible to keep the levels of such impurities below about 1 ppm in the metal, thus ensuring that even if all the impurity is deposited within the reactor (itself unlikely) it is still not a major source of cobalt input to the system.

It should be noted that all such concerns about adding impurities are eased by using a dilute reagent. If it is desired to maintain no greater than 100 mg input of cobalt in an EDTA decontamination performed at 0.1 M ($\sim$ 3%) the maximum allowable cobalt in the EDTA would be 0.01 ppm.

The nuclear properties of the ligands under consideration, which contain only C, H, O and N will not present any unfamiliar difficulties.

5.4 THE DECONTAMINATION

The only preparation of the reactor necessary for the decontamination would be to remove lithium from the reactor coolant to the lowest practical concentration (reactor pH $\sim$ 5 - 6). Since any oxygen dissolved in the coolant will waste the capacity of the reagent this should be removed by a prior addition of hydrazine if necessary.

The decontamination solution would then be added to the reactor coolant and circulated throughout the pipework. The pH should remain within the range of the acetic acid buffer.

After the decontamination is complete the reactor coolant contains the normal constituents plus ligand complexes of vanadium, iron, nickel, Co-60, acetate or formate ion and some free ligand. All the constituents other than acetate or formate may be removed by a hydrogen form cation-exchange resin, e.g.

$$Fe^{II}(bipy)_3^{2+} + 2\ Resin - H^+ \rightarrow 2\ Resin - Fe^{II}(bipy)_3^{2+} + 2\ H^+$$

$$bipy + Resin - H^+ \rightarrow Resin-(bipy\ H)^+$$

In studies of this cation-exchange process it has been shown that less than 1% of metal ions and no detectable bipyridyl appear in the column effluent.

The acetate ions may be removed by anion exchange in the hydroxide/borate form at a pH between the borate and acetate buffers. After these procedures and appropriate lithium additions, the reactor coolant is in its original chemical condition.

Preliminary experiments with vanadous picolinate indicated that its ion-exchange behaviour was similar to that of the bipyridyl system.

5.5 WASTE TREATMENT

It is not envisaged that the cation resin, which contains the activity, should be further chemically treated, but would be stored for an appropriate period ($\sim$ 50 years) to allow decay of Co-60 or would be disposed of by solidification and burial.

If, however, it was desired to recover the vanadium for further use 2-Normal acid regenerates the column and treatment of the acid regenerant by alkaline oxidation would yield a precipitate of hydroxides of the radioactive metal ions. The vanadium, which would remain in solution (and the picolinate ligand) could then be recovered. Any Cr-51 activity remaining in solution would decay in a period of $\sim$ 1 year.

APPENDIX A6

6.0 SUMMARY AND CONCLUSIONS

In order to reduce Man Rem exposure in LWRs a method of decontamination is being developed to remove the activated oxide crud prior to man access. Ideally, low concentrations of cleaning reagents should be employed so as to minimise circuit corrosion and the volume of waste arisings. Experiments have been conducted to determine the factors which control the chemical dissolution of oxides typical of LWR primary circuits. The presence of a single-electron reducing agent is central to obtaining rapid dissolution of oxides where the predominant species is Fe^{III}. This conclusion has allowed the development of a number of decontaminating agents based on low oxidation-state transition metal ion reductants (LOMI). These are capable of dissolving synthetic PWR oxides up to two orders of magnitude faster than conventional decontaminating reagents based on mixtures of complexing acids, even when the LOMI reagent is present at only one hundredth the concentration of the conventional chemicals. The radiation chemistry of these reagents has been examined and most will be suitable for component or part circuit decontamination whereas a few can be applied to a full circuit including the fuelled core. The application of LOMI reagents to a PWR circuit is discussed. The main conclusions of the study are :-

1) The rates of dissolution of nickel ferrite, haematite and magnetite are controlled by the rate of reduction of Fe^{III} to Fe^{II}.

2) For rapid dissolution it is not sufficient simply to have a reagent which is thermodynamically capable of reducing Fe^{III}, the reagent must also provide a low-activation-energy route for electron transfer to the solid surface.

3) Reagents which promote rapid electron transfer in homogeneous solutions have also proved successful in dissolving iron oxides. One of these, V^{2+}, dissolves nickel ferrite four orders of magnitude faster than reagents such as EDTA, oxalic/citric acid and HCl when present at only 10% of the concentration of these conventional reagents.

4) Dissolution experiments in which only the thermodynamic solubility of cations was increased by the addition of strong chelating agents, resulted in only small changes in rate when compared with the influence of efficient, non-complexing reducing agents.

5) Reagent systems based on V^{2+} in combination with 2,2'-bipyridyl or picolinic acid have been developed which decontaminated at a usable rate 9% Cr steel and SGHWR riser pipework at temperature $\sim 80^{o}C$ and at pH's in the range 4.5 - 6.5. A decontamination factor of 36 was achieved with the 321 stainless steel SGHWR specimen after 36 hours exposure in V^{2+} picolinate at concentrations $\sim$ 0.1%.

6) Methods have been developed for the ion-exchange removal of both the reagents and the dissolved activity which minimises the volume of active waste arisings.

7) Chelating agents such as picolinic acid, EDTA and NTA are sufficiently radiation stable for use in the active core of a water reactor. 2,2'bipyridyl is, however, only suitable for use in out of core regions.

8) To decontaminate the primary circuit of a 1000 MWe PWR with vanadium picolinate will require $\sim$ 90 kg of vanadium, 80 kWh for its reduction and 1 metric tonne (1 te) of picolinic acid. The waste arisings would be contained on 5 m^3 of ion exchange resin.

APPENDIX A7

7.0 REFERENCES

Abramovitch, S. and Rabani, J., 1976, J. Phys. Chem., 80, 1562.

Anbar, M., Bambenek, M. and Ross, A.B., 1973, NSRDS-NBS 43.

Anbar, M., Munoz, R.A. and Rona, P., 1963, J. Phys. Chem., 67, 2708.

Baker, B.R. and Melita, B.D., 1965, Inorg. Chem., 4, 848.

Bansal, K.M., Grätzel, M., Henglein, A. and Janata, R., 1973, J. Phys. Chem.,77, 16.

Bansal, K.M. and Sellers, R.M., 1975, J. Phys. Chem., 79, 1775.

Basolo, F. and Pearson, R.G., "Mechanisms of Inorganic Reactions" 2nd Edition (John Wiley, New York, 1967).

Baxendale, J.H., Hardy, H.R. and Sutcliffe, L.H., 1951, Trans. Far. Soc., 47, 963.

Baybartz, R.D., 1961, U.S. Patent 2981643.

Beattie, J.K. and Basolo, F., 1967, Inorg. Chem., 6, 2069.

Behar, D., Czapski, G., Rabani, J., Dorfman, L.M. and Schwarz, H.A., 1970., J. Phys. Chem., 74, 3209.

Bennett, L.E. and Taube, H., 1968, Inorg. Chem., 7, 254.

Bhattacharyya, S.N. and Kundu, K.P., 1971, Int. J. Radiat. Phys. Chem., 3, 1.

Bhattacharyya, S.N. and Kundu, K.P., 1972a, Int. J. Radiat. Phys. Chem., 4, 31.

Bhattacharyya, S.N. and Kundu, K.P., 1972b, Radiat. Res., 51, 45.

Bhattacharyya, S.N. and Kundu, K.P., 1976, Radiat. Eff., 29, 231.

Bhattacharyya, S.N. and Srisankar, E.V., 1977, Radiat. Res., 71, 325.

Bhattacharyya, S.N. and Srisankar, E.V., 1978, J.C.S. Faraday I, 74, 622.

Bradbury, D., 1978, in "Water Chemistry of Nuclear Reactor Systems", British Nuclear Energy Society, London, p.373.

Brauer, G., 1965, "Handbook of Preparative Inorganic Chemistry", 2nd Ed.(Academic Press), p.1277.

Buitenhuis, R., 1977, Thesis, University of Amsterdam.

Buxton, G.V. and Sellers, R.M., 1977, Coordinat. Chem. Rev., 22, 195.

Candlin, J.P., Halpern, J. and Trimm, D.L., 1964, J. Amer. Chem. Soc., 86, 1019.

Cotton, F.A. and Wilkinson, G., 1966, "Advanced Inorganic Chemistry", 2nd Ed., (Interscience, New York), p. 822.

Crabtree, J.M., Marsh, D.W., Williams, R.J.P. and Fernelius, W.C., 1961, Proc. Chem. Soc., 336,

Diebler, H. and Sutin, N., 1964, J. Phys. Chem.,68, 174.

Dultz, G. and Sutin, N., 1964, J. Am. Chem. Soc., 86, 829.

Eichler, E. and Wahl, A.C., 1958, J. Am. Chem. Soc., 80, 4145.

George, P. and Irume, D.H., 1957, J. Chem. Soc.,587.

Johnson, A.B., Dillon, R.L., Griggs, B. and Remark, J.F., 1978, Battelle N.W. Report BN-SA-7032.

Kametani, H. and Azuma, K., 1968, Trans. Met. Soc. AIME, 242, 1025.

Lappin, A.G. and McAuley, A., 1975, J.C.S. Dalton, 1560.

Lati, J., Koresh, J. and Meyerstein, D., 1975. Chem. Phys. Lett., 33, 286.

Lati, J. and Meyerstein, D., 1972, Inorg. Chem., 11, 2397.

Lati, J. and Meyerstein, D., 1975, Int. J. Radiat. Phys. Chem., 7, 611.

Lati, J. and Meyerstein, D., 1978, J.C.S. Dalton, 1105.

Marcus, R.A., 1964, Ann. Rev. Phys. Chem., 15, 155.

Margalova, T.K., 1965, Thermal Engineering, 12, 51.

Matijevic, E. and Rubio, J., 1978, EPRI Project RP966-1, 1977/78 Ann. Report.

Mercier, R.C. and Paris, M.R., 1964, Comptes Rendues, 259, 2445.

Mercier, R.C., Bonnett, M. and Paris, M.R., 1965, Bull. Soc. Chim., France, 2926, 3577.

Meyerstein, D., 1971, Inorg. Chem., 10, 2244.

Pitzer, E.C., 1961, General Electric Co., Report KAP2-M-ECP-8, Knolls Atomic Power Laboratory.

Pryor, M.J. and Evans, U.R., 1950, J. Chem. Soc., 1259.

Rantell, A., Jones, R.F. and Furlong, V.E., 1976, CEGB Report No. SSD/MID/N16/76.

Rao, P.S., Simic, M. and Hayon, E., 1975, J. Phys. Chem., 79, 1260.

Rigg, T., Scholes, G. and Weiss, J., 1952, J. Chem. Soc., 3034.

Rodliffe, R.S., Private Communication.

Ross, A.B., 1975, NSRDS-NBS43 Supplement.

Sandler, Y.L., 1978, "Structure and Solubility of PWR Primary Corrosion Products", Corrosion 78, Paper No. 158, Houston, U.S.A.

Sandler, Y.L. and Kunig, R.H., 1977, Nucl. Sci. and Eng., December.

Sellers, R.M., 1979a, CEGB Report No. RD/B/N4429.

Sellers, R.M., 1979b, CEGB Report No. RD/B/N4430.

Simic, M. and Ebert, M., 1971, Int. J. Radiat. Phys. Chem., 3, 259.

Swallow, A.J., 1978, Prog. React. Kinet., 9, 195.

Valverde, N., 1976, Ber Bunsenges Phys. Chem., 80, 330.

Wickham, D.G., 1967, Inorg. Syn., 9, 152.